

ROLE OF ASPARTATE AMINOTRANSFERASES AspB AND AspC IN THE WhiB7-CONTROLLED INTRINSIC  
DRUG RESISTANCE SYSTEM OF MYCOBACTERIA

by

Carol Ka Lo Ng

BSc (Hon), University of British Columbia 2005

A THESIS SUBMITTED IN PARTIAL FULFILMENT OF THE REQUIREMENTS FOR THE DEGREE OF  
MASTER OF SCIENCE

in

THE FACULTY OF GRADUATE STUDIES  
(Microbiology and Immunology)

THE UNIVERSITY OF BRITISH COLUMBIA  
(Vancouver)

October 2012

© Carol K L Ng, 2012

## Abstract

Intrinsic resistance of the intracellular pathogen *Mycobacterium tuberculosis* is one of the main reasons that the disease tuberculosis is difficult to treat and why it remains as one of the world's most prevalent and dangerous infectious diseases. The intrinsic resistance regulator WhiB7 controls a regulon that contains many genes predicted to have physiological functions including aspartate aminotransferases, *aspB* and *aspC*. Multi-drug susceptibility was observed in an *aspC* mutant and an *aspB* constitutive expression strain. The expression of *aspC* was positively regulated by WhiB7 while expression of *aspB* downregulated *whiB7* expression. The fitness of *Mycobacterium smegmatis* was affected negatively by oxaloacetate and positively by  $\alpha$ -ketoglutarate, substrates of aspartate aminotransferase, which then altered the growth inhibition by antibiotics. Recombinant AspB and AspC both catalyze measurable transamination of aspartate and  $\alpha$ -ketoglutarate. AspC plays an important role in mycobacteria physiology as deletion of this gene caused many growth deficiencies. Furthermore, the physiological role of AspC extended beyond amino acid intermediary metabolism to redox homeostasis and oxidative stress detoxification. These results revealed a link between intrinsic antibiotic resistance and metabolism mediated through AspB and AspC. Since antibiotic resistance in mycobacterium is a complex function of its physiology, it is important to screen for tuberculosis drugs under growth conditions that resemble those found *in vivo*.

## **Preface**

Dr. Gaye Sweet performed the catalase activity assay experiments. Experimental design and analysis of the data were a collaborative effort between Dr. Sweet and Carol Ng.

Steady-state kinetic determination of AspB was done in collaboration with Antonio Ruzzini in the group of Dr. Lindsay E. Eltis (University of British Columbia). Purified protein was supplied by Carol Ng.

The work in this thesis is conducted with approval from University of British Columbia Office of Research and in accordance with the University of British Columbia Policies and Procedures, Biosafety Practices and Public Health Agency of Canada Guidelines. The protocols in this work were approved by the UBC Biosafety Committee. The certificate number is B07-0169.

## Table of contents

<b>Abstract .....</b>	<b>ii</b>
<b>Preface.....</b>	<b>iii</b>
<b>Table of contents.....</b>	<b>iv</b>
<b>List of tables.....</b>	<b>vii</b>
<b>List of figures.....</b>	<b>viii</b>
<b>List of abbreviations .....</b>	<b>x</b>
<b>Acknowledgments.....</b>	<b>xii</b>
<b>1. Introduction .....</b>	<b>1</b>
1. 1. <i>Mycobacterium tuberculosis</i> and antibiotic resistance .....	1
1. 2. The WhiB family of proteins .....	2
1. 3. Oxidative stress and tuberculosis pathogenesis.....	3
1. 4. Physiological changes induced by antibiotics .....	5
1. 5. Mycobacterial amino acid aminotransferases.....	7
1. 6. Project rationale .....	8
<b>2. Materials and methods.....</b>	<b>9</b>
2. 1. Cloning and reagents .....	13
2. 2. Growth conditions .....	13
2. 3. Constitutive expression strain construction .....	13
2. 4. Mutant construction .....	14
2. 5. Construction of double mutant $\Delta aspB\Delta aspC$ .....	14
2. 6. Drug susceptibility testing.....	15
2. 7. Growth kinetics .....	15
2. 8. Antibiotic kill curve .....	15
2. 9. RNA isolation.....	16
2. 10. Quantitative real-time PCR.....	16

2. 11. NAD-NADH pool isolation and NAD cycling assay .....	16
2. 12. Hydrogen peroxide and menadione disc assay .....	17
2. 13. Preparation of cell lysate .....	17
2. 14. Catalase assay .....	18
2. 15. Phylogenic analysis of AspB <sub>Mtb</sub> and AspC <sub>Mtb</sub> .....	18
2. 16. Cloning of <i>aspB</i> and <i>aspC</i> in pGEX4T-1 .....	18
2. 17. Purification of GST-tagged AspB <sub>Mtb</sub> and AspC <sub>Mtb</sub> .....	18
2. 18. Thrombin cleavage of GST-tagged AspB <sub>Mtb</sub> and AspC <sub>Mtb</sub> .....	19
2. 19. Cloning of <i>aspB</i> and <i>aspC</i> in pET expression vectors.....	19
2. 20. Expression of recombinant His-tagged AspB <sub>Mtb</sub> and AspC <sub>Mtb</sub> .....	19
2. 21. Purification of recombinant His-tagged AspB <sub>Mtb</sub> and AspC <sub>Mtb</sub> .....	20
2. 22. Removal of His tag from AspB <sub>Mtb</sub> .....	20
2. 23. Cloning and expression of AspC <sub>Mtb</sub> without fusion tags .....	21
2. 24. Cloning and expression of AspC <sub>Mtb</sub> in <i>M. smegmatis</i> .....	21
2. 25. Aspartate aminotransferase assay.....	21
<b>3. Results.....</b>	<b>23</b>
3. 1. Expression of <i>whiB7</i> upregulates <i>aspC</i> .....	23
3. 2. Expression of <i>whiB7</i> and <i>aspC</i> is upregulated by tetracycline.....	24
3. 3. Optimal <i>whiB7</i> induction by tetracycline requires <i>aspC</i> .....	26
3. 4. Constitutive expression of <i>aspB</i> downregulates <i>whiB7</i> and <i>aspC</i> in tetracycline-induced cultures .....	26
3. 5. The $\Delta$ <i>aspC</i> mutant exhibits growth deficiencies.....	28
3. 6. The $\Delta$ <i>aspC</i> is able to catalyze glutamate but not aspartate .....	30
3. 7. $\alpha$ -ketoglutarate complements $\Delta$ <i>aspC</i> mutant's growth deficiencies .....	30
3. 8. Passaging the $\Delta$ <i>aspC</i> mutant in media containing $\alpha$ -ketoglutarate suppresses the growth rate defect but does not shorten lag phase .....	32
3. 9. The $\Delta$ <i>aspB</i> $\Delta$ <i>aspC</i> double mutant is not an amino acid auxotroph .....	32
3. 10. Opacification of 7H10 by $\Delta$ <i>aspC</i> mutant.....	34

3. 11. The $\Delta whiB7$ mutant, $\Delta aspC$ mutant, and <i>aspB</i> constitutive expression strains are antibiotic sensitive .....	35
3. 12. Complementation of antibiotic susceptibility of the $\Delta aspC$ mutant .....	35
3. 13. Effects of antibiotics on the growth kinetics of the $\Delta aspC$ mutant .....	38
3. 14. Differential killing of the $\Delta aspC$ mutant by clarithromycin .....	42
3. 15. Oxaloacetate and $\alpha$ -ketoglutarate modulate the rate of recovery from stationary phase growth and adaptation to bacteriostatic drugs .....	43
3. 16. Deletion of <i>aspC</i> causes a shift in intracellular redox homeostasis.....	46
3. 17. Increased oxidative stress in the $\Delta aspC$ mutant.....	46
3. 18. Phylogenic analysis corroborates <i>aspB</i> and <i>aspC</i> as putative aminotransferases .....	50
3. 19. Complementation of aspartate auxotrophy in <i>E. coli</i> with AspB <sub>Mtb</sub> and AspC <sub>Mtb</sub> .....	56
3. 20. Amino acid auxotroph DL39 does not exhibit general growth deficiencies and does not show increased antibiotic susceptibility .....	58
3. 21. Expression and purification of AspB <sub>Mtb</sub> and AspC <sub>Mtb</sub> .....	61
3. 22. Aspartate aminotransferase activity of AspB <sub>Mtb</sub> and AspC <sub>Mtb</sub> .....	73
<b>4. Discussion .....</b>	<b>75</b>
4. 1. <i>aspB</i> and <i>aspC</i> expression is linked to <i>whiB7</i> expression .....	75
4. 2. Intermediary metabolism of mycobacteria is linked to intrinsic antibiotic resistance .....	78
4. 3. Role of AspB and AspC in mycobacteria physiology .....	82
4. 4. Implicated roles for AspC in redox homeostasis and oxidative stress detoxification .....	84
4. 5. Concluding remarks .....	87
<b>References .....</b>	<b>88</b>

## List of tables

Table 1. Plasmids and strains used in this study.....	10
Table 2. Primers used in this study.....	12
Table 3. Growth properties of $\Delta aspB$ and $\Delta aspC$ mutants in cultures containing aspartate and glutamate as carbon and/or nitrogen sources.....	31
Table 4. Antibiotic susceptibility profiles of the $\Delta whiB7$ mutant, <i>hsp-aspB</i> expression, and the $\Delta aspC$ mutant strains of <i>M. smegmatis</i> .....	36
Table 5. Effect of antibiotics and putative aspartate transaminase substrates on time of recovery from stationary phase growth arrest.....	45
Table 6. Functions of anchor residues in family I aminotransferases. ....	55
Table 7. Amino acid auxotrophic strain DL39 does not show changes in antibiotic susceptibility. ....	59
Table 8. Expression of <i>AspC<sub>Mtb</sub></i> in <i>E. coli</i> and <i>M. smegmatis</i> .....	72
Table 9. Specific activities of purified aspartate aminotransferases.....	74
Table 10. Comparison of steady state kinetic parameters determined for <i>AspC<sub>Mtb</sub></i> and <i>AspC<sub>Eco</sub></i> . ....	74

## List of figures

Figure 1. Detoxification of reactive oxygen species.....	4
Figure 2. Oxidative damage via Fenton’s reaction occurs in 3 steps.....	6
Figure 3. Reaction catalyzed by aspartate aminotransferases.....	23
Figure 4. Expression of <i>aspC</i> was upregulated by <i>whiB7</i> .....	25
Figure 5. Expression responses of <i>whiB7</i> , <i>aspB</i> , and <i>aspC</i> to tetracycline.....	25
Figure 6. Interactive regulation of <i>aspB</i> , <i>whiB7</i> and <i>aspC</i> .....	27
Figure 7. Growth kinetics of <i>M. smegmatis</i> wild-type, $\Delta$ <i>aspB</i> , $\Delta$ <i>aspC</i> , <i>hsp-aspB</i> <sub>Mtb</sub> , <i>hsp-aspC</i> <sub>Mtb</sub> , and $\Delta$ <i>aspC</i> complemented.....	29
Figure 8. Growth of the $\Delta$ <i>aspC</i> mutant was modulated by addition of aspartate aminotransferase substrates.....	31
Figure 9. Allowing the $\Delta$ <i>aspC</i> mutant to adapt to growth in media containing $\alpha$ -ketoglutarate did not suppress the extended lag phase growth deficiency.....	33
Figure 10. Growth kinetics of double mutant $\Delta$ <i>aspB</i> $\Delta$ <i>aspC</i> .....	33
Figure 11. Opacification of 7H10 by the $\Delta$ <i>aspC</i> mutant.....	34
Figure 12. Complementation of antibiotic susceptibility of the $\Delta$ <i>aspC</i> mutant by constitutive expression of <i>aspC</i> <sub>Mtb</sub> or addition of $\alpha$ -ketoglutarate.....	37
Figure 13. The time required for wild-type mc <sup>2</sup> 155 to adapt and grow in media containing antibiotics is dependent on antibiotic concentration.....	39
Figure 14. The difference between wild-type and the $\Delta$ <i>aspC</i> mutant growth kinetics in media containing antibiotic.....	40
Figure 15. Differential killing of the $\Delta$ <i>aspC</i> mutant by clarithromycin.....	42
Figure 16. Effect of $\alpha$ -ketoglutarate and oxaloacetate supplementation on growth kinetics and antibiotic inhibition of growth in wild-type <i>M. smegmatis</i> .....	44
Figure 17. The $\Delta$ <i>aspC</i> mutant has an increased redox state.....	47

Figure 18. Sensitivity of mutants $\Delta aspB$ and $\Delta aspC$ to oxidative stress compounds hydrogen peroxide and menadione .....	48
Figure 19. Higher oxidative stress in the $\Delta aspC$ mutant reflected in catalase activity.....	49
Figure 20. Phylogenetic tree showing amino acid homology of various aminotransferases .....	52
Figure 21. Neighbor-joining phylogenetic tree of aspartate aminotransferases from different organisms .	54
Figure 22. Vector maps of pUC19::hsp- <i>aspB</i> and pUC19::hsp- <i>aspC</i> .....	57
Figure 23. Amino acid auxotroph DL39 has a lower cell density at stationary phase .....	59
Figure 24. Oxaloacetate inhibited growth of <i>E. coli</i> at 40mM and 80mM .....	60
Figure 25. Expression vector maps for GST-tagged recombinant protein expression .....	62
Figure 26. Purification of AspB <sub>Mtb</sub> and AspC <sub>Mtb</sub> using GST affinity chromatography .....	63
Figure 27. Removal of GST-tag from recombinant protein GST-AspB <sub>Mtb</sub> .....	64
Figure 28. GST-AspC <sub>Mtb</sub> contain many putative secondary thrombin cleavage sites .....	66
Figure 29. Thrombin cleavage of GST-AspC <sub>Mtb</sub> .....	67
Figure 30. His-tagged AspB <sub>Mtb</sub> and AspC <sub>Mtb</sub> expression vectors.....	68
Figure 31. Purified AspB <sub>Mtb</sub> and His-tag removal .....	69
Figure 32. Purification of C-terminal His-tagged AspC <sub>Mtb</sub> .....	70
Figure 33. Schematic representation of the proposed antibiotic induced regulatory network of <i>whiB7</i> , <i>aspB</i> , and <i>aspC</i> .....	77

## List of abbreviations

<b>Abbreviation</b>	<b>Expanded</b>
ADC	albumin dextrose catalase
AES	allelic exchange substrate
AspAT	aspartate aminotransferase
AT	aminotransferase
BCA	bicinchoninic acid
cDNA	complementary deoxyribonucleic acid
cfu	colony forming unit
CLR	clarithromycin
DMSO	dimethyl sulfoxide
DNA	deoxyribonucleic acid
DTT	dithiothreitol
<i>Eco</i>	<i>Escherichia coli</i>
EDTA	ethylenediaminetetraacetic acid
GST	glutathione s-transferase
HEPES	4-(2-hydroxyethyl)-1-piperazineethanesulfonic acid
his	hexa-histidine
hsp / hsp60	heat shock promoter
INH	isoniazid
IPTG	isopropyl $\beta$ -D-1-thiogalactopyranoside
LB	Luria-Bertani
MDR	multidrug resistant
MIC	minimum inhibitory concentration
mRNA	messenger ribonucleic acid
<i>Msm</i>	<i>Mycobacterium smegmatis</i>
<i>Mtb</i>	<i>Mycobacterium tuberculosis</i>
MTT	[3-(4,5-dimethylthiazol-2-yl)-2,5-diphenyl tetrazolium bromide; thiazolyl blue
MWCO	molecular weight cut off
NAD <sup>+</sup>	nicotinamide adenine dinucleotide (oxidized form)
NADH	nicotinamide adenine dinucleotide (reduced form)
NADPH	nicotinamide adenine dinucleotide phosphate
OAA	oxaloacetate
OADC	oleic acid albumin dextrose catalase
PAGE	polyacrylamide gel electrophoresis
PB	Proskauer Beck
PBS	phosphate buffered saline
PCR	polymerase chain reaction
PEG	polyethylene glycol
PMSF	phenylmethanesulfonyl fluoride
qRT-PCR	quantitative real-time PCR
RNI	reactive nitrogen species

ROS	reactive oxygen species
SDS	sodium dodecyl sulfate
SPT	spectinomycin
TB	tuberculosis
TET	tetracycline
WT	wild-type
XDR	extensively drug resistant
YT	yeast extract tryptone
$\alpha$ KG	alpha ketoglutarate

## **Acknowledgments**

I wish to offer my deepest gratitude to Dr. Charles Thompson for giving me this opportunity to do a graduate project under his supervision, and whose guidance and support enabled me to explore and expand my abilities.

I would like to thank my committee members, Dr. William Mohn and Dr. Lindsay Eltis for their counsel and support.

I wish to acknowledge the generosity of the Hallam, Eltis, Mohn, and Murphy labs for the use of their equipment.

Special thanks to Dr. Santiago Ramón-García who first started me out on this project and for continual enthusiasm and input into this research. I would like to also express my sincere gratitude towards Dr. Gaye Sweet for invaluable guidance throughout this program and for critical reading of this thesis.

It was an honour and pleasure to work alongside my lab mates in the Thompson lab both past and present, especially Leah Lim and Jan Burian, their friendship and lively discussions was what created such a positive work environment.

Above all, I owe a great debt of gratitude to my family and friends whose infinite support is from where I drew the courage to pursue my passion in research. Profound thanks go to my parents for their unfailing love and support throughout the pursuit of this degree. Words cannot express how much their support has meant throughout my life, especially now.

The research project was funded in part by a Graduate Entrance Scholarship from the University of British Columbia. Additional funding was provided by CIHR and Lung Association grants awarded to Dr. Charles Thompson.

## 1. Introduction

### 1. 1. *Mycobacterium tuberculosis* and antibiotic resistance

The acid-fast bacterium *M. tuberculosis* is the causative agent of tuberculosis. Tuberculosis remains one of the top infectious causes of mortality, with 8.8 million incident cases and 1.4 million deaths worldwide in 2010 [1]. The current treatment for tuberculosis is a combination of four antibiotics administered over a course of 6 months. Noncompliance or abandonment of treatment is the major impediment to effective therapy due to the long and sometimes unpleasant regimen required to cure tuberculosis. This further contributes to the emergence of drug resistant mutants. The development of drug-resistance is a growing problem for tuberculosis control. Multidrug-resistant TB (MDR-TB) and extensively drug-resistant TB (XDR-TB) are forms of tuberculosis that are even more difficult and expensive to treat because they fail to respond to standard first- and second-line therapy [2,3]. There are an estimated 290,000 cases of MDR-TB in 2010 making antibiotic resistant tuberculosis a global health concern [1].

Acquired drug resistance to the two most powerful front-line antibiotics used to treat tuberculosis, isoniazid and rifampicin, is on the rise. In 1994, mono resistance to isoniazid and rifampicin was found at a rate of 4.1% and 0.2% respectively [4]. In a 2012 report, the frequency of these resistances had increased to 9.3% and 0.3% [5]. To further hinder treatment, mycobacteria have high intrinsic resistance to most naturally occurring antibiotics, including many commonly-used broad-spectrum drugs. In contrast to acquired drug resistance, which occurs via random mutation or horizontal gene transfer, intrinsic resistance is the natural resistance of the bacterial species and is typically chromosomally encoded. The intrinsic resistance of mycobacteria has conventionally been attributed to the mycolic acid-containing cell envelope as it may serve as a barrier to antibiotic entry by diffusion [6]. In addition to decreased permeability of the bacterial envelope, the *M. tuberculosis* chromosome contains intrinsic resistance genes that encode efflux pumps [7] [8],  $\beta$ -lactamases [9] [10], and ribosome methyltransferases [11] [12]. Clearly, *M. tuberculosis* has evolved many mechanisms to counteract the actions of antibiotics.

Mutations conferring antibiotic resistance in *M. tuberculosis* are often found associated with a cost which reduces the fitness of the bacterium [13] [14]. Furthermore, physiological state and growth rate of the bacteria can also influence antibiotic susceptibility [15,16]. Intrinsic resistance mechanisms of *M. tuberculosis* would appear to have strong links to the general physiology of the bacterium.

## 1. 2. The WhiB family of proteins

WhiB homologues are highly conserved throughout the Actinomycetales order with most species containing multiple orthologs [17]. WhiB proteins are small (87 to 130 amino acid residues), putative transcription factors with conserved structural characteristics such as a glycine-rich helix-turn-helix motif that could interact with RNA polymerase. WhiB proteins also possess four near-invariant cysteine residues arranged as C-X<sub>19-36</sub>-C-X-X-C-X<sub>5-7</sub>-C which may act as ligands for a metal cofactor and are predicted to have a role in sensing redox change [18].

WhiB proteins have been implicated in a variety of functions from sporulation in *Streptomyces coelicolor* [17] to oxidative stress in *Corynebacterium glutamicum* [19]. The *M. tuberculosis* genome has seven annotated *whiB* genes implicated in a variety of physiological processes including cell division, pathogenesis, starvation and detection of stress conditions [20]. All *M. tuberculosis* WhiB proteins, except for WhiB2, have disulfide reductase activity [20]. While these assays typically are based on reduction of insulin, WhiB1 can catalyze reduction of at least one *M. tuberculosis* protein [20]. WhiB1 acts in a thioredoxin-like manner to reduce GlgB, a mycobacterial enzyme important in carbohydrate metabolism [21]. WhiB2 regulates expression of genes that are involved in cell division [22]. WhiB3 controls fatty acid metabolism [23]. The seven *M. tuberculosis whiB* genes were differentially expressed during different growth phases and in response to environmental stresses such as pH, nutrient starvation, antibiotic assault, and oxidative stress [24,25] [26]. Experimental evidence has shown that both WhiB1 and WhiB3 coordinate redox-sensitive Fe-S clusters that are sensitive to oxygen and nitric oxide [27] [28]. In general, WhiB proteins are used by *M. tuberculosis* to coordinate specific expression of proteins that the bacterium requires for survival under unfavourable conditions.

The transcriptional regulator WhiB7 has a central role in regulation of intrinsic multidrug resistance [29]. WhiB7 controls expression of antibiotic resistance genes including *tap* (Rv1258c), an efflux transporter, *erm*, a methyltransferase (Rv1988), and *eis* (Rv2416c), an aminoglycoside acetyltransferase [29]. The efflux pump Tap confers tetracycline resistance by extruding the antibiotic from the cell [30,31]. *ermMT* encodes a methyltransferase which causes methylation of 23S rRNA leading to resistance against macrolides [11]. The gene *eis*, initially named for enhanced intracellular survival in macrophages [32], confers kanamycin resistance by acetylating the antibiotic as well as host signalling molecules resulting in suppression of host immune responses [33] [34]. Deletion of *whiB7* in *M. tuberculosis*, *M. smegmatis*, or *M. bovis* BCG renders the strain sensitive to a broad spectrum of antibiotics such as macrolides, rifampicin, streptomycin, tetracycline and chloramphenicol [29]. The expression of *whiB7* is induced by antibiotics, fatty acids, redox-modifying compounds, and immediately after entry to macrophages [29] [35,36]. The *M. smegmatis whiB7* mutant is deficient in mycothiol, the major low-molecular-weight thiol produced by mycobacteria, linking *whiB7* to redox homeostasis [35]. These results suggest that WhiB7 links bacterial physiology and redox homeostasis to intrinsic antibiotic resistance.

### 1. 3. Oxidative stress and tuberculosis pathogenesis

The success of *M. tuberculosis* as an intracellular pathogen depends on its survival within host macrophages. The macrophage creates a highly oxidative environment by producing reactive oxygen species (ROS) [37] [38] in response to infection. To survive the exposure to exogenous, host-derived oxidative stress, *M. tuberculosis* must employ strategies to sense and respond to changes in its microenvironment. WhiB proteins have been implicated in this process. WhiB1, WhiB2, and WhiB3 transcription activators differentially bound to DNA sequences in promoters depending on its redox state [27] [39] [40]. Similarly, the activity of WhiB7 was strongly induced by a more reduced cytoplasmic environment [35]. These sensors allow *M. tuberculosis* to detect oxidative stress and make the appropriate response, such as expression of detoxifying factors and modulating cellular metabolism, to promote survival inside the host.

In order to survive within macrophages, *M. tuberculosis* must withstand the toxicity of ROS produced by phagocyte NADPH oxidase (NOX2/gp91<sup>phox</sup>) [41]. Activated macrophages generate superoxide molecules and other ROS by transporting electrons across the plasma membrane from cytosolic NADPH to molecular oxygen [42]. The thick, mycolic acid-containing cell wall of *M. tuberculosis* limits diffusion of toxic molecules but the bacteria also contain an arsenal of mechanisms to detoxify ROIs before they can cause damage to the bacteria. To counteract the deleterious effects of ROS such as superoxides and hydroxyl radicals, *M. tuberculosis* requires superoxide dismutase (SOD) and catalase to convert the ROS to water and molecular oxygen. The *M. tuberculosis* genome contains two SODs: *sodA* and *sodC*. The function of catalase in *M. tuberculosis* is performed by a single enzyme, KatG, which functions in two other capacities: peroxidase and peroxyntirite [43] [44] [45]. AhpCD, another oxidative stress detoxifier, encode alkyl hydroperoxidases to neutralize the alkyl hydroperoxides generated by the reaction between lipids and superoxides and is required for survival in macrophages [46,47,48,49]. SodC is localized to the mycobacterial cell envelope [50] and is essential to resistance against the initial oxidative burst generated by IFN $\gamma$ -activated macrophages [51]. *sodA* and *katG* are required for growth of *M. tuberculosis in vitro* [52] and appear to be important during mouse infections. SodA and KatG are exported by the SecA2 virulence secretion system; *M. tuberculosis*  $\Delta$ *secA2* is unable to grow in non-activated macrophages and showed reduced growth in mice due to the bacteria being defective in SodA and KatG export [53,54]. KatG confers protection against both hydrogen peroxide [55] [56] and peroxyntirite [45]. The *M. tuberculosis katG* mutant was attenuated in wild-type mice but virulent in mice lacking NOX2 [41]. While more research is required for better understanding of the mechanisms of ROS detoxification in *M. tuberculosis*, their detoxification genes are needed for virulence.

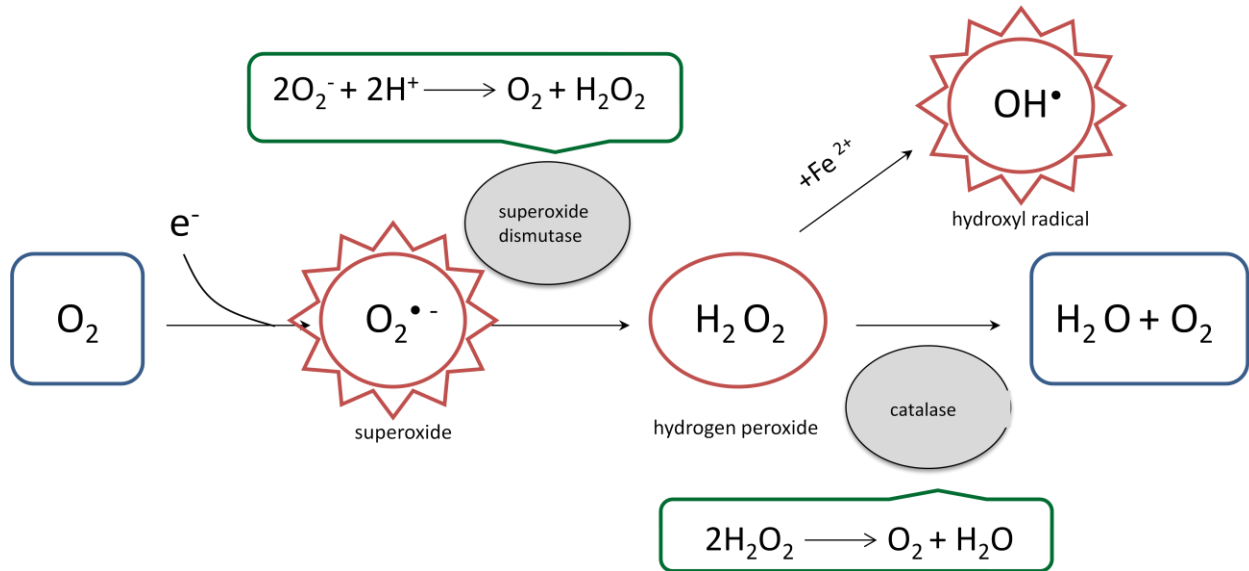


Figure 1. Detoxification of reactive oxygen species. Organisms that grow aerobically and pathogens that encounter immune cells in the host are routinely exposed to oxidative stress in the form of reactive oxygen species (ROS) such as oxygen radicals, hydrogen peroxide, and hydroxyl radicals. Detoxification enzymes, SodA and SodC, convert oxygen radicals to hydrogen peroxide. Hydrogen peroxide can react to form hydroxyl radicals through Fenton's reaction, requiring the catalase activity of KatG to degrade hydrogen peroxide to water and molecular oxygen.

#### 1. 4. Physiological changes induced by antibiotics

Antibiotics and their antibacterial activities are rigorously studied for their potential use as therapeutics. Traditionally it is thought that antibiotics cause growth inhibition by a singular cellular target within systems such as DNA replication or repair, protein synthesis, or cell wall turnover. However, global expression studies have revealed that changes in expression profiles induced by subinhibitory concentrations of antibiotics can be diverse and some are within genes not related to the target function [57] [58] [59] [60] [61] [62]. In mycobacteria, inactivation of one of a number of genes with roles in physiology and metabolism leads to a multidrug sensitive phenotype; *mmpA*, a porin protein [63], *fbpA*, a cell wall biosynthesis gene [6], *pknG*, a serine/threonine kinase related to glutamine/glutamate metabolism [64,65] and *asnB*, an asparagine synthetase [66]. The fact that these genes with physiological roles in transport, metabolism, or cell envelope functions are activated in response to antibiotic exposure implicates physiology of the bacterium to play a role in antibiotic resistance.

The redox-responsive transcription regulator WhiB7 is a central regulator of intrinsic resistance. In addition to induction of expression by antibiotics, the activation of *whiB7* is triggered by small molecules that are known to perturb respiration, redox balance and transmembrane ion flux [35]. Furthermore, the expression of *whiB7* is highly dependent on the reducing potential in the cytoplasm and on the main mycobacterial thiol antioxidant, mycothiol [35], placing this transcription regulator at the junction between redox homeostasis and antibiotic resistance. Indeed, antibiotics have been shown to cause both oxidative [67] [68] and reductive stress [69]. A large body of work by the Collins lab indicates that bactericidal antibiotics instigate the production of hydroxyl radicals produced from hydrogen peroxide via Fenton's reaction and cause bacterial cell death via oxidative damage [67] [70] [71]. Many bacteria produce catalases and peroxidases to scavenge hydrogen peroxide and protect themselves from reactive oxygen species. *E. coli* and many other bacteria rely on the action of alkylhydroperoxide reductase (Ahp), a NAD(P)H peroxidase, for the detoxification of hydrogen peroxide [72] [73]. The action of Ahp, like other antioxidation systems, involves the transfer of electrons between pools of NAD(P)H, FADH, and thiol redox compounds (Burian, J, 2012, in review). Mycothiol and other thiol-reducing agents require reducing power in order to eliminate the oxidative stress. Therefore, the cytoplasmic redox potential of mycobacteria is kept reduced in order to maintain a pool of thiols in preparation for any oxidoreductive stress brought on by the host immune system [46].

During infection, the cytoplasmic redox potential of *M. tuberculosis* is highly reduced. This redox imbalance is likely generated through metabolic pathways such as hypoxia, inhibition of respiration by nitric oxide, and  $\beta$ -oxidation of lipids [74], pathways which are upregulated in *M. tuberculosis* during infection. These processes all generate a high NADH/NAD<sup>+</sup> ratio making the regeneration of NAD<sup>+</sup> important for redox homeostasis and survival of the bacilli [75] [76]. A role for redox imbalance has also been implicated in the mechanism of antibiotic action. In contrast to the traditional thought that antibiotics act on a single target, a proposed mechanism by Kohanski, Collins and coworkers points to an

additional underlying mechanism in which bactericidal antibiotics cause oxidative stress and bacterial death is brought on by the toxic accumulation of reactive oxygen species [67,71,77]. While hydrogen peroxide cannot directly oxidize DNA, it can react very rapidly with transition metals. Hydroxyl radicals are generated through reaction of hydrogen peroxide with ferrous iron via Fenton's reaction (Figure 2 reaction 1). Hydroxyl radicals are powerful oxidants and react with the base or sugar residues of DNA, resulting in base modification and DNA breakage (Figure 1 reaction 2). The ferric iron can be reduced back to ferrous state by a reductant and the reaction cycles to generate more hydroxyl radicals (Figure 1 reaction 3)[78] [79] [80]. The tricarboxylic acid (TCA) cycle is a source of the reductant NADH and TCA cycle mutants were less susceptible to bactericidal drugs [67]. The results which led to this proposed pathway were derived from *E. coli* experiments but similar results have been observed with *Staphylococcus* [67], *Pseudomonas* [80], *Listeria* [81], *Leishmania* [82], and *Acinetobacter* [83] suggesting that this phenomenon may extend to all bacteria (and protozoans) and perhaps even *Mycobacterium*. The poorly understood but significant role of redox homeostasis and antioxidation in *M. tuberculosis* resistance could prove to be a good target candidate for tuberculosis therapy and deserves additional study.

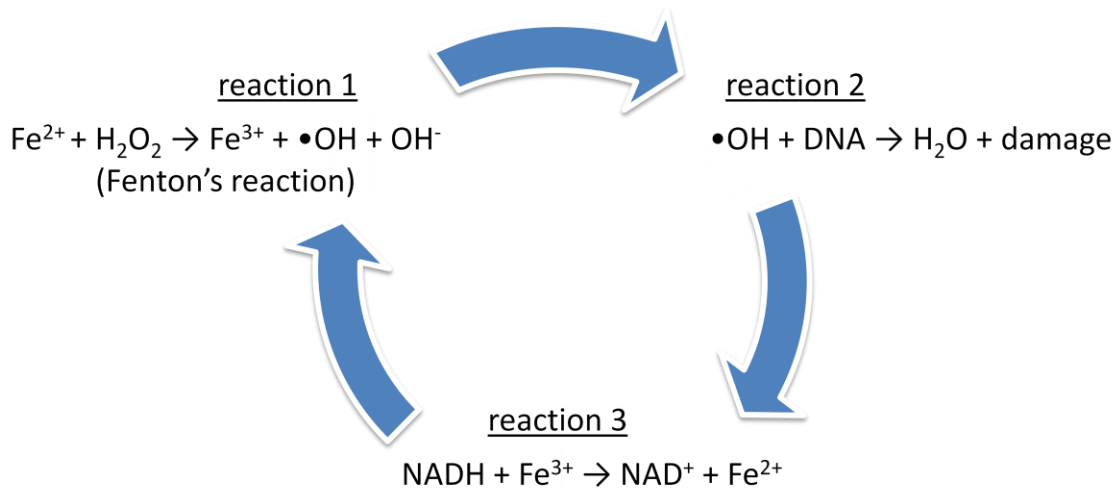


Figure 2. Oxidative damage via Fenton's reaction occurs in 3 steps. Hydroxyl radicals are formed through reactions with hydrogen peroxide and free iron. Radicals cause DNA damage and mutagenesis. Iron II is regenerated by a reducing agent (NADH).

## 1. 5. Mycobacterial amino acid aminotransferases

Bacteria encode enzymes for the synthesis of all twenty amino acids required for protein synthesis [84]. Pyridoxal 5'-phosphate-dependent transaminase performs the final biosynthetic step in these pathways, converting keto acid precursors into  $\alpha$ -amino acids. In the hopes of identifying inhibitors of aminotransferases for target-based tuberculosis drug development, the structures of several aminotransferases of *M. tuberculosis* have been solved, including phosphoserine aminotransferase (SerC, Rv0884c) [85], histidinol phosphate aminotransferase (HisC2, Rv3772) [86] and branched-chain amino acid aminotransferase (IlvE, Rv2210c) [87]. There are two putative aspartate aminotransferases annotated in *M. tuberculosis* genome, *aspB* (Rv3565) and *aspC* (Rv0337c). The transamination reaction of aspartate serves as a link between amino acid and carbon metabolism. Aspartate aminotransferases form aspartate from oxaloacetate, an intermediate of the TCA cycle, via a transamination reaction with glutamate. Aspartate can then act as an intermediate for the biosynthesis of other amino acids such as asparagine, threonine, isoleucine, methionine, and lysine [88]. Furthermore, aspartate is required in central physiological pathways such as pyrimidine ribonucleotide, purine nucleotide and nicotinamide dinucleotide biosynthesis [88]. Aspartate aminotransferases catalyze the reversible reaction of transamination between a dicarboxylic  $\alpha$ -amino acid and the corresponding  $\alpha$ -keto-acids by a ping-pong bi-bi mechanism with pyridoxal 5'-phosphate (PLP) as a cofactor [89].

The *M. tuberculosis* genome contains a large conserved gene cluster involved in cholesterol catabolism as a carbon source during infection [90]. The expression of genes for growth of *M. tuberculosis* on lipids such as cholesterol is controlled by two TetR- type regulators, KstR (Rv3574) and KstR2 (Rv3557c) [91,92]. *aspB* belongs to a regulon controlled by the transcriptional repressor KstR2 [92]. Deletion of KstR2 in *M. smegmatis* de-repressed genes in the regulon including *aspB*, resulting in increased expression [92]. *aspB* is located on the *M. tuberculosis* genome within an operon that includes fatty acid CoA ligase and acyl-CoA dehydrogenases [92]. KstR2 control the expression of genes required for utilizing cholesterol as a carbon source during infection is implicated [91]. The *aspC* gene does not appear to be part of any operon. *aspC* was identified as being required for growth *in vitro* [93].

## 1. 6. Project rationale

Expression of both *aspB* (Rv3565) and *aspC* (Rv0337c) genes were dependent on WhiB7 in a microarray experiment (unpublished data, Thompson Lab). When *whiB7* was expressed, both by antibiotic induction and from a plasmid promoter, the expression of *aspB* was downregulated. Conversely, the expression of *aspC* was upregulated along with *whiB7* expression. As putative aspartate aminotransferases, AspB and AspC have predicted functions in amino acid intermediary metabolism. That *aspB* and *aspC* were in the WhiB7 regulon strongly suggested that they could contribute to antibiotic resistance in Mycobacteria. WhiB7 responds to changes to cell metabolism by sensing and responding to changes in cytoplasmic redox potential. Based on the observation that WhiB7 responds to redox stress and controls expression of metabolic genes such as *aspB* and *aspC*, we hypothesized that mycobacterial intermediary metabolism plays a role in the WhiB7-controlled antibiotic resistance system mediated through AspB and AspC.

## 2. Materials and methods

Table 1. Plasmids and strains used in this study.

Plasmid/Strain	Relevant features	References
pMV361	Single-copy, L5 integration-proficient mycobacterial expression vector containing kanamycin resistance, integrase gene, and the hsp60 promoter upstream of a multiple cloning site	[94]
pMV361:: <i>aspB</i>	pMV361 expressing <i>aspB</i> (Rv3565) from hsp60	
pMV361:: <i>aspC</i>	pMV361 expressing <i>aspC</i> (Rv0337c) from hsp60	
pMV361:: <i>whiB7</i> <sub>Mtb</sub>	pMV361 expressing <i>whiB7</i> (Rv3197a) from hsp60	
pMV361:: <i>whiB7</i> <sub>Msm</sub>	pMV361 expressing <i>whiB7</i> (MSMEG_1953) from hsp60	
p004S-AES <i>aspB</i>	plasmid containing AES for <i>aspB</i> <sub>Msm</sub> deletion	
pYUB854-AES <i>aspC</i>	plasmid containing AES for <i>aspC</i> <sub>Msm</sub> deletion	
pJV53	acetamide inducible expression of the Che9c recombination genes	[95]
pYUB870	for transient expression of $\gamma\delta$ –resolvase	[96]
pGEX4T-1:: <i>aspB</i>	pGEX4T-1 (GE) cloned with <i>aspB</i> for GST-tagged AspB expression	
pGEX4T-1:: <i>aspC</i>	pGEX4T-1 (GE) cloned with <i>aspC</i> for GST-tagged AspC expression	
pET19b:: <i>aspB</i>	pET19b (Novagen) cloned with <i>aspB</i> for His-tagged AspB expression	
pET30b:: <i>aspC</i>	pET30b (Novagen) cloned with <i>aspC</i> for His-tagged AspC expression	
pET19b:: <i>aspC</i>	pET19b (Novagen) cloned with <i>aspC</i> for His-tagged AspB expression	
pET30b:: <i>aspC1</i>	pET30b (Novagen) cloned with <i>aspC</i> for tag free AspC expression	
pGro7, pTf-2, pG-KJE8, pTf16	expression of chaperone proteins GroEL, GroES, GrpE, Tf, DnaJK	Takara Bio
pYUB1062	acetamide inducible protein expression vector expression in mycobacteria	[97]
pYUB1062:: <i>aspC</i>	pYUB1062 cloned with <i>aspC</i> expression in mc <sup>2</sup> 4517	
pUC19:: <i>hsp-aspB</i> <sub>Mtb</sub>	expression of <i>aspB</i> from hsp60 promoter in <i>E. coli</i>	
pUC19:: <i>hsp-aspC</i> <sub>Mtb</sub>	expression of <i>aspC</i> from hsp60 promoter in <i>E. coli</i>	
<i>E. coli</i> TOP 10	general cloning	
<i>E. coli</i> Rosetta™ 2	protein expression. pRARE2 expresses tRNAs for rare codons	
<i>E. coli</i> BL21	protein expression	
<i>E. coli</i> BL21 (DE3)	protein expression. $\lambda$ DE3 expresses T7 RNA polymerase	
mc <sup>2</sup> 4517	mycobacteria strain for T7-based expression	[97]
mc <sup>2</sup> 155	wild-type <i>M. smegmatis</i>	
mc <sup>2</sup> 155 $\Delta$ <i>whiB7</i>	$\Delta$ <i>whiB7</i> mutant	
mc <sup>2</sup> 155 $\Delta$ <i>aspB</i>	$\Delta$ <i>aspB</i> mutant	
mc <sup>2</sup> 155 $\Delta$ <i>aspC</i>	$\Delta$ <i>aspC</i> mutant	

mc <sup>2</sup> 155 $\Delta aspB \Delta aspC$	$\Delta aspB \Delta aspC$ double mutant	
mc <sup>2</sup> 155 pMV361	wild-type vector control	
mc <sup>2</sup> 155 pMV361:: <i>aspB</i>	constitutive <i>aspB</i> <sub>Mtb</sub> expression	
mc <sup>2</sup> 155 pMV361:: <i>aspC</i>	constitutive <i>aspC</i> <sub>Mtb</sub> expression	
mc <sup>2</sup> 155 pMV361:: <i>whiB7</i> <sub>Mtb</sub>	constitutive <i>whiB7</i> <sub>Mtb</sub> expression	
mc <sup>2</sup> 155 pMV361:: <i>whiB7</i> <sub>Msm</sub>	constitutive <i>whiB7</i> <sub>Msm</sub> expression	
$\Delta aspC$ pMV361:: <i>aspC</i> <sub>Mtb</sub>	mutant $\Delta aspC$ with constitutive expression of <i>aspC</i> <sub>Mtb</sub>	
DL39	<i>E. coli</i> mutant in <i>aspC</i> , <i>tyrB</i> , and <i>ilvE</i> ; auxotrophic for Val, Leu, Ile, Tyr, Phe, Asp	[98]
MG1655	wild-type laboratory strain of <i>E. coli</i> K-12	
DL39 pUC19	DL39 vector control	
DL39 pUC19:: <i>hsp-aspB</i> <sub>Mtb</sub>	DL39 that constitutively expresses <i>aspB</i> <sub>Mtb</sub>	
DL39 pUC19:: <i>hsp-aspC</i> <sub>Mtb</sub>	DL39 that constitutively expresses <i>aspC</i> <sub>Mtb</sub>	

Table 2. Primers used in this study

Primer	Sequence (restriction site)	Purpose
BOO-13	TTTCGAATTCGTGACGGATCGTGTC (EcoRI)	aspB <sub>Mtb</sub> forward primer
BOO-14	GCAAAGCTTCTATTGGCTCGGCAG (HindIII)	aspB <sub>Mtb</sub> reverse primer
BOO-15	AGGGAATTCGTGGACAACGATGGC (EcoRI)	aspC <sub>Mtb</sub> forward primer
BOO-16	TAGAAGCTTCTATTGCCGTAAC TG (HindIII)	aspC <sub>Mtb</sub> reverse primer
BOO-30	CCATGAATTCATGACTGCTCCGACCACGG (EcoRI)	whiB7 <sub>Msm</sub> forward primer
BOO-31	AAATAAGCTTGATCAGGCGGCGGC (HindIII)	whiB7 <sub>Msm</sub> reverse primer
BOO-32	GATATAGAATTCGTGTCGGTACTGACAGTCCCC (EcoRI)	whiB7 <sub>Mtb</sub> forward primer
BOO-33	TAGAAAGCTTCTATGCAACAGCATCCTTGC-3' (HindIII)	whiB7 <sub>Mtb</sub> reverse primer
BOO-34	TTTTTTTTCCATAAATTGGCGTTGTTGTTGCTGCGGG (PflMI)	AES for Msmeg_6017 ( <i>aspB<sub>Msm</sub></i> )
BOO-42	TTTTTTTTCCATTTCTTGGGCGGTCGTTTCATCTCACCC (PflMI)	AES for Msmeg_6017 ( <i>aspB<sub>Msm</sub></i> )
BOO-36	TTTTTTTTCCATAGATTGGCGTGCGAGGCAACTCCTATG(PflMI)	AES for Msmeg_6017 ( <i>aspB<sub>Msm</sub></i> )
BOO-43	TTTTTTTTCCATCTTTTGGCCAACGACCGTTCCTGTC (PflMI)	AES for Msmeg_6017 ( <i>aspB<sub>Msm</sub></i> )
BOO-61	TTTTTTCTTAAGAAGCCCGCAGCCACAGAGG (AflII)	AES for Msmeg_0688 ( <i>aspC<sub>Msm</sub></i> )
BOO-62	TTTTTTCTAGATCGTGGACTGGGTGAACGTG (XbaI)	AES for Msmeg_0688 ( <i>aspC<sub>Msm</sub></i> )
BOO-63	TTTTTTAGATCTCCCAGGTGTACGACATCCAC (BglII)	AES for Msmeg_0688 ( <i>aspC<sub>Msm</sub></i> )
BOO-64	TTTTTTACTAGTGCCGTGGTCGCAACCTTTC (SpeI)	AES for Msmeg_0688 ( <i>aspC<sub>Msm</sub></i> )
BOO-103	GACCCGGCGCCAAGAAGACC	forward primer upstream of <i>aspC</i>
BOO-105	CCGCGAAGGTCAGGCACGTC	reverse primer downstream of <i>aspC</i>
BOO-119	CCGTGACCCACGCGCAAG	forward primer upstream of <i>aspB</i>
BOO-120	GACGTTGCGGACGCGGTCC	reverse primer downstream of <i>aspB</i>
BOO-92	ACGTTCTCGGTGGTGTGCG	reverse primer for <i>hyg</i>
BOO-104	CACCGATCCGAGGAACTGGC	Hyg down (fw)
prAB49	CCAAAAACCATCTGCTGGAG	mysA <sub>Msm</sub> forward primer for qRT-PCR
prAB50	AGGTTGCCTTCTGGATGAG	mysA <sub>Msm</sub> reverse primer for qRT-PCR
prAB47a	TCCATTGCGATGACTGCTC	whiB7 <sub>Msm</sub> forward primer for qRT-PCR
prAB48	GTTCTCGGCGAACCACAG	whiB7 <sub>Msm</sub> reverse primer for qRT-PCR
prAspB_fw	GGGTCTGCTGACGCACTAC	aspB <sub>Msm</sub> forward primer for qRT-PCR
prAspB_rv	CAGCGAGTTGTGCGGTGTA CT	aspB <sub>Msm</sub> reverse primer for qRT-PCR
prAspC_fw	ATCCCGGCACCCGACTACCC	aspC <sub>Msm</sub> forward primer for qRT-PCR
prAspC_rv	CCACGATCGCCTTGGTGC GT	aspC <sub>Msm</sub> reverse primer for qRT-PCR
BOO-78	TTTTGGATCCGT GAC GGA TCG TGT CGC (BamHI)	aspB <sub>Mtb</sub> forward primer
BOO-79	TTTTGAATTCCTA TTG GCT CGG CAGC (EcoRI)	aspB <sub>Mtb</sub> reverse primer
BOO-80	TTTTGGATCCGTG GAC AAC GAT GGC ACCATTG (BamHI)	aspC <sub>Mtb</sub> forward primer

BOO-81	TTTTGAATTCCTA TTG CCG GTA ACT GACCAGGAAG (EcoRI)	aspC <sub>Mtb</sub> reverse primer
BOO-106	TTTTCATATG GT GAC GGA TCG TGT CGC (NdeI)	aspB <sub>Mtb</sub> forward primer
BOO-107	TTTTGGATCC CTA TTG GCT CGG CAGC (BamHI)	aspB <sub>Mtb</sub> reverse primer
BOO-108	TTTTCATATG GTG GAC AAC GAT GGC ACCATTG (NdeI)	aspC <sub>Mtb</sub> forward primer
BOO-109	TTTTGGATCC CTA TTG CCG GTA ACT GACCAGGAAG (BamHI)	aspC <sub>Mtb</sub> reverse primer
BOO-110	TTTT GGTACC TTG CCG GTA ACT GACCAGGAAG (KpnI) mutated stop codon	aspC <sub>Mtb</sub> reverse primer

## 2. 1. Cloning and reagents

*E. coli* TOP 10 (Invitrogen) was used for general cloning procedures. Media components were purchased from Difco. All DNA primers were synthesized by Integrated DNA Technologies, Inc. All PCRs were performed using Dynazyme EXT polymerase (New England Biolabs) according to the manufacturer's protocol with buffer sometimes supplemented with 5% (v/v) DMSO. Restriction enzymes, purchased from New England Biolabs and Rapid DNA Dephos & Ligation Kit from Roche Applied Bioscience, were used in all molecular cloning protocols following standard recombinant DNA techniques. Plasmids pET19b and pET30b were purchased from Novagen. Plasmid DNA pGEX4T-1 was purchased from GE Healthcare. Fine chemicals were acquired from Sigma unless otherwise indicated. Strains, plasmids, and oligonucleotides used are summarized in Tables 1 and 2.

## 2. 2. Growth conditions

The bacterial strains used are listed in Table 1. *E. coli* strains were grown in LB medium at 37°C with shaking. Antibiotics (ampicillin 100 µg/ml, kanamycin 300 µg/ml, chloramphenicol 34 µg/ml) were added to the medium when necessary. *M. smegmatis* mc<sup>2</sup>155 strains and its derived mutants were routinely grown in Middlebrook 7H9 broth (Difco) supplemented with 0.05% tyloxapol, 0.2% glycerol, and 10% albumin-dextrose-catalase (ADC; Difco) or on Middlebrook 7H10 agar (Difco) supplemented with 0.5% glycerol, and 10% oleic acid-albumin-dextrose-catalase (OADC; Difco). Cultures were aerated using an orbital shaker at 200 rpm or culture roller drum at level 5. For experiments investigating nutritional growth requirements of *M. smegmatis*, Proskauer Beck (PB) medium was used (36.7 mM KH<sub>2</sub>PO<sub>4</sub>, 37.8 mM NH<sub>4</sub>Cl, 2.4 mM MgSO<sub>4</sub>•7H<sub>2</sub>O, 11.6 mM magnesium citrate, 2% v/v glycerol). 0.05% tyloxapol (v/v) was added to 7H9 and PB medium to promote dispersed growth except in the case with drug susceptibility testing using alamar blue or MTT assay in microwells. Minimal media 56/2 (Glucose, 0.3%; KH<sub>2</sub>PO<sub>4</sub>, 0.5 g/L; Na<sub>2</sub>HPO<sub>4</sub>, 0.93 g/L; (NH<sub>4</sub>)<sub>2</sub>SO<sub>4</sub>, 0.2 g/L; tri-sodium citrate 0.14 g/L; MgSO<sub>4</sub>•7H<sub>2</sub>O, 20 mg/L; FeSO<sub>4</sub>•7H<sub>2</sub>O, 2.5 mg/L; Ca(NO<sub>3</sub>)<sub>2</sub>•4H<sub>2</sub>O, 0.7 mg/L; amino acids 50 µg/ml; 1.5% agar, pH 7.6) was used as the minimal medium for *E. coli* nutritional requirement studies[99].

## 2. 3. Constitutive expression strain construction

Strains that constitutively express *M. smegmatis* *whiB7* (MSMEG\_1953), *M. tuberculosis* *whiB7* (Rv3197a), *aspB* (Rv3565) and *aspC* (Rv0337c) in *M. smegmatis* were generated by cloning into the integrative vector pMV361 that drives expression from a heat-shock promoter (hsp60). The genes were amplified from *M. tuberculosis* H37Rv or *M. smegmatis* mc<sup>2</sup> 155 genomic DNA (for primers refer to Table 2) with engineered EcoR1 and HindIII restriction sites (*whiB7*<sub>Msmv</sub> BOO-30 and BOO-31; *whiB7*<sub>Mtb</sub> BOO-32

and BOO-33; *aspB*, BOO-13 and BOO-14; *aspC*, BOO-15 and BOO16). The PCR fragments were digested and cloned into pMV361 digested with EcoR1 and HindIII. The cloned vectors were transformed into mc<sup>2</sup>155 to create hsp promoter-driven constitutive expression strains (hsp-*whiB7*<sub>Mtb</sub>, hsp-*aspB*<sub>Mtb</sub> and hsp-*aspC*<sub>Mtb</sub>).

## 2. 4. Mutant construction

Knockout strains of *aspB*<sub>Msm</sub> (MSMEG\_6017) and *aspC*<sub>Msm</sub> (MSMEG\_0688) in *M. smegmatis* mc<sup>2</sup>155 were generated by allele exchange using recombineering technique [95]. The allelic exchange substrate (AES) for *aspC*<sub>Msm</sub> deletion was prepared by amplifying the upstream and downstream flanking regions and cloning them on either side of the hygromycin-resistant gene in the shuttle vector pYUB854. The upstream region was amplified from genomic DNA using primers BOO-61 and BOO-62 and cloned between AflII and XbaI sites in pYUB854. The downstream region was amplified with primers BOO-63 and BOO-64 and cloned between BglII and SpeI. The linear *aspC*<sub>Msm</sub> AES was removed from pYUB854 by AflII and SpeI digestion and electroporated into mc<sup>2</sup>155 expressing Che9c recombination genes from pJV53. Construction of the mc<sup>2</sup>155  $\Delta$ *aspB*<sub>Msm</sub> mutant was carried out following a similar strategy. The *aspB*<sub>Msm</sub> flanking regions were amplified from genomic DNA using primers BOO-34 and BOO-42 for the upstream region and BOO-36 and BOO-43 for the downstream region. A PflMI restriction enzyme site was engineered at the 5' end of each primer. The amplicons were digested with PflMI and cloned into PflMI-digested p0004s vector arms. P0004s is a delivery vector that contains lambda phage *cos* sites, a *hyg* resistance marker, and a *sacB* cassette (T. Hsu and W. R. Jacobs, Jr., unpublished data). The linearized *aspB*<sub>Msm</sub> AES was generated with BamHI digestion and electroporated into mc<sup>2</sup>155 expressing recombineering functions from pJV53. For deletion of both *aspB* and *aspC*, colonies resistant to hygromycin and kanamycin were screened for precise allele replacements by PCR using primers specific to the hygromycin cassette (BOO-92 and BOO-104) and primers outside the flanking sequences (BOO-119 and BOO-120 for *aspB* and BOO-103 and BOO-105 for *aspC*).

## 2. 5. Construction of double mutant $\Delta$ *aspB* $\Delta$ *aspC*

The double mutant was constructed by first removing the hygromycin resistance gene from the  $\Delta$ *aspB* single deletion mutant. The specialized *res-hyg-res* gene cassette employed to construct the *aspB* knockout mutant contains the specific DNA binding sites (*res*) for a site-specific  $\gamma\delta$  –resolvase, the product of the *tnpR* gene of *E. coli* transposon Tn1000, cloned under the expression control of mycobacterial promoter hsp60. Excision of the hygromycin resistance cassette was achieved by transient expression of the  $\gamma\delta$  –resolvase from the pYUB870 plasmid, with subsequent loss of the *sacB*-

expressing pYUB870 plasmid via negative selection via plating onto medium containing sucrose [96]. The second mutation,  $\Delta aspC$ , was introduced into the unmarked  $\Delta aspB$  mutant using the original hygromycin selection as in the construction of the single deletion mutant.

## 2. 6. Drug susceptibility testing

MTT and resazurin assays were used to determine whether expression of  $aspB_{Mtb}$  or  $aspC_{Mtb}$  or deletion of  $aspB_{Msm}$  or  $aspC_{Msm}$  affected the drug susceptibility of *M. smegmatis*. Stationary phase cultures were diluted to an  $A_{600\text{nm}}$  of 0.005 and added to microtiter plates containing 2-fold dilutions of antibiotics and incubated at 37°C for 48 hours. At 48 hours MTT reagent was added. Cultures were incubated at 37°C for 2 hours before addition of solubilising solution (10% SDS). For *E. coli*, cultures were seeded into the wells at  $OD_{600\text{nm}} = 0.001$  and incubated at 37°C for 6 hours. MTT reagent was added followed by incubation for 30 min at 37°C prior to addition of solubilisation solution. The absorbance at 570nm was measured to quantify the amount of purple formazan precipitate formed. The minimal inhibitory concentration (MIC) was set as the lowest concentration of antibiotic to give a reduction of more than 90% of  $OD_{570\text{nm}}$  reading of the untreated control MIC. For resazurin assay, the initial setup was essentially the same but the cultures were incubated for 24 hours before the addition of the resazurin reagent followed by an additional incubation of 24 hours at 37°C. A change from blue to pink indicated growth of bacteria, and the MIC was defined as the last concentration at which resazurin remained blue.

## 2. 7. Growth kinetics

*M. smegmatis* strains were seeded into the microtitre wells of honeycomb plates with antibiotics (for susceptibility testing) or intermediary metabolites (for nutritional growth requirement determination) and incubated in a Bioscreen C kinetic growth reader at 37 °C with constant shaking at maximum amplitude. Growth was monitored by the machine by measuring  $OD_{600\text{nm}}$ .

## 2. 8. Antibiotic kill curve

Time-kill curves were performed in shaken flask cultures in 7H9 media at 37°C. Wild-type and mutant  $\Delta aspC$  was inoculated to give a starting  $OD_{600\text{nm}}$  of 0.001 and grown to early exponential phase ( $OD_{600\text{nm}} = 0.5$ ) at which point a bactericidal concentration of clarithromycin was added at 15  $\mu\text{g}/\text{ml}$  (about 30 times MIC). Surviving bacteria were counted by cfu plating every 2 hours onto 7H10 (10% OADC). Colonies were counted after 48 h incubation at 37°C.

## 2. 9. RNA isolation

Total mRNA from *M. smegmatis* was isolated by a standard technique [100]. Briefly, *M. smegmatis* was grown to early exponential phase ( $OD_{600nm} = 0.4-0.6$ ). Some samples were treated with tetracycline at  $0.8 \mu\text{g/ml}$  (equivalent to four times the MIC for wild-type) for 1 hour at  $37^\circ\text{C}$ . Guanidine lysis buffer (5 M guanidine thiocyanate, 17 mM sodium lauroyl sarcosinate, 28.5 mM tri-sodium citrate, 0.5% (v/v) Tween 80, 0.7% (v/v) 2-mercaptoethanol) was added to the culture at a ratio of 4 to 1. Bacterial cells were then pelleted by centrifugation (4000 rpm for 15min at  $4^\circ\text{C}$ ) and disrupted in 1 ml of TRIzol reagent (Life Technologies) with 0.1 mm silica beads in a FastPrep-24 bead-beater (MP Biomedicals). Cell debris was removed by centrifugation at full speed in a microcentrifuge for 10 min and the lysate was extracted with an equal volume of chloroform/isoamyl alcohol 24:1. Total nucleic acid was precipitated using 30 mM sodium acetate in isopropyl alcohol. Nucleic acid samples were then treated for 30 min at  $37^\circ\text{C}$  with Turbo DNase (Ambion) and final RNA clean-up was done using RNA spin mini columns (GE Healthcare) according to the manufacturer's instructions.

## 2. 10. Quantitative real-time PCR

cDNA was synthesized from 250 ng of total mRNA using qScript cDNA Synthesis kit (Quanta Biosciences) as per manufacturer's instructions. Each 25- $\mu\text{l}$  reaction mixture included cDNA from 25 ng of RNA,  $1 \mu\text{M}$  of each primer pair, and Perfecta SYBR Green SuperMix (Quanta Biosciences). The reactions were monitored in a CFX96 real-time System (Bio-Rad Laboratories Inc.). Thermocycling parameters used were  $95^\circ\text{C}$  for 3 min, and 35 cycles of  $95^\circ\text{C}$  for 30 s,  $55^\circ\text{C}$  for 30 s,  $72^\circ\text{C}$  for 30 s. Amplification specificity was assessed by melting curve analyses. Oligonucleotides for amplification of *M. smegmatis* *whiB7*, *aspB* and *aspC* are listed in Table 2. The degrees of expression change were normalized to an internal control, *mysA*, using primers prAB49 and prAB50 and the significance of differential gene expression in each sample, relative to the non-treated wild-type control was calculated using the  $2^{-\Delta\Delta\text{Ct}}$  method. Analysis was performed on triplicate biological samples that were assayed in duplicate. Genomic DNA contamination was measured by real-time PCR of RNA not treated with reverse transcriptase and found to be insignificant.

## 2. 11. NAD-NADH pool isolation and NAD cycling assay

$\text{NAD}^+$  and NADH levels were measured by a sensitive cycling assay [101,102,103]. *M. smegmatis* strains were grown to early exponential phase ( $OD_{600nm} = 0.2-0.4$ ). Some cells were treated with tetracycline ( $0.8 \mu\text{g/ml}$ ) for 1 hour before extraction of  $\text{NAD}^+$  and NADH. Cells were pelleted by centrifugation and split in two for extraction with 0.2 M HCl (for  $\text{NAD}^+$  determination) or 0.2 M NaOH (for NADH

determination). The samples were incubated at 50°C for 10 min and then cooled on ice. The cell extracts were neutralized by adding an equal volume of 0.1 M NaOH (for NAD<sup>+</sup> determination) or 0.1 M HCl (for NADH determination). Cell debris was removed via centrifugation and the supernatant used in the cycling assay immediately.

In a microtiter plate, 10 µl of extract was added to 180 µl of reagent solution consisting of 110 mM Bicine buffer, pH 8.0, 11% (v/v) ethanol, 4.4 mM EDTA, pH 8.0, 0.47 mM MTT, and 3.7 mM phenazine ethosulfate. The assay was initiated by the addition of 10 µl alcohol dehydrogenase (1 mg/ml in 0.1 M Bicine buffer, pH 8.0) and the absorbance at 570nm was read at intervals of 20 seconds. The concentrations of NAD<sup>+</sup> and NADH in the extracts were extrapolated from a standard curve constructed using 0.01-0.05 mM solutions of NAD<sup>+</sup> or NADH. The change in absorbance ( $\Delta A_{570nm}/\text{min}$ ) reflects the concentration (mM) of NAD<sup>+</sup> or NADH in extracts. The final concentration of NAD<sup>+</sup> and NADH was expressed as micromolar per gram of dry weight of cells (µM/g). All determinations were based on triplicate biological experiments.

## **2. 12. Hydrogen peroxide and menadione disc assay**

Sensitivity to hydrogen peroxide was assessed by disc diffusion. Twenty ml of 7H9 agar [0.2% (v/v) glycerol and 1.5% (w/v) agar] were poured into standard 100 mm diameter petri plates. Plates were overlaid with 10 ml of 7H9 top agar [(0.2% (v/v) glycerol and 0.5% (w/v) agar] inoculated with stationary phase culture to 10<sup>5</sup> cfu/ml. Five µl of 30% hydrogen peroxide solution or 50 mM menadione was applied to a blank assay disc (6 mm diameter, BD) placed in the centre of the plate. Zones of inhibition were measured after incubation at 37°C for 48 hours.

## **2. 13. Preparation of cell lysate**

The catalase activity in whole cell lysate was determined in untreated and hydrogen peroxide treated cultures. Cultures were grown to exponential phase ( $OD_{600} = 0.5$ ) and subjected to 3.6 mM and 20 mM hydrogen peroxide treatment or PBS control for 1 hour at 37°C. Cells were harvested by centrifugation (5000 rpm for 25 min at 4°C) and the cell pellet was washed three times in dH<sub>2</sub>O and resuspended in 0.1 mM phenylmethylsulfonyl fluoride, 50 mM triethylamine (pH 7.8), concentrating the cells 200-fold. The cells were lysed with 0.1 mm silica beads in a FastPrep-24 bead-beater (MP Biomedicals). The glass beads and cell wall were pelleted by centrifugation at 10,000 X g for 30 min at 4°C. The supernatant was transferred to a fresh tube and its protein concentration was determined using Pierce Micro BCA Protein Assay Kit according to manufacturer's instructions.

## 2. 14. Catalase assay

The determination of catalase activity was based on an assay previously described by Beers and Sizer [104]. Briefly, 10  $\mu$ L of the lysate was added to 890  $\mu$ L of 100 mM potassium phosphate, pH7.0. 100  $\mu$ L of 100 mM H<sub>2</sub>O<sub>2</sub> was added and the decrease in absorbance at 250 nm was monitored for 2 min using a Varian Cary 5000 spectrophotometer. The linear part of the curve was used to quantitate the rate of H<sub>2</sub>O<sub>2</sub> removal using molar extinction coefficient  $\epsilon_{250}=16.69 \text{ M}^{-1}\text{cm}^{-1}$ . One unit of catalase was defined as the amount of lysate that catalysed the decomposition of 1  $\mu$ mol H<sub>2</sub>O<sub>2</sub> per min at 25°C. The catalase activity was expressed as specific activity, units per mg total protein.

## 2. 15. Phylogenetic analysis of AspB<sub>Mtb</sub> and AspC<sub>Mtb</sub>

Protein sequences were obtained from Uniprot ([www.uniprot.org](http://www.uniprot.org)) and aligned using Clustal X2, followed by manual adjustments [105]. Phylogenetic trees were constructed using the Neighbor-joining algorithm in Mega 5 [106].

## 2. 16. Cloning of *aspB* and *aspC* in pGEX4T-1

The genes *aspB* and *aspC* from *M. tuberculosis* H37Rv were cloned from genomic DNA using primers BOO-78 and BOO-79 (*aspB*) and BOO-80 and BOO-81 (*aspC*). The PCR fragments were ligated into pGEX4T-1 (GE Healthcare) pre-digested with BamH1 and EcoR1 for expression of recombinant fusion proteins with an N-terminal Glutathione S-transferase (GST) tag. The recombinant fusion proteins contained an engineered thrombin cleavage site for the removal of the tag after affinity purification. The expression vectors were transformed into BL21 *E. coli*; transformants with ampicillin resistance were selected. A single colony was inoculated into selective media and grown overnight with shaking at 37°C. The overnight culture was diluted 200-fold into 2xYT media containing ampicillin (100  $\mu$ g/ml) and grown at 37°C until OD<sub>600nm</sub> 0.4 was reached. Expression was induced with 0.25 mM IPTG for 17 hours at room temperature. Cells were harvested by centrifugation (4000 rpm, 15 min) and stored at -80°C.

## 2. 17. Purification of GST-tagged AspB<sub>Mtb</sub> and AspC<sub>Mtb</sub>

Purification of GST-tagged AspB and AspC was based on the method described by Frangioni and Neel [107]. Cells were resuspended in STE buffer (10mM Tris, pH 8.0, 150 mM NaCl, 1mM EDTA) with 1.5% sarkosyl and 2% triton. Cells were lysed by bead beating in a FastPrep-24 (MP Biomedicals) for 3 rounds of 30 seconds at level 5. The lysate was centrifuged for 40 min at 10 000 g to remove unbroken cells and

inclusion bodies. The supernatant was then loaded onto a Glutathione Sepharose 4B column (GE Healthcare) and the column was washed with STE buffer. Purified GST-AspB<sub>Mtb</sub> and GST-AspC<sub>Mtb</sub> were eluted from the column using 10 mM reduced glutathione in STE buffer (Figure 24). De-salting and buffer exchange into 10 mM Tris, pH8.0 was performed using centrifugal filter units (Amicon) with a 30 kDa MWCO. The purity of the purified recombinant fusion protein was assessed using SDS-PAGE.

## **2. 18. Thrombin cleavage of GST-tagged AspB<sub>Mtb</sub> and AspC<sub>Mtb</sub>**

Removal of the affinity tag was performed at room temperature for 10 min at a 100:1 molar ratio of the protein with human  $\alpha$ -thrombin (Haematologic Technologies Inc.). At the end of the incubation, thrombin was inactivated using 1 mM PMSF followed by a second round of Glutathione Sepharose affinity chromatography.

## **2. 19. Cloning of *aspB* and *aspC* in pET expression vectors**

DNA fragments encoding the genes *aspB* Rv3565 (BOO-106 and BOO-107) and *aspC* Rv0337c (BOO-108 and BOO-109) were cloned from *M. tuberculosis* genomic DNA, using primers with engineered NdeI and BamHI recognition sequences. The PCR products were directionally cloned into pET19b for heterologous expression of recombinant AspB and AspC with an N-terminal hexa-histidine (His) fusion tag. Additionally the *aspC* gene was amplified without the stop codon using primers BOO-108 and BOO-110 and was directionally cloned between NdeI and KpnI sites of pET30b to attach a His tag at the C-terminus of the recombinant protein. Both pET19b and pET30b included an engineered enterokinase cleavage site between the His-tag and recombinant protein.

## **2. 20. Expression of recombinant His-tagged AspB<sub>Mtb</sub> and AspC<sub>Mtb</sub>**

The expression vectors were electroporated into BL21 (DE3) or Rosetta™ 2 (Novagen®) *E. coli* expression strains. The transformants were plated onto LB agar plates containing ampicillin (100  $\mu$ g/ml), kanamycin (30  $\mu$ g/ml) and chloramphenicol (34  $\mu$ g/ml) whenever necessary. For expression with chaperone proteins, pET30b::*aspC* was co-transformed with one of the following: pGro7, pTf-2, pG-KJE8, or pTf16 (Takara Bio Inc.) and plated on kanamycin and chloramphenicol selection plates.

Starter cultures were made from a single colony inoculated into LB broth containing antibiotics for plasmid maintenance and grown overnight at 37°C with shaking. The starter culture was diluted 200-fold into 1 litre 2xYT media, grown at 37°C with shaking until an OD<sub>600nm</sub> of ~0.4, and induced using 0.1 mM

IPTG. To induce the expression of chaperone proteins, L-arabinose (1 mg/ml) and/or tetracycline (2 ng/ml) were used. Induction proceeded at room temperature overnight (~17 h). The cells were harvested by centrifugation at 4000 g for 15 min and frozen at -80°C until further use.

## **2. 21. Purification of recombinant His-tagged AspB<sub>Mtb</sub> and AspC<sub>Mtb</sub>**

The cell pellets were thawed on ice and resuspended in lysis buffer containing 50 mM NaH<sub>2</sub>PO<sub>4</sub> pH 7.8, 300 mM NaCl, 0.06mM pyridoxal 5'-phosphate hydrate, 2% Triton and 1 mM DTT. The cells were lysed by five 30 second cycles of sonication on ice. The lysate was clarified by centrifugation at 10 000 g for 40 min. The recombinant protein was purified using a Ni-NTA Agarose (Qiagen) column according to manufacturer's protocol. Briefly, the clarified supernatant was loaded onto the column which was then washed with 10 column volumes of wash buffer (50 mM NaH<sub>2</sub>PO<sub>4</sub> pH 8.0, 300 mM NaCl, 100 mM imidazole). The recombinant protein was eluted using 2 column volumes of elution buffer (75 mM HEPES pH 7.8, 150 mM NaCl and 250 mM imidazole). The recombinant His-tagged AspB protein was observed to have a molecular weight of ~45 kDa and the recombinant His-tagged AspC protein had an observed molecular weight of ~51 kDa, consistent with sizes predicted by their nucleotide sequences. The eluted recombinant proteins were dialyzed in 2 l of 50 mM HEPES pH 7.8 overnight at 4°C. The volumes of the purified recombinant proteins were reduced using PEG 8000. The His tag from both recombinant proteins was removed using the engineered enterokinase site. The purity of the recombinant proteins was examined by SDS PAGE.

## **2. 22. Removal of His tag from AspB<sub>Mtb</sub>**

The His tag was removed by incubating a 6000:1 molar ratio of AspB with enterokinase (NEB Inc.) for 10 h at room temperature. The reaction was stopped by the addition of 1.5 mM PMSF followed by the removal of the enterokinase with a Benzamidine Sepharose (Sigma) column. Centrifugal filter units (Amicon) with a 30 kDa MWCO were used for concentration and buffer exchange into 10 mM HEPES buffer pH 7.8. The removal of the His tag was monitored via SDS-PAGE and it was determined that >95% of the fusion tags had been cleaved. Purified AspB aliquots were frozen with liquid nitrogen and stored at -80°C until use.

## 2. 23. Cloning and expression of AspC<sub>Mtb</sub> without fusion tags

The *aspC* gene fragment was cut out from pET19b::*aspC* using NdeI and BamHI and cloned into pET30b creating pET30b::*aspC1* for expression of AspC without any fusion tags. The plasmid was transformed into Rosetta 2™ *E. coli* and kanamycin-resistant colonies were selected. Expression of AspC was analogous to steps described in section “Expression of recombinant His-tagged AspB and AspC” (Section 2. 21) except AspC expression was induced with 1 mM IPTG for 3 h at 37°C or 0.05 mM IPTG overnight at 15°C. The expression and solubility of AspC was monitored using SDS PAGE.

## 2. 24. Cloning and expression of AspC<sub>Mtb</sub> in *M. smegmatis*

The *aspC* gene fragment was removed from pET30b::*aspC* using NdeI and KpnI and cloned into pYUB1062 [97] creating pYUB1062::*aspC*. The expression vector for C-terminus His tagged AspC fusion protein was electroporated into mc<sup>2</sup> 4517 *M. smegmatis* expression strain [97] and plated onto 7H10 hygromycin selection plates. A starter culture was prepared by inoculating a single colony into 10 ml 7H9 containing hygromycin B and the culture was grown at 37°C for 24 h. 1 ml of the primary culture was inoculated into 50 ml of the same 7H9 media and was grown at 37°C to OD<sub>600nm</sub> 0.6-0.8. Subsequently expression of AspC was induced with 0.2% (w/v) acetamide and expression proceeded at 37°C for 22 h. After 22 h, the cells were harvested by centrifugation (4000 rpm for 15min at 4°C), resuspended in lysis buffer II (50 mM NaH<sub>2</sub>PO<sub>4</sub> pH 7.8, 300 mM NaCl) and lysed with 0.1 mm silica beads in a FastPrep-24 bead-beater (MP Biomedicals). Expression and solubility of AspC was observed using SDS PAGE.

## 2. 25. Aspartate aminotransferase assay

The aspartate aminotransferase activity of purified recombinant AspB and AspC was assayed by coupling the aspartate aminotransferase reaction with malate dehydrogenase, and measuring the oxidation of NADH spectrophotometrically at 340 nm [108] [109]. Briefly, the final substrate mixture contained 200 mM HEPES buffer, pH 7.5; 10 mM aspartate; 10 mM α-ketoglutarate; 0.1 mM NADH, 2 μM pyridoxal 5'-phosphate; and 0.5 μg/ml malate dehydrogenase. Reaction rates at 25°C were determined by following the decrease in absorbance at 340 nm with a Varian Cary 5000 spectrophotometer. Calculations were based on extinction coefficient for NADH (ε<sub>340</sub> = 6220 M<sup>-1</sup>cm<sup>-1</sup>). One unit of AAT activity equals 1 μmol of product generated per minute at 25°C.

Steady-state kinetic parameters, K<sub>m</sub> values were determined for aspartate and α-ketoglutarate in the assay system described above. Initial reactions rates were measured by varying the α-ketoglutarate

concentration while aspartate concentration was held constant at 10mM and vice versa as aspartate concentration was varied as  $\alpha$ -ketoglutarate was fixed at 1.5 mM. The concentration of the enzyme used in each assay was 130 nM. Curves were fit using the equation for a substituted-enzyme mechanism in LEONORA.

### 3. Results

#### 3. 1. Expression of *whiB7* upregulates *aspC*

The transcription factor encoded by *whiB7* is required for the induction of genes that encode conventional resistance determinants, including an antibiotic modifying enzyme (*eis* [110,111]), a target modifying enzyme (*erm37*[12,112]), and antibiotic transporter (*tap* [113]) [29]. Intriguingly, Morris *et al.* reported that some primary metabolic genes were also under *whiB7* control. Further analyses of the microarray data suggested that expression of two homologous genes annotated as aspartate transaminases (*aspB*, Rv3565; *aspC*, Rv0337c) were affected by *whiB7* expression. Comparing expression levels between *whiB7* overexpressing *M. tuberculosis* and wild-type, *aspB* was downregulated three-fold (ratio of 0.34) and *aspC* was upregulated ratio of 3.64 (unpublished data, Thompson lab). Members of this family of proteins catalyze a reversible transamination reaction involving interconversions of  $\alpha$ -keto acids and their partnered amino acids [114], thereby serving as central hubs of metabolism. Although these enzymes may catalyze reactions involving multiple amino acid/  $\alpha$ -keto acid partners, they are often called glutamate-oxaloacetate transaminases (Figure 3).

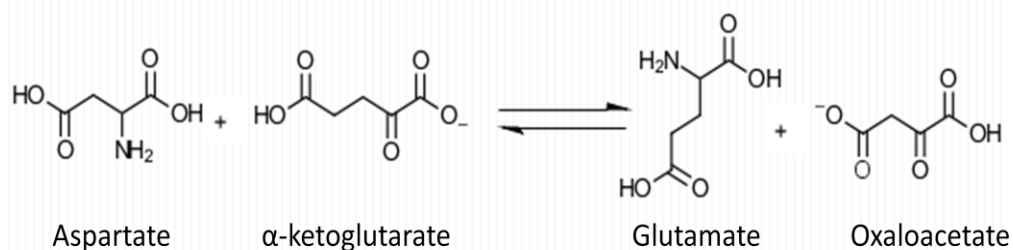


Figure 3. Reaction catalyzed by aspartate aminotransferases. The genes *aspB* and *aspC* are both annotated to be aspartate aminotransferases. Aspartate aminotransferases catalyze a pyridoxal-5'phosphate-dependent (PLP-dependent) reversible reaction that transfers an amino group from glutamate to  $\alpha$ -ketoglutarate forming aspartate and oxaloacetate [115].

Initial experiments were designed to explore the interdependencies of *aspB*, *aspC*, and *whiB7* expression and how this might relate to metabolism and intrinsic drug resistance. *whiB7<sub>Mtb</sub>* (Rv3197a) and *whiB7<sub>Msm</sub>* (MSMEG\_1953) were cloned into pMV361 to provide constitutive expression in *M. smegmatis*. Since *whiB7* orthologs in *M. tuberculosis* and *M. smegmatis* share 75% amino acid identity, *M. smegmatis* was adopted as a convenient surrogate system to study the regulation of gene expression of *whiB7*, *aspB*, and *aspC*. *mysA* (MSMEG\_2758) encoding the primary sigma factor  $\sigma^A$ , was used as an internal control for normalization of *aspB*, *aspC*, and *whiB7* expression levels. Rates of *aspB* and *aspC* transcription were

measured by qRT-PCR in wild-type when *whiB7*<sub>Mtb</sub> or *whiB7*<sub>Msm</sub> were constitutively expressed from the heat-shock protein (hsp) promoter [94,116,117]. Relative to the wild-type strain transformed with the empty vector, constitutive transcription of *whiB7*<sub>Mtb</sub> and *whiB7*<sub>Msm</sub> resulted in a 7.5-fold increase in *aspC* expression (Figure 4). Under these conditions *aspB* expression was not significantly changed by *whiB7*<sub>Mtb</sub>. This result suggests that *aspC*, but not *aspB*, expression may be controlled by transcription of *whiB7*.

### 3. 2. Expression of *whiB7* and *aspC* is upregulated by tetracycline

In *M. tuberculosis* (and *Streptomyces lividans*), *whiB7* is induced by various antibiotics including tetracycline [29]. To validate the use of *M. smegmatis* as a surrogate model system, cultures were treated with tetracycline at 0.8 µg/ml (about four-times the MIC of tetracycline in the wild-type strain) for 1 hour and the expression of *whiB7*<sub>Msm</sub> was measured using qRT-PCR. This treatment induced expression of *whiB7*<sub>Msm</sub> over 1000-fold (Figure 5A). The expression of *aspC* in the same tetracycline-treated RNA samples was induced 4-fold (Figure 5B).

To more clearly understand the dependence of *aspB* and *aspC* expression on *whiB7* and antibiotics, transcription was measured in both wild-type and  $\Delta$ *whiB7* after tetracycline treatment. The expression of *aspC* in untreated  $\Delta$ *whiB7* cultures was slightly (about 50%) depressed relative to the wild-type strain (Figure 5B). While *aspC* was induced more than four-fold in wild-type by tetracycline, this did not occur in the tetracycline-treated  $\Delta$ *whiB7* strain (Figure 5B). These observations demonstrated *whiB7*-dependent upregulation of *aspC* in response to tetracycline. Parallel experiments showed that expression of *aspB* was not significantly affected by tetracycline treatment or *whiB7* deletion (Figure 5B)

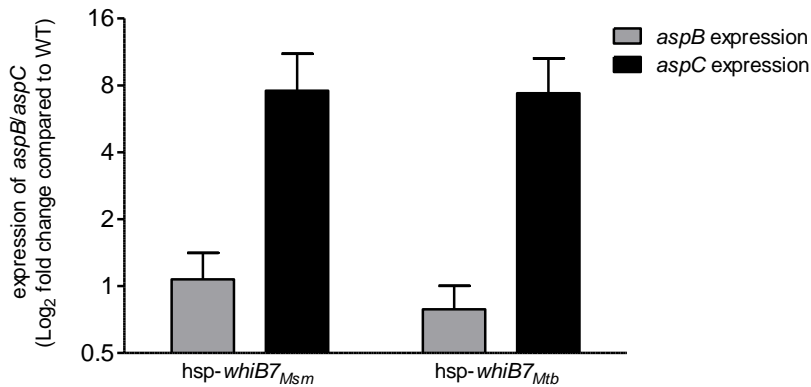


Figure 4. Expression of *aspC* was upregulated by *whiB7*. Expression of *aspB* and *aspC* in *M. smegmatis* that constitutively expresses *whiB7*<sub>Mtb</sub> or *whiB7*<sub>Msm</sub> from hsp60 promoter was measured by qRT-PCR. Constitutive expression of *whiB7*<sub>Mtb</sub> increased the expression of *aspC* seven-fold compared to wild-type. The expression of *aspB* was not significantly affected. Mean data from 3 biological experiments are reported.

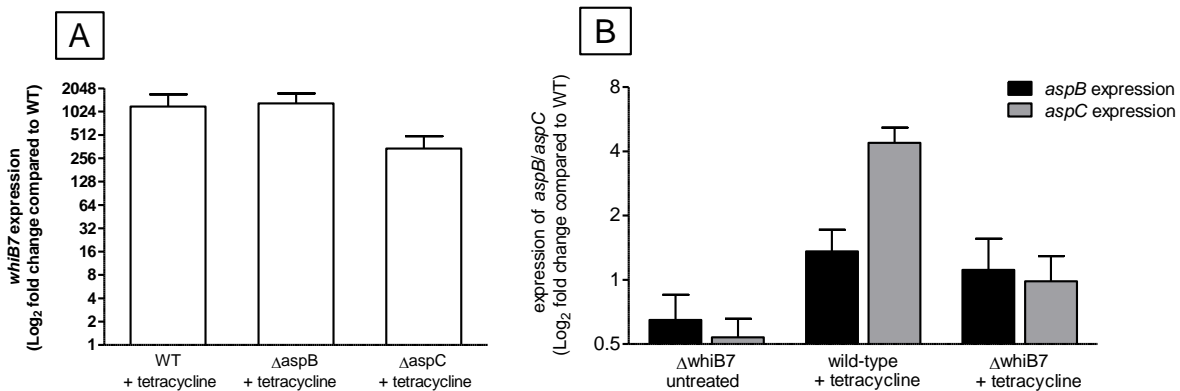


Figure 5 Expression responses of *whiB7*, *aspB*, and *aspC* to tetracycline. (A) Wild-type and mutants Δ*aspB* and Δ*aspC* were treated with 0.8 μg/ml tetracycline for 1 h and *whiB7* expression levels compared to untreated wild-type. *whiB7* was strongly upregulated in response to tetracycline and the deletion of *aspB* did not affect this response. The expression of *whiB7* in response to tetracycline treatment was significantly reduced in Δ*aspC*. (B) Expression of *aspC* in wild-type and Δ*whiB7*. Expression of *aspC* increased in response to tetracycline treatment. Deletion of *whiB7* downregulated *aspC* in untreated samples and abrogated upregulation of *aspC* in response to tetracycline. Mean data from 3 biological experiments are reported.

### 3. 3. Optimal *whiB7* induction by tetracycline requires *aspC*

Cultures of mutant strains  $\Delta aspB$  and  $\Delta aspC$  were tetracycline treated and relative *whiB7* expression levels were determined using qRT-PCR to assess whether those genes affected *whiB7* expression in response to tetracycline. As shown in Figure 5A, the  $\Delta aspB$  mutant strain had the same *whiB7* tetracycline induced upregulation as the wild-type while the *whiB7* expression in the  $\Delta aspC$  mutant was significantly lower (340-fold versus over 1000-fold in wild-type). This suggested that *whiB7* upregulation in response to tetracycline is enhanced by *aspC*.

### 3. 4. Constitutive expression of *aspB* downregulates *whiB7* and *aspC* in tetracycline-induced cultures

The *M. tuberculosis* *aspB<sub>Mtb</sub>* and *aspC<sub>Mtb</sub>* genes were cloned and expressed in *M. smegmatis* from an integrative vector with constitutive transcription from hsp promoter (pMV361::*aspB<sub>Mtb</sub>* and pMV361::*aspC<sub>Mtb</sub>*) generating strains that constitutively expressed *aspB<sub>Mtb</sub>* and *aspC<sub>Mtb</sub>* (*hsp-aspB<sub>Mtb</sub>* and *hsp-aspC<sub>Mtb</sub>*). To determine whether constitutive *aspB* and *aspC* expression affected expression of *whiB7* in response to antibiotics, *whiB7* transcripts were measured in cultures constitutively expressing these genes with and without tetracycline induction. In untreated wild-type cultures, constitutive expression of *aspB* (*hsp-aspB<sub>Mtb</sub>*) reduced expression of *whiB7* about 95% and the strong tetracycline induced upregulation of *whiB7* expression was eliminated (Figure 6A). Measurement of *aspC* in these samples revealed a similar trend; upregulation of *aspC* in response to tetracycline was not observed in the *hsp-aspB<sub>Mtb</sub>* strain (Figure 6B). In contrast, expression of *aspC<sub>Mtb</sub>* increased *whiB7* expression by 3.8-fold in untreated cultures but did not significantly alter *whiB7* upregulation in tetracycline treated cultures. (Figure 6A).

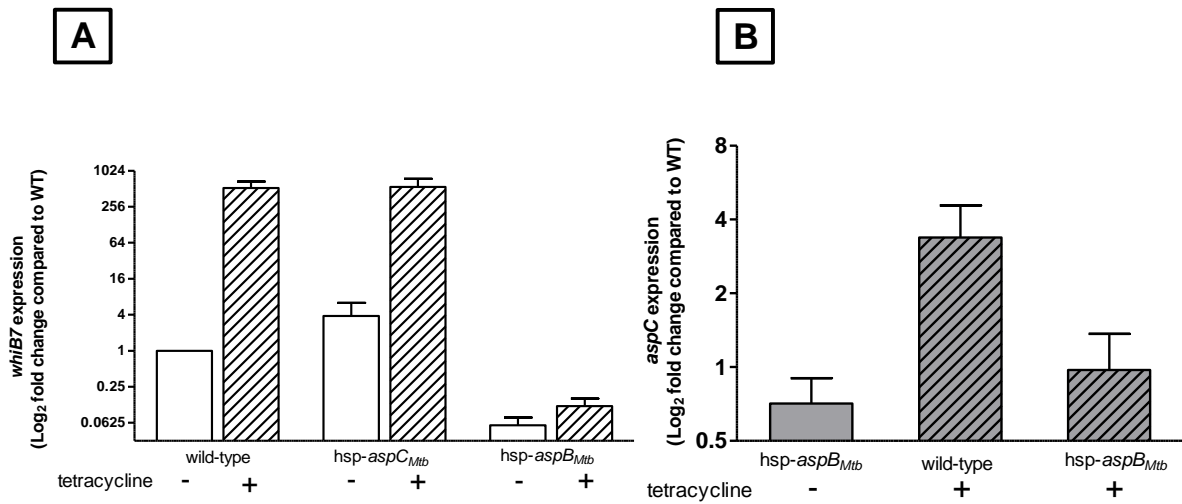


Figure 6. Interactive regulation of *aspB*, *whiB7* and *aspC*. (A) *whiB7* expression in *aspB<sub>Mtb</sub>* and *aspC<sub>Mtb</sub>* constitutive expression strains. Constitutive expression of *aspB<sub>Mtb</sub>* downregulated *whiB7* expression in untreated and tetracycline treated cultures. Constitutive expression of *aspC<sub>Mtb</sub>* increased levels of transcription in untreated cultures. (B) Expression of *aspC* in the *hsp-aspB<sub>Mtb</sub>* strain. Constitutive expression of *aspB<sub>Mtb</sub>* also prevented tetracycline-induced upregulation of *aspC*. Mean data from 3 biological experiments are reported.

### 3. 5. The $\Delta aspC$ mutant exhibits growth deficiencies

*aspB* and *aspC* are both annotated as aspartate aminotransferases, enzymes that are central to intermediary metabolism. To test the hypothesis that *aspB* and/or *aspC* are needed for growth, knock-out mutant strains of *aspB*<sub>Msm</sub> (MSMEG\_6017) and *aspC*<sub>Msm</sub> (MSMEG\_0688) were constructed using a mycobacterial recombineering system [95].

Growth kinetics of mutant and constitutive-expression strains were analyzed in either nutrient rich (7H9 supplemented with ADC; Figure 7A) or minimal (Proskauer Beck (PB) medium; Figure 7B). Strains  $\Delta aspB$ , *hsp-aspB*<sub>Mtb</sub> and *hsp-aspC*<sub>Mtb</sub> grew at the same rate as wild-type *M. smegmatis* in both media. However, in both complete 7H9 media and minimal media PB  $\Delta aspC$  exhibited growth deficiencies, including a prolonged lag phase, decreased rate of exponential growth, and decreased cell density at stationary phase. For example, in PB medium, deletion of *aspC* increased the doubling time approximately two-fold (from 6-6.5 hrs to 12-14 hrs); rolling cultures of wild-type *M. smegmatis* achieved a stationary phase OD<sub>600nm</sub> of 5.0-5.5 while  $\Delta aspC$  only reached OD<sub>600nm</sub> of 3.0-3.4. The lag phase of the  $\Delta aspC$  mutant was generally 6 hours (in 7H9 rich medium) and 12 hours (in PB minimal medium) longer than that of wild-type (Figures 7A and 7B). Finally,  $\Delta aspC$  also grew as smaller colonies on both 7H10 and PB agar plates. Transformation of  $\Delta aspC$  with an integrative construct that constitutively expressed *aspC*<sub>Mtb</sub> (pMV361::*aspC*<sub>Mtb</sub>) fully restored growth defects on both media\_(results with PB cultures are shown in Figure 7C).

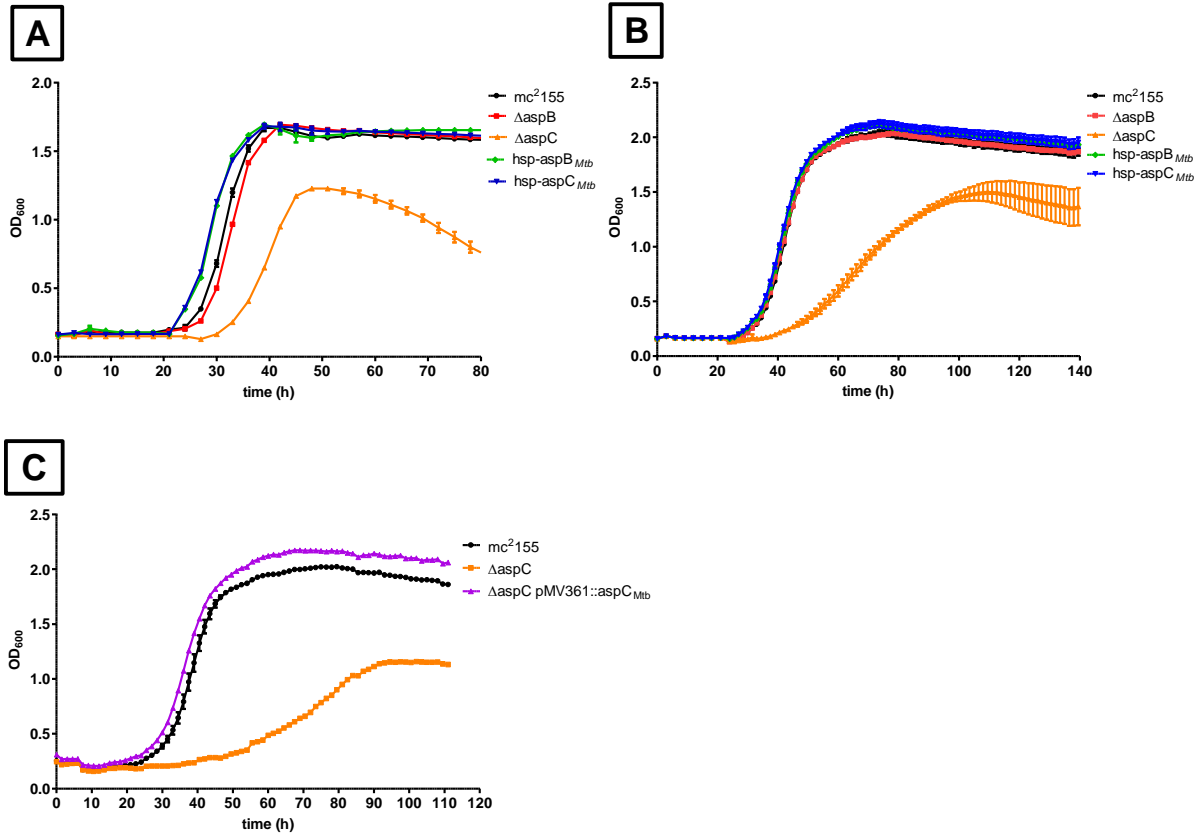


Figure 7. Growth kinetics of *M. smegmatis* wild-type (black),  $\Delta aspB$  (red),  $\Delta aspC$  (orange),  $hsp-aspB_{Mtb}$  (green),  $hsp-aspC_{Mtb}$  (blue), and  $\Delta aspC$  complemented (purple). Strains were grown in nutrient-rich 7H9 with ADC (A) and PB minimal media (B) (C). Growth curves are representative of quadruplicate wells. Bars indicate standard error.

### **3. 6. The $\Delta aspC$ is able to catalyze glutamate but not aspartate**

Since the use of amino acids to provide carboxylic acids or ammonia as intermediary metabolites require aminotransferases, the ability of *aspB* and *aspC* mutants to utilize aspartate and glutamate as carbon and nitrogen sources were tested. Wild-type and  $\Delta aspB$  and  $\Delta aspC$  mutants were inoculated into PB salts (without  $\text{NH}_4\text{Cl}$ ) containing glycerol (1% v/v) and 40mM glutamate or aspartate to test the ability of the strains to use these amino acids as nitrogen sources. In other cultures, glycerol was omitted in order to determine whether these amino acids could serve as sources of both carbon and nitrogen. In all these media, the *aspB* mutation had no growth phenotype; its growth kinetics were similar to wild-type. Growth of the  $\Delta aspC$  mutant was not impaired (relative to wild-type) when cultures were grown with glutamate as nitrogen source; growth was slightly impaired in media with glutamate as the source of both carbon and nitrogen (Table 3). In contrast, the *aspC* mutant strain grew poorly with aspartate as its nitrogen source and could not grow using aspartate as both carbon and nitrogen sources.

### **3. 7. $\alpha$ -ketoglutarate complements $\Delta aspC$ mutant's growth deficiencies**

To further investigate whether the growth deficiencies observed in  $\Delta aspC$  mutant were due to a lack of one of its putative substrates, growth rates were determined in PB minimal medium supplemented with aspartate, glutamate, oxaloacetate or  $\alpha$ -ketoglutarate. Oxaloacetate did not significantly affect the growth of the  $\Delta aspC$  mutant at 20mM and 40mM (data not shown). The presence of  $\alpha$ -ketoglutarate increased the growth rate of  $\Delta aspC$  in a dose-dependent manner and allowed it to grow at a rate similar to that of wild-type at 60 mM  $\alpha$ -ketoglutarate (Figure 8A). The prolonged lag phase of  $\Delta aspC$  was not shortened by  $\alpha$ -ketoglutarate (Figure 8A). Aspartate and glutamate did not improve the growth of  $\Delta aspC$  and did not affect the growth of wild-type cultures. However, at higher concentrations of aspartate and glutamate growth of  $\Delta aspC$  mutant was further delayed, showing that the mutant may have defects in catabolising these amino acids (Figure 8B).

Table 3. Growth properties of  $\Delta aspB$  and  $\Delta aspC$  mutants in cultures containing aspartate and glutamate as carbon and/or nitrogen sources. Growth was tested on minimal Proskauer Beck salts <sup>1</sup> supplemented with the indicated carbon and nitrogen sources at 37°C.

Addition to PB salts	Strain		
	mc <sup>2</sup> 155	$\Delta aspB$	$\Delta aspC$
1% glycerol + 40 mM L-glutamate	+++	+++	+++
1% glycerol + 40 mM L-aspartate	+++	+++	+
40 mM L-glutamate	++	++	+
40 mM L-aspartate	++	++	-

Growth represented by symbols (in order of decreasing growth) +++, ++, +, - .

<sup>1</sup> 36.7 mM monopotassium phosphate, 2.4 mM magnesium sulfate, 0.4 mM sodium citrate, pH 7.4

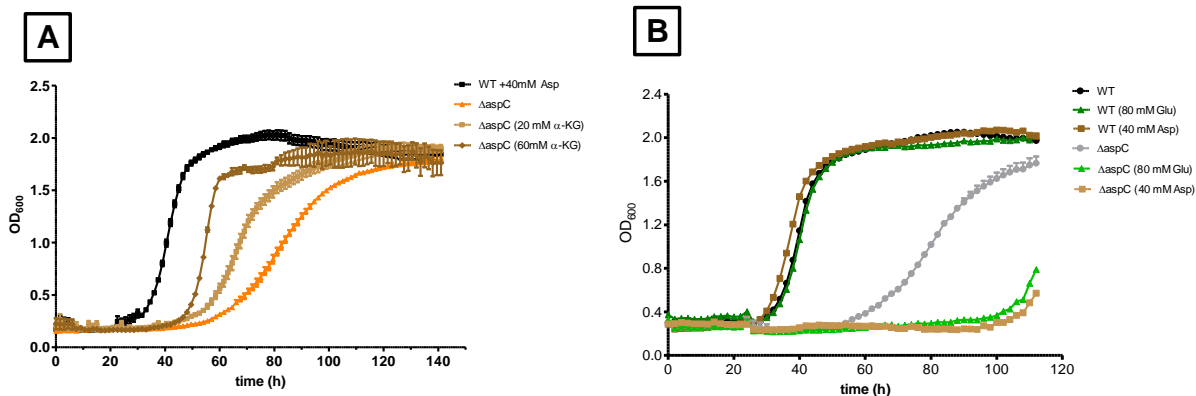


Figure 8. Growth of the  $\Delta aspC$  mutant was modulated by addition of aspartate aminotransferase substrates. (A) Effect of  $\alpha$ -ketoglutarate on growth kinetics of  $\Delta aspC$  in PB media. The supplementation of  $\alpha$ -ketoglutarate at 60mM into the medium restored the doubling rate to wild-type levels. (B) Addition of glutamate and aspartate at high concentrations (80 mM and 40 mM respectively) inhibits growth of  $\Delta aspC$  mutant but wild-type growth is unaffected. Growth curves are representative of quadruplicate wells. Error bars indicate standard error. OD<sub>600</sub>, OD at 600 nm.

### **3. 8. Passaging the $\Delta aspC$ mutant in media containing $\alpha$ -ketoglutarate suppresses the growth rate defect but does not shorten lag phase**

The growth deficiencies of mutant  $\Delta aspC$  could be partially complemented by the inclusion of  $\alpha$ -ketoglutarate in the growth medium. When  $\alpha$ -ketoglutarate was supplemented in the medium, both the reduced growth rate and lowered cell density at stationary phase of the  $\Delta aspC$  mutant was restored to wild-type levels. However, the longer lag phase remained (Figure 8A). Since the prolonged lag phase could be the time required for  $\Delta aspC$  mutant to make the necessary metabolic adaptations for growth on  $\alpha$ -ketoglutarate, pre-cultures of wild-type, mutant  $\Delta aspC$  and complemented strain  $\Delta aspC$  pMV361::*aspC* were grown in 7H9 medium. The second pre-culture of the  $\Delta aspC$  mutant was inoculated into the same media that also contained 40 mM  $\alpha$ -ketoglutarate. The stationary phase cultures were washed and re-inoculated in PB (with 0.05% tyloxapol) medium with and without 40 mM  $\alpha$ -ketoglutarate, and seeded into microwells in quadruplicates for growth analysis using the Bioscreen C kinetic growth reader. The mutant  $\Delta aspC$  grown in PB media without  $\alpha$ -ketoglutarate still exhibited growth deficiencies (longer lag, reduced growth rate, and lowered cell density at stationary phase) compared to wild-type (Figure 9). Addition of  $\alpha$ -ketoglutarate to the medium suppressed only the growth rate and cell density at stationary phase but not the prolonged lag regardless of whether or not the pre-culture contained  $\alpha$ -ketoglutarate. This result shows that the prolonged lag phase of the  $\Delta aspC$  mutant is not due to a nutritional deficiency or toxicity that can be overcome with passaging in  $\alpha$ -ketoglutarate-containing media.

### **3. 9. The $\Delta aspB \Delta aspC$ double mutant is not an amino acid auxotroph**

The  $\Delta aspB \Delta aspC$  double mutant was able to grow on a standard media for testing auxotrophy M9 minimal media (Figure 10A). In 7H9 liquid media, growth kinetic analyses revealed that the double mutant  $\Delta aspB \Delta aspC$  had growth deficiencies similar to the single mutant  $\Delta aspC$  (Figure 10B). The double mutant had a prolonged lag phase as with the single mutant  $\Delta aspC$ , but the double mutant replicated faster (doubling rates of 5.7 hours and 4.7 hours for  $\Delta aspC$  and  $\Delta aspB \Delta aspC$  respectively). It is likely the growth deficiencies in both strains were due to the deletion of *aspC* but the second deletion in *aspB* may relieve slightly the toxicity caused by the single  $\Delta aspC$  mutant. Understanding the physiological roles of *aspB* and *aspC* individually would contribute to understanding the effect of deletions of both *aspB* and *aspC* to *M. smegmatis* physiology.

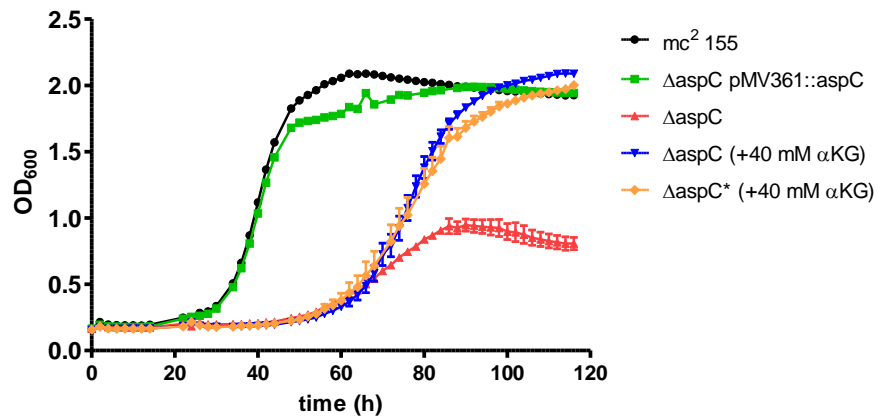


Figure 9. Allowing the  $\Delta$ *aspC* mutant to adapt to growth in media containing  $\alpha$ -ketoglutarate did not suppress the extended lag phase growth deficiency. Growth of wild-type *mc*<sup>2</sup> 155, mutant  $\Delta$ *aspC*, and complemented strain  $\Delta$ *aspC* pMV361::*aspC* in PB media. Constitutive expression of *aspC*<sub>Mtb</sub> complemented the mutant's growth deficiencies. Addition of  $\alpha$ -ketoglutarate suppressed only the reduced doubling rate and lower cell density at stationary but not the prolonged lag phase. Passaging the mutant in  $\alpha$ -ketoglutarate ( $\Delta$ *aspC*\*) did not shorten the lag phase of the mutant.

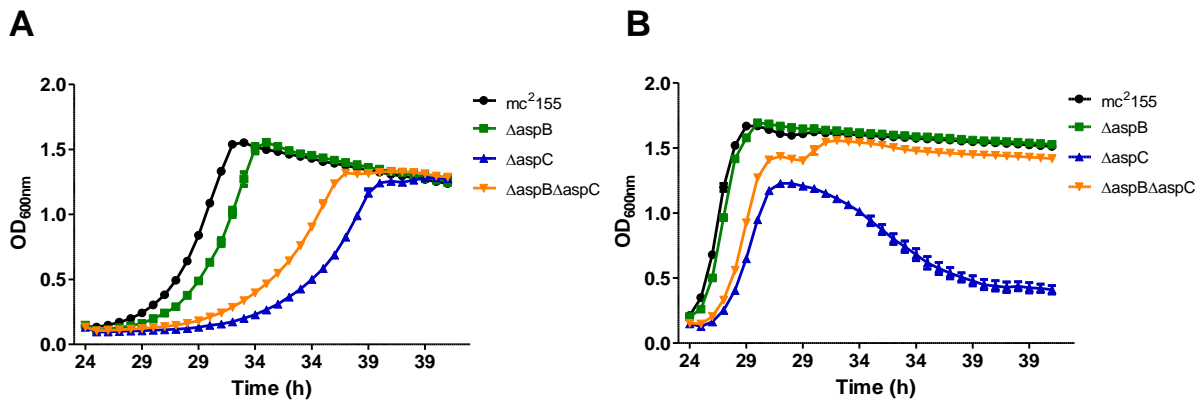


Figure 10. Growth kinetics of double mutant  $\Delta$ *aspB* $\Delta$ *aspC*. (A) in M9 minimal salt media and (B) in rich media 7H9 (10% ADC). The double mutant was not auxotrophic and displayed growth defects similar to mutant  $\Delta$ *aspC*.

### 3. 10. Opacification of 7H10 by $\Delta aspC$ mutant

The  $\Delta aspC$  mutant generated a white, opaque, diffuse zone surrounding the colonies (opacification) when grown on Middlebrook 7H10 (with 10% OADC) (Figure 11A). The white effect can be mimicked by reducing the pH of the media.

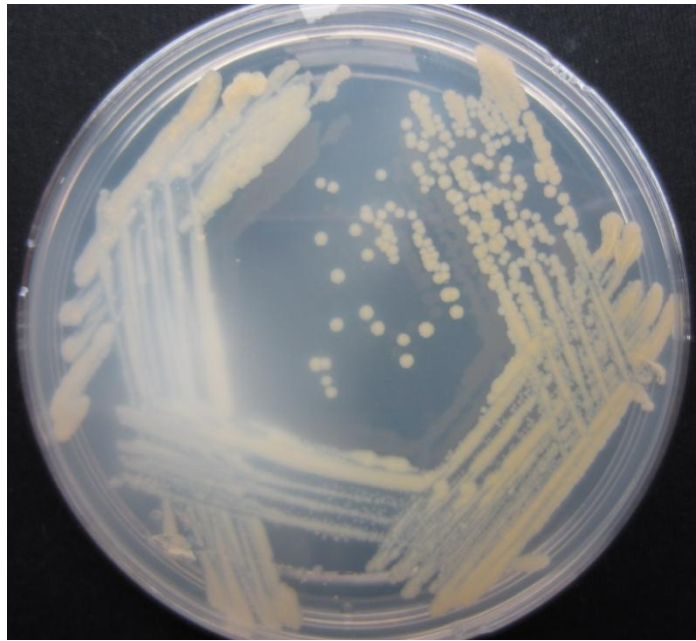


Figure 11. Opacification of 7H10 by the  $\Delta aspC$  mutant. Growth of mutant  $\Delta aspC$  on 7H10 with 10% OADC yields a white opaque colour.

### 3. 11. The $\Delta whiB7$ mutant, $\Delta aspC$ mutant, and $aspB$ constitutive expression strains are antibiotic sensitive

Deletion of *whiB7* in *M. tuberculosis* or *M. smegmatis* made them sensitive to an assortment of antibiotics including rifampicin and erythromycin [29,35]. To test whether the expression of *asp* genes affect antibiotic sensitivity, strains in which they were constitutively expressed (*hsp-aspB<sub>Mtb</sub>*, *hsp-aspC<sub>Mtb</sub>*) or inactivated ( $\Delta aspB$ , and  $\Delta aspC$ ) were subjected to antibiotic susceptibility profiling using resazurin or MTT assays. MICs were determined for fourteen antibiotics representing different structures and targets. Their MICs were compared to wild-type with no plasmid or transformed with an empty pMV361 vector.

While the drug sensitivities of  $\Delta aspB$  and *hsp-aspC<sub>Mtb</sub>* strains were identical to wild-type,  $\Delta aspC$  and *hsp-aspB<sub>Mtb</sub>* strains were more sensitive to many antibiotics (Table 4).  $\Delta whiB7$  and *hsp-aspB<sub>Mtb</sub>* were 4 to 16-fold more sensitive than wild-type to drugs targeting the ribosome, including chloramphenicol, clarithromycin, clindamycin, roxithromycin, spectinomycin and tetracycline. The  $\Delta aspC$  mutant was also more susceptible to drugs targeting protein synthesis including clindamycin, spectinomycin, clarithromycin and roxithromycin. While both *hsp-aspB<sub>Mtb</sub>* and  $\Delta aspC$  sensitivity profiles affected activities of the same set of ribosome targeting antibiotics, they exhibited a different susceptibility profile for drugs targeting RNA polymerase (rifampicin) or affecting cell envelope synthesis (isoniazid, clofazimine, and possibly triclosan). Transformation of the mutant  $\Delta aspC$  with a plasmid encoding *aspC<sub>Mtb</sub>* complemented the antibiotic sensitivity (Figure 12). Furthermore, the increased antibiotic susceptibility of mutant  $\Delta aspC$  was also studied using growth kinetic analysis (Figure 14).

### 3. 12. Complementation of antibiotic susceptibility of the $\Delta aspC$ mutant

The antibiotic susceptibility of *M. smegmatis*  $\Delta aspC$  was partially complemented (tetracycline, clarithromycin, and spectinomycin were tested) by constitutive expression of the *M. tuberculosis* *aspC* gene as determined by MTT assay (Figure 12). Similarly, addition of  $\alpha$ -ketoglutarate to the growth medium increased the growth rate of the mutant and suppressed the antibiotic susceptibility of  $\Delta aspC$  (Figure 12). It is interesting to note that addition of  $\alpha$ -ketoglutarate caused the strain to become more resistant to isoniazid (32-fold more resistant than wild-type (Figure 12).

Table 4. Antibiotic susceptibility profiles of the  $\Delta whiB7$  mutant, *hsp-aspB* expression, and the  $\Delta aspC$  mutant strains of *M. smegmatis*. The MIC of the strains including wild-type towards the antibiotics was determined using the MTT cell viability assay described in Section 2 .6.

target	compound	<u>fold susceptibility relative to wild-type</u>		
		$\Delta whiB7$	<i>hsp-aspB</i> <sub>Mtb</sub>	$\Delta aspC$
cell wall	ethambutol	--	--	--
	isoniazid	--	--	2
	triclosan	4	4	--
protein synthesis	capreomycin	--	--	--
	chloramphenicol	4	4	--
	clarithromycin	8	8	16
	clindamycin	8	4	2-4
	fusidic acid	2	--	2-4
	roxithromycin	8	8	16
	spectinomycin	16	4	2
	streptomycin	--	--	--
	tetracycline	4	4	--
RNAP	rifampicin	--	--	8
other	clofazimine	--	--	2

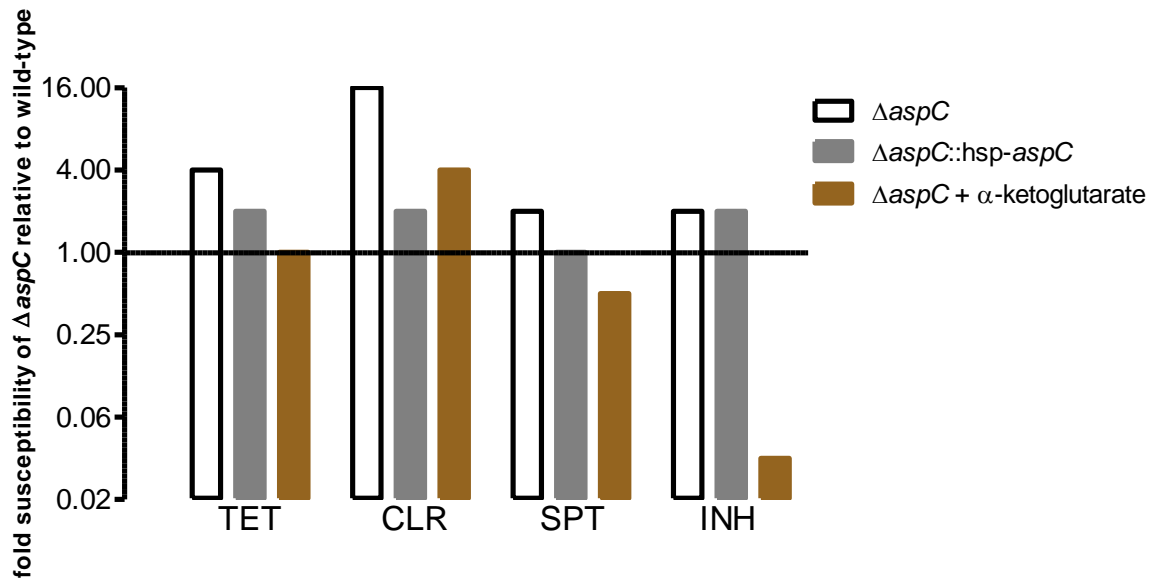


Figure 12. Suppression of antibiotic susceptibility of the  $\Delta aspC$  mutant by constitutive expression of  $aspC_{Mtb}$  or addition of  $\alpha$ -ketoglutarate. Mutant  $\Delta aspC$ , complemented strain  $\Delta aspC$  pMV361:: $aspC_{Mtb}$ , and wild-type mc<sup>2</sup> 155 were grown in the presence of 2-fold dilutions of tetracycline, clarithromycin, spectinomycin, and isoniazid in PB medium. After 2 days of growth at 37°C, the MIC was determined using MTT cell viability assay. The constitutive expression of  $aspC_{Mtb}$  or presence of  $\alpha$ -ketoglutarate (50 mM) in the media partially suppressed the antibiotic sensitivity of the mutant.

### 3. 13. Effects of antibiotics on the growth kinetics of the $\Delta aspC$ mutant

The kinetic growth response of wild-type *M. smegmatis* and the  $\Delta aspC$  mutant to nine of the antibiotics used in the antibiotic susceptibility profiling were also assessed with growth curves. Nine antibiotics (clarithromycin, tetracycline, chloramphenicol, clindamycin, clofazimine, fusidic acid, rifampicin, roxithromycin, and spectinomycin) were tested at five concentrations each, together with control growth curves of wild-type and the  $\Delta aspC$  mutant (92 growth curves in total).

Treatment of cultures with antibiotics, generally affected growth both by prolonging the lag phase and slightly increasing the doubling time. With both phenomena, the time for the strain to achieve a certain cell density increased. The growth curve data was plotted to show the effect of antibiotic concentration and the time to reach half of the maximum  $OD_{600nm}$  – as illustrated in Figure 13. Figure 13A shows growth curves of antibiotic-treated wild-type mc<sup>2</sup>155 and Figure 13B shows an alternate presentation of the same data, to show the effect of antibiotic concentration on growth delay. With this type of graph, the slope is proportional to the growth inhibition effect. The steeper the slope, the greater the increases in lag phase with higher antibiotic concentration. The growth curves of wild-type mc<sup>2</sup>155 and the  $\Delta aspC$  mutant in the presence of nine different antibiotics were analyzed using this graphical representation (Figure 14). With clarithromycin, roxithromycin, rifampicin, and clindamycin, the curves representing the  $\Delta aspC$  mutant have steeper slope and lay above and to the left of the wild-type. This shows that the growth kinetic inhibition (i.e. length of lag phase, doubling rate) was greater in  $\Delta aspC$  mutant than in the wild-type and that the mutant experiences orders of magnitude of more growth inhibition than wild-type. With fusidic acid, spectinomycin, and clofazimine the curves representing the  $\Delta aspC$  mutant has a similar slope compared to wild-type but the mutant curve still lie above the wild-type curve. This demonstrated that while the growth inhibition of  $\Delta aspC$  mutant was more than wild-type, the effect of increasing concentrations was similar. When there was no change in susceptibility in the  $\Delta aspC$  mutant compared to wild-type, the curves overlap, as is the case with tetracycline and chloramphenicol.

The growth curve data correlated with the results of the MTT assay for MIC determination (Table 4). When the mutant growth curve had a steeper slope than the wild-type curve (clarithromycin, roxithromycin, rifampicin), the fold susceptibility was higher (eight- to sixteen-fold more susceptible as compared to wild-type). A slight increase in susceptibility (two- to four-fold more susceptible as compared to wild-type) corresponded to the mutant curve having a similar slope to the wild-type curve but with the mutant curve lying above the wild-type curve (clindamycin, fusidic acid, and spectinomycin). The growth curve analysis once again showed that deletion of *aspC* caused the strain to be more susceptible to a number of antibiotics. In addition, this analysis revealed that the susceptibility of the  $\Delta aspC$  mutant increase was due the increased growth lag, akin to the effect of oxaloacetate and antibiotics on the growth of wild-type (Table 5 and Figure 16).

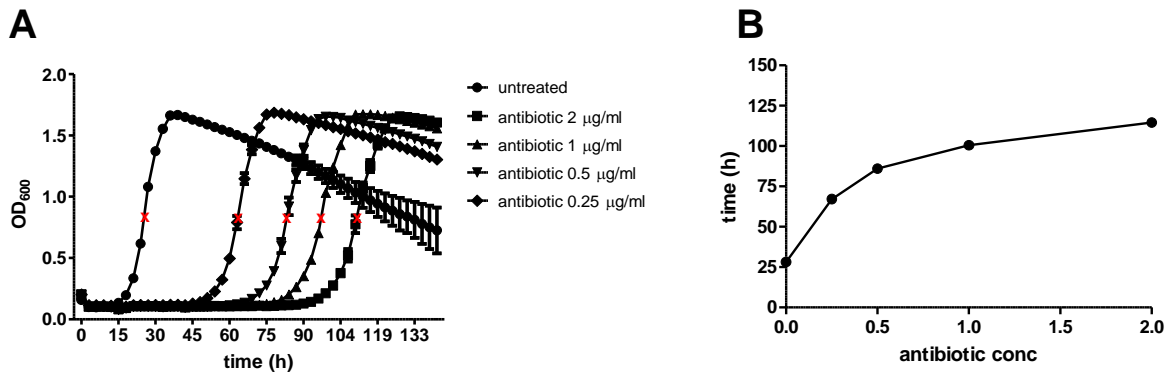
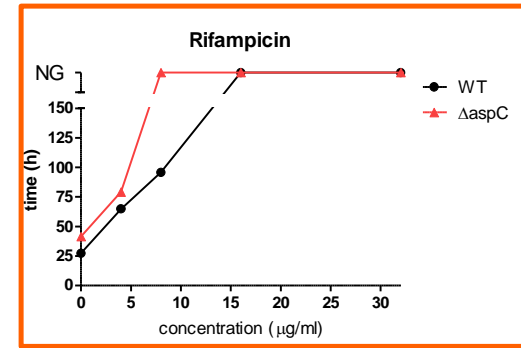
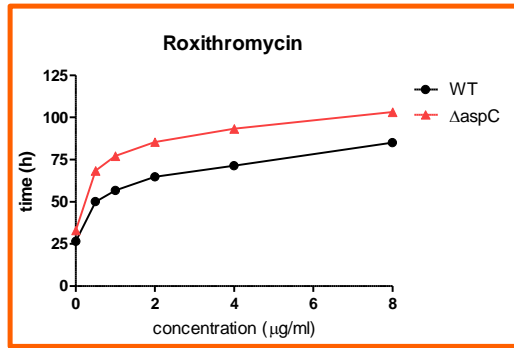
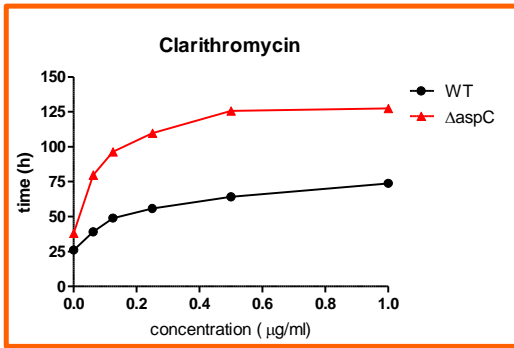
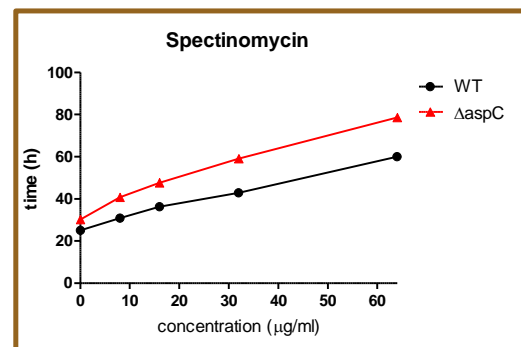
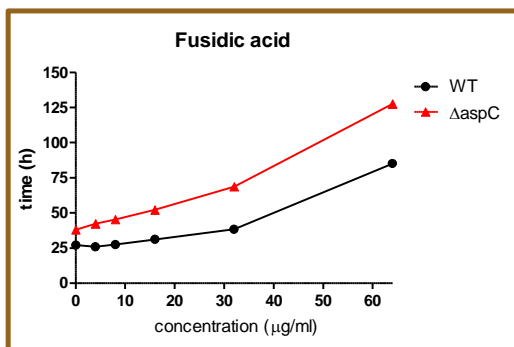
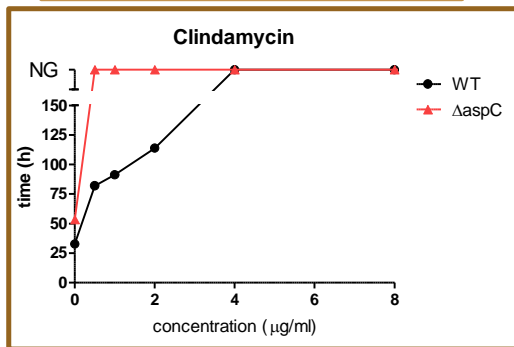


Figure 13. The time required for wild-type  $mc^2155$  to adapt and grow in media containing antibiotics is dependent on antibiotic concentration. (A) The time for recovery from stationary phase was increased by inoculation into various concentrations (0.25 – 2.0  $\mu\text{g/ml}$ ) of antibiotics. The growth at  $OD_{600\text{nm}}$  was monitored for 6 days. The time spent in lag phase was proportional to the concentration of the antibiotic. The point at which half-maximum  $OD_{600\text{nm}}$  (about 0.83) is marked by a red 'x' on each growth curve (B) The data from growth curves is represented as time to reach half-maximum  $OD_{600\text{nm}}$  versus antibiotic concentration.

**$\Delta aspC$  is 8-16 fold more susceptible**



**$\Delta aspC$  is 2-4 fold more susceptible**



**$\Delta aspC$  is not more susceptible**

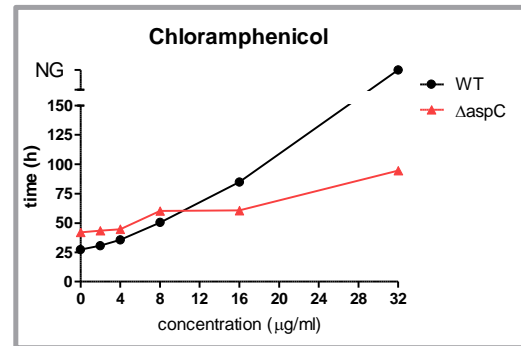
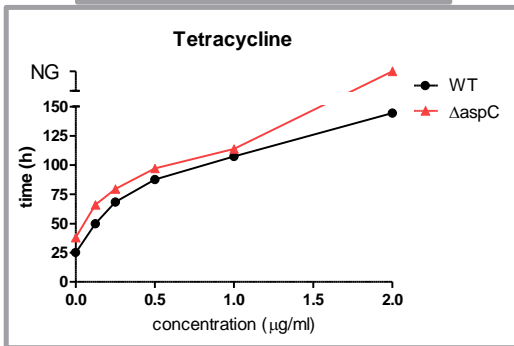
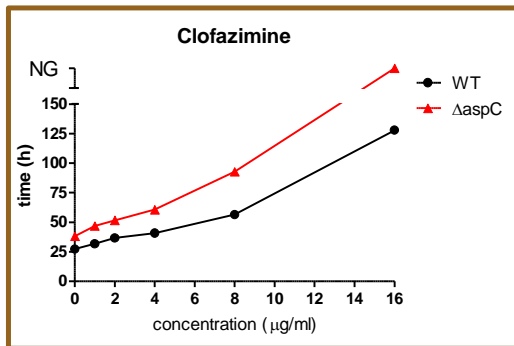


Figure 14. The difference between wild-type and the  $\Delta aspC$  mutant growth kinetics in media containing antibiotics. Stationary phase cultures of wild-type and mutant  $\Delta aspC$  were inoculated into media containing various concentration of nine antibiotics (clarithromycin, tetracycline, chloramphenicol, clindamycin, clofazimine, fusidic acid, rifampicin, roxithromycin, and spectinomycin). Growth of the bacteria was monitored at OD<sub>600nm</sub> for six days. The time for each cell growth to reach half-maximum OD<sub>600nm</sub> of its respective strain was plotted against antibiotic concentrations. No growth is indicated on the second segment of y-axis marked 'NG'. The difference between susceptibility of mutant  $\Delta aspC$  and wild-type towards an antibiotic determined by MTT MIC determination is indicated by border colors around each plot. Orange (8 to 16 fold more susceptible), brown (2 to 4 fold more susceptible), grey (not more susceptible)

### 3. 14. Differential killing of the $\Delta aspC$ mutant by clarithromycin

Time-kill curve experiment was performed to evaluate the susceptibility of mutant  $\Delta aspC$  compared to wild-type  $mc^2155$ . The mutant  $\Delta aspC$  was previously observed to have increased susceptibility to clarithromycin using both the MTT cell viability assay (Table 4) and growth curve analyses (Figure 14). Here the  $\Delta aspC$  strain exhibited a slower rate of death compared to wild-type (Figure 15). After 24 hours, wild-type  $mc^2155$  had decreased  $5 \log_{10}$  cfu/mL while mutant  $\Delta aspC$  only had a decrease of  $3 \log_{10}$  cfu/mL suggesting that mutant  $\Delta aspC$  is more resistant to killing by clarithromycin.

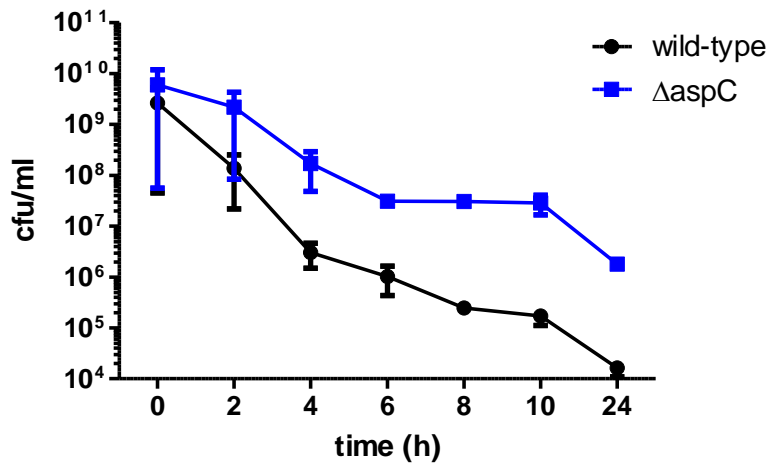


Figure 15. Differential killing of the  $\Delta aspC$  mutant by clarithromycin. Logarithmic phase cultures were treated with clarithromycin ( $15 \mu\text{g/ml}$ ). Samples were taken every 2 hours for cfu plating. The  $\Delta aspC$  maintained higher cell viability compared to wild-type at every time point. Data shown represents results from 2 biological experiments.

### 3. 15. Oxaloacetate and $\alpha$ -ketoglutarate modulate the rate of recovery from stationary phase growth and adaptation to bacteriostatic drugs

In addition to the classical lag phase observed after inoculation of stationary phase cultures into fresh medium, *M. smegmatis* also displayed a lag phase in response to bacteriostatic antibiotic treatments. When inoculated from antibiotic-free cultures into media containing low concentrations of bacteriostatic antibiotics (tetracycline, spectinomycin, or clarithromycin), onset of growth of *M. smegmatis* was delayed (Figure 16A). In both cases,  $\alpha$ -ketoglutarate in the medium consistently decreased the delay caused by antibiotics (Figure 16B-D). In contrast, oxaloacetate consistently prolonged the growth delay of the bacteria due to the presence of antibiotics (Figure 16B-D). Data are summarized in Table 5 and explained in more detail below.

Wild-type cultures growth in PB medium supplemented with 40 mM  $\alpha$ -ketoglutarate consistently entered exponential phase 4 to 5 hours earlier than in medium without  $\alpha$ -ketoglutarate (three independent experiments are shown in Figure 16B-D; Table 5). Conversely, growth in medium supplemented with 40 mM oxaloacetate delayed exponential phase by 24 to 27 hours (Figure 16B-D; Table 5). Based on these observations, we hypothesized that the drug sensitivity of  $\Delta aspC$  might be related to changes in intracellular concentrations of oxaloacetate and  $\alpha$ -ketoglutarate. To test this hypothesis, we analyzed the effects of oxaloacetate and  $\alpha$ -ketoglutarate on the growth inhibition activity of antibiotics. We used growth curve analysis to observe the growth inhibition of antibiotics alone and in combination with oxaloacetate or  $\alpha$ -ketoglutarate. Because  $\Delta aspC$  exhibited sensitivities to antibiotics of diverse classes we also chose to use drugs representing different ribosomal targets in order to determine whether the effects of oxaloacetate and  $\alpha$ -ketoglutarate are also similarly non-specific with respect to the class of antibiotic. Individually tetracycline (0.125  $\mu\text{g/ml}$ ), clarithromycin (0.25  $\mu\text{g/ml}$ ) and spectinomycin (4  $\mu\text{g/ml}$ ) delayed the growth of wild-type from 36 hours to 51, 63, and 64 hours respectively (Table 5, Figure 16A). When oxaloacetate was added to the medium at 40 mM the growth of *M. smegmatis* was delayed further by 64, 96, and 118 hours for tetracycline, clarithromycin, and spectinomycin respectively as compared to media without oxaloacetate. Conversely,  $\alpha$ -ketoglutarate promoted growth with and without antibiotic treatment. When  $\alpha$ -ketoglutarate was added to the medium, the growth delay of antibiotics was decreased to 44, 36, and 53 hours for tetracycline, clarithromycin and spectinomycin respectively. In summary, oxaloacetate potentiated the growth inhibition actions of antibiotics whereas  $\alpha$ -ketoglutarate increased the fitness of the bacterium, antagonizing the inhibition of antibiotics.

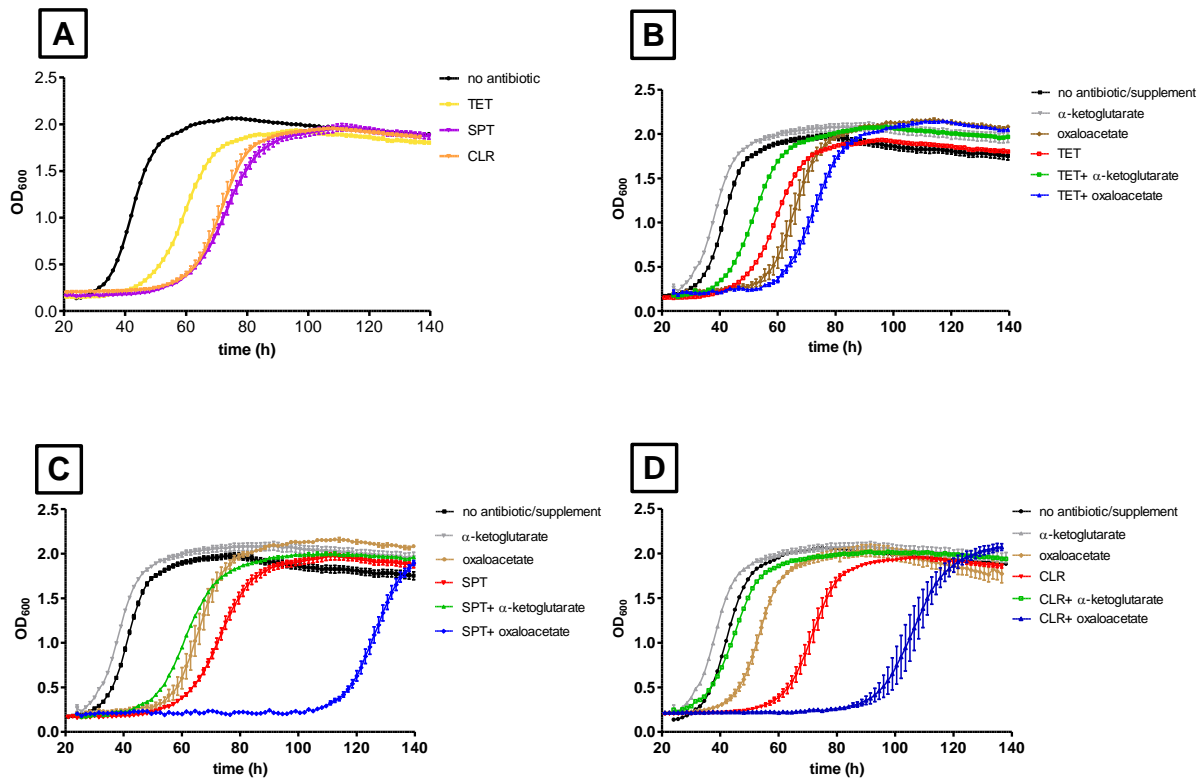


Figure 16. Effect of  $\alpha$ -ketoglutarate and oxaloacetate supplementation on growth kinetics and antibiotic inhibition of growth in wild-type *M. smegmatis*. (A) Growth of wild-type mc<sup>2</sup>155 in PB medium with 1/4-fold MICs of tetracycline (0.125  $\mu$ g/ml, TET, yellow), spectinomycin (4.0  $\mu$ g/ml, SPT, purple), or clarithromycin (0.25  $\mu$ g/ml, CLR, orange). (B-D)  $\alpha$ -ketoglutarate and oxaloacetate were added into PB at 40 mM. Oxaloacetate (tan) delayed growth of *M. smegmatis* and potentiated the effects of tetracycline (B), spectinomycin (C), and clarithromycin (D) (blue). The onset of growth was accelerated by the addition of  $\alpha$ -ketoglutarate (grey) and the growth delay due to tetracycline, spectinomycin, and clarithromycin was diminished with  $\alpha$ -ketoglutarate (green). Growth curves are representative of quadruplicate wells. Error bars indicate standard error. OD<sub>600</sub>, OD at 600 nm. Data are summarized in Table 5.

Table 5. Effect of antibiotics and putative aspartate transaminase substrates on time of recovery from stationary phase growth arrest. The table summarizes the time required to establish exponential growth defined at  $OD_{600nm} = 0.5$  in PB media supplemented with oxaloacetate and  $\alpha$ -ketoglutarate at 40mM and/or ¼-fold MIC sub-inhibitory concentrations of tetracycline (0.125  $\mu$ g/ml), clarithromycin (0.25  $\mu$ g/ml) or spectinomycin (4  $\mu$ g/ml).

Antibiotic ( $\mu$ g/ml)	Time to reach $OD_{600nm} = 0.5$ (hours)		
	Proskauer Beck	PB + $\alpha$ -ketoglutarate	PB + oxaloacetate
no treatment	36	31	58
tetracycline (0.125)	51	44	64
clarithromycin (0.25)	63	36	96
spectinomycin (4)	64	53	118

### 3. 16. Deletion of *aspC* causes a shift in intracellular redox homeostasis

By analogy to other bacteria, and metabolic pathways predicted by genome sequences, aspartate is likely to be a precursor for the nicotinamide adenine dinucleotide (NAD<sup>+</sup>) biosynthetic pathway in mycobacteria [118]. WhiB7 also plays a role in redox homeostasis and influences expression of *aspB* and *aspC*. Based on this information, we speculated that *asp* genes might have roles in maintaining intracellular redox balance. Since NADH and NAD<sup>+</sup> levels and ratios are important indicators of redox, we measured the levels of reduced (NADH) and oxidized (NAD<sup>+</sup>) nicotinamide adenine dinucleotide; these were quantified in wild-type,  $\Delta whiB7$ ,  $\Delta aspB$ ,  $\Delta aspC$  mutants, *hsp-aspB<sub>Mtb</sub>*, and *hsp-aspC<sub>Mtb</sub>* overexpression strains in early exponential phase (Figure 17A). A trend observed in mutant  $\Delta aspB$ , *hsp-aspB<sub>Mtb</sub>* and *hsp-aspC<sub>Mtb</sub>* was a decrease in the pools of NAD<sup>+</sup> (63%, 54%, and 58% of wild-type levels respectively) and no significant changes in NADH. The overall effect on the NADH:NAD<sup>+</sup> ratios of  $\Delta aspB$ , *hsp-aspB<sub>Mtb</sub>* and *hsp-aspC<sub>Mtb</sub>* was minor. The  $\Delta aspC$  mutant was notably different in that its pool of NADH and NAD<sup>+</sup> increased. This reflected the fact that while its NAD<sup>+</sup> levels were unchanged, NADH levels were elevated 2.5-fold relative to wild-type (Figure 17A). The higher NADH:NAD<sup>+</sup> ratio indicates a more reduced intracellular redox state (Figure 17B). In conclusion, deletion of *aspC* resulted in an increased pool of NADH and NAD<sup>+</sup> and a major shift in intracellular redox suggesting that it may be linked to redox homeostasis.

### 3. 17. Increased oxidative stress in the $\Delta aspC$ mutant

The  $\Delta aspC$  mutant was more sensitive to hydrogen peroxide and to ROS inducer menadione, as determined via a disc assay. Stronger growth inhibition of the  $\Delta aspC$  mutant compared to wild-type was indicated by larger zones of inhibitions (Figure 18). It should be noted that the observed sensitivity may be a by-product of the slower outgrowth of the  $\Delta aspC$  mutant which would allow more time for the diffusion of compound from the disc into the medium.

Results showing sensitivity of the  $\Delta aspC$  mutant to hydrogen peroxide and menadione led to the hypothesis that *aspC* may be linked to oxidative stress response in mycobacteria. Catalase is one of the pathways for detoxification of oxidative stress. In mycobacteria, catalase (KatG) is expressed in response to hydrogen peroxide [119] [120] by relieving the repression of *katG* by the oxidative stress response regulator OxyS [121]. The amount of catalase typically reflects the level of oxidative stress in the bacterium. The catalase activities of exponential phase cultures were determined by directly measuring the decrease of hydrogen peroxide by catalase in lysates. The catalase activity measured in the lysate of the  $\Delta aspC$  mutant was determined to be about four times that of wild-type (Figure 19A). Deletion or constitutive expression of *aspB* did not significantly affect catalase activity (Figure 19A). Treatment with hydrogen peroxide (20 mM) for 1 hour resulted in no change in wild-type catalase activity whereas the  $\Delta aspC$  mutant had a decreased catalase activity (about 36% decrease) (Figure 19B).

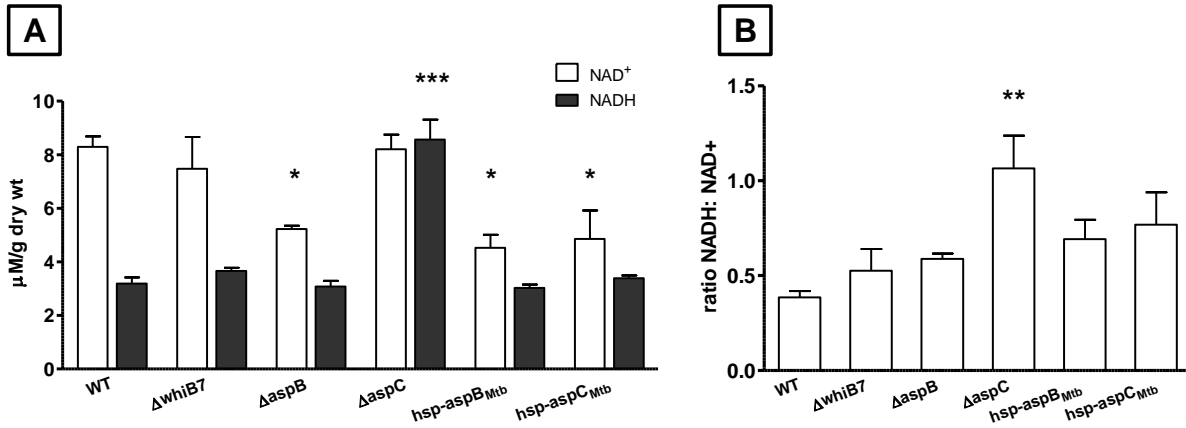


Figure 17. The  $\Delta aspC$  mutant has an altered redox state. (A) Determination of intracellular levels of NAD<sup>+</sup> and NADH in wild-type,  $\Delta whiB7$ ,  $\Delta aspB$ ,  $\Delta aspC$  mutants,  $hsp-aspB_{Mtb}$ , and  $hsp-aspC_{Mtb}$  overexpression strains. Mutant  $\Delta aspB$ ,  $hsp-aspB_{Mtb}$  and  $hsp-aspC_{Mtb}$  had decreased concentrations of oxidized NAD<sup>+</sup>. (B) The redox ratio (NADH:NAD<sup>+</sup>) was calculated from NAD<sup>+</sup> and NADH levels from A. The  $\Delta aspC$  mutant had more than double the concentration of NADH compared to wild-type causing the redox potential of the cytoplasm to become more reduced as indicated by the NADH:NAD<sup>+</sup> ratio. Results from triplicate measurements of 3 biological experiments. Values are the means  $\pm$  standard error. \* ( $P \leq 0.05$ ), \*\* ( $P \leq 0.01$ ), \*\*\* ( $P \leq 0.001$ ).

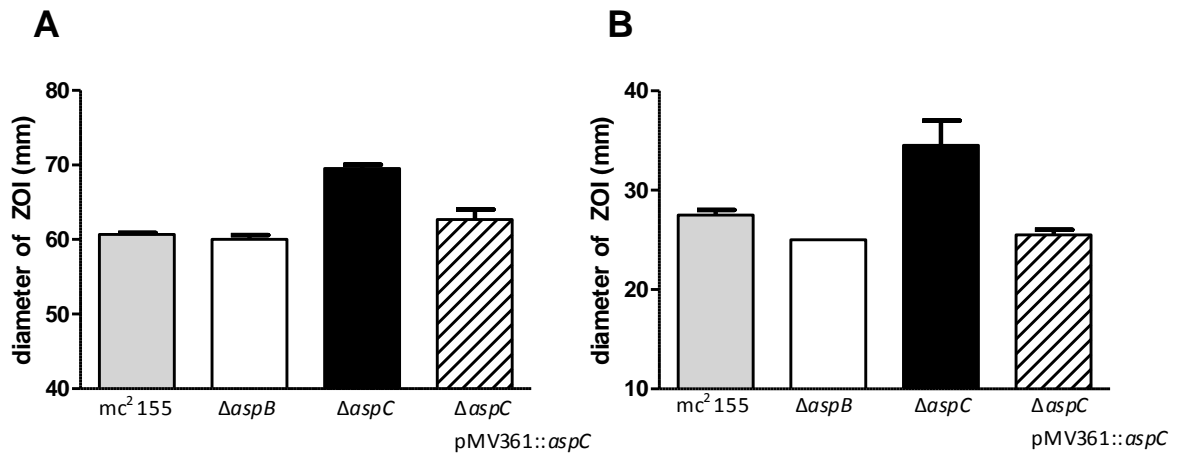


Figure 18. Sensitivity of mutants  $\Delta aspB$  and  $\Delta aspC$  to oxidative stress compounds hydrogen peroxide and menadione. The diameter of the zone of inhibition around the disc containing (A) 5  $\mu$ l of 30% hydrogen peroxide and (B) 5  $\mu$ l of 50 mM menadione solution was measured after incubation at 37°C for 48 h. The  $\Delta aspC$  mutant was more sensitive to both hydrogen peroxide and menadione as indicated by the larger zones of inhibition compared to wild-type. The sensitivity was suppressed in the complemented strain. Mutant  $\Delta aspB$  did not exhibit any sensitivity to either hydrogen peroxide or menadione.

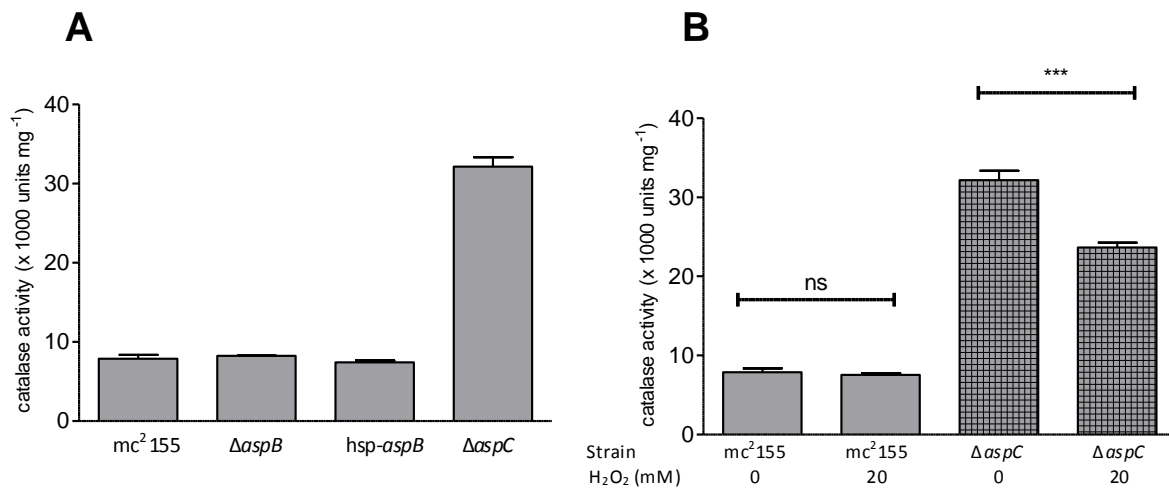


Figure 19. Higher oxidative stress in the  $\Delta$ aspC mutant reflected in catalase activity. (A) Catalase activity measured in total lysate of wild-type,  $\Delta$ aspB,  $\Delta$ aspC mutants, and hsp-aspB<sub>Mtb</sub> strains. The catalase activity found in  $\Delta$ aspC was four times that of wild-type. (B) Catalase activity in response in hydrogen peroxide treatment (20 mM H<sub>2</sub>O<sub>2</sub> for 1 hour). The catalase activity decreased after hydrogen peroxide exposure in the  $\Delta$ aspC mutant but was not affected in wild-type. ns (not significant), \*\*\* (P ≤ 0.0001).

### 3. 18. Phylogenetic analysis corroborates *aspB* and *aspC* as putative aminotransferases

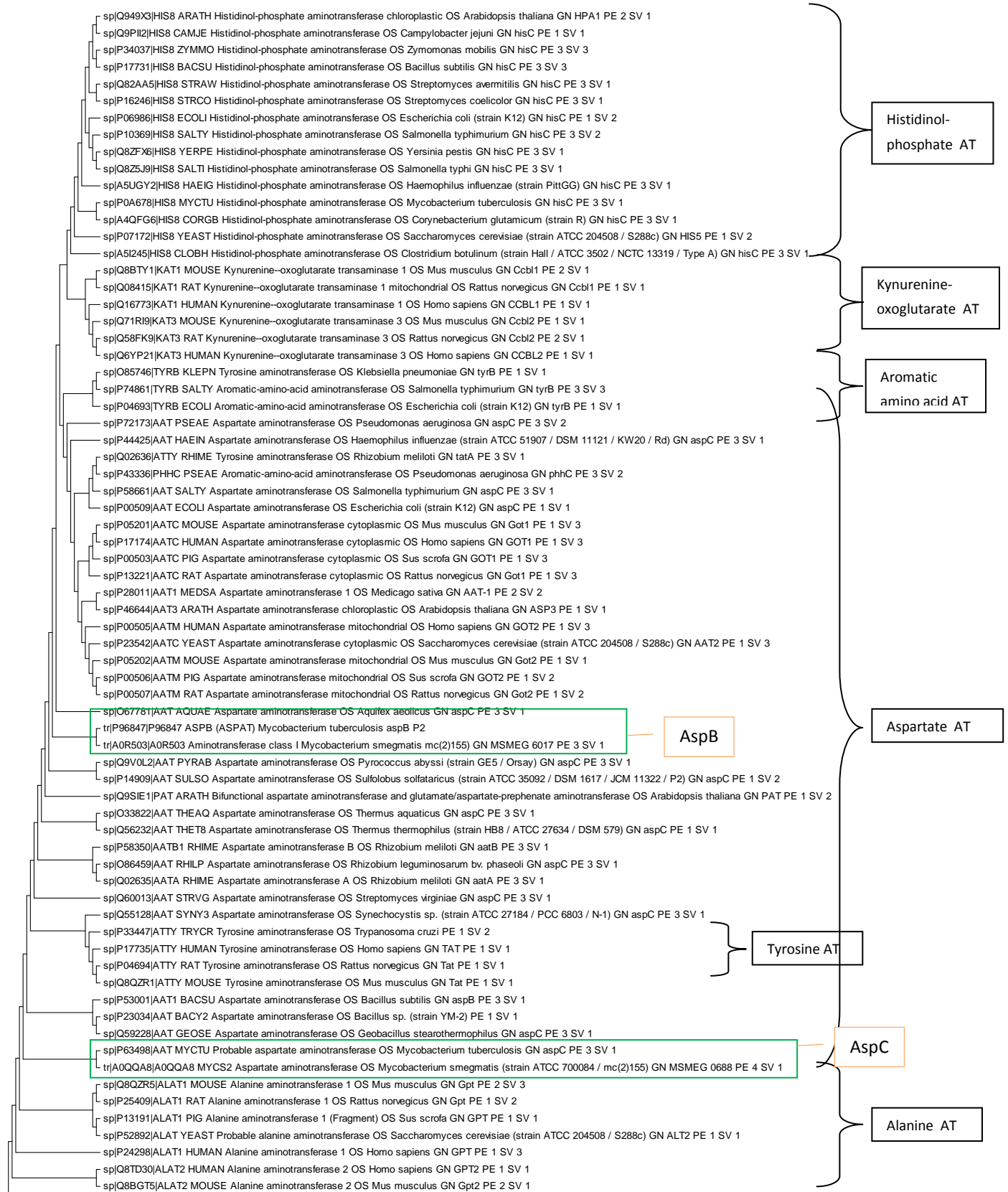
The function of AspB and AspC was analyzed using a phylogenetic approach based on amino acid sequence homology. Both AspB and AspC are annotated as aspartate aminotransferases. Aligning AspB<sub>Mtb</sub> and AspC<sub>Mtb</sub> sequences showed that they share 30% amino acid identity.

Under the premise that aminotransferases with similar catalytic activities would exhibit sequence homology, AspB and AspC amino acid sequences were compared to five classes of aminotransferases that are closely related to aspartate aminotransferases functionally and phylogenetically. Figure 20 shows comparison of 87 sequences of enzymes that are biochemically characterized as aspartate aminotransferases: alanine aminotransferases (EC 2.6.1.2), tyrosine aminotransferases (EC2.6.1.5), kynurnine-oxoglutarate aminotransferases (EC2.6.1.7), histidinol-phosphate aminotransferases (EC 2.6.1.9), aromatic amino acid aminotransferases, and branched-chain amino acid aminotransferases. As an internal control *M. tuberculosis* IlvE was included as it is the only mycobacterial aminotransferase to be structurally and functionally characterized [87]. As predicted, the *M. tuberculosis* IlvE clustered with the branched chain amino acid aminotransferases of *Pseudomonas*, *Staphylococcus* and *Haemophilus*. AspB was found clustered with aspartate aminotransferases of *S. solfataricus* and *T. thermophilus*. AspC was found with other aspartate aminotransferases as well (*Bacillus sp.*, *G. stearothermophilus*) but the proximity to alanine aminotransferases could suggest another function.

To examine the phylogenetic relationship of mycobacterial AspB and AspC with aspartate aminotransferases from plants, animals, protozoa, eubacteria and archeobacteria, a phylogram was constructed using the Neighbor-joining method. Aspartate aminotransferases are classified into the aminotransferase family I which is again separated into subgroups on the basis on their amino acid sequence [122,123] [124]. Subgroup Ia generally contain aspartate aminotransferases from eubacteria, eukaryotes, animals and plants while subgroup Ib contain almost exclusively aspartate aminotransferases from prokaryotes, including protozoa, archaeobacteria and eubacteria [125]. The amino acid sequence identities between subgroups Ia and Ib are only ~15% [125]. Figure 21 shows a phylogenetic tree of aspartate aminotransferases from different organisms. In the tree, AspB and AspC from *M. tuberculosis* clustered with other bacterial aspartate aminotransferases supporting potential structural and functional similarity to other bacterial aspartate aminotransferases. It is interesting that while AspB and AspC clustered with other Ib subgroup prokaryote-type aspartate aminotransferases, their sequences did not cluster with the main subgroup Ib branch: each occupies a separate periphery branch in the phylogeny tree.

Extensive work has been done in the field of eukaryotic and prokaryotic aspartate aminotransferases and key catalytic residues important for their function have been defined. The conserved active residues important to the function of family I aminotransferases have been thoroughly studied using X-ray crystallographic studies and site-directed mutagenesis experiments. We performed sequence alignment

analysis between aspartate aminotransferase from *E. coli* (AspC) and cytosolic aspartate aminotransferase from *Sus scrofa* (pig) and found that AspB and AspC from *M. tuberculosis* and *M. smegmatis* also appeared to have most of the conserved active residues of family I aminotransferases (Table 6). In addition, the signature amino acid motifs surrounding the conserved residues were found in AspB and AspC. An interesting note was that AspC from *M. tuberculosis* and *M. smegmatis* had an arginine residue that aligns with Arg292, which is found in subgroup Ia aspartate aminotransferases. This residue recognizes the distal carboxyl groups of dicarboxylate substrates. Aspartate aminotransferases from subgroup Ib typically rely on a Lys109 to perform this function but this residue was not found in either AspB or AspC. Studies on the substitution of Arg292 have shown that aspartate aminotransferase activity was greatly decreased by the mutation while other pyridoxal 5'-phosphate-dependent catalytic activities such as  $\beta$ -decarboxylation and racemization of L-aspartate increased [126]. Based on phylogenetic analysis, AspB and AspC possess sequence similarities to the family I within the protein superfamily of aminotransferases which includes aspartate aminotransferases. The arginine catalytic residue characteristic of subgroup Ia was found in AspC but not AspB. The absence of this important catalytic residue could have consequences for the enzymatic activity of AspB.



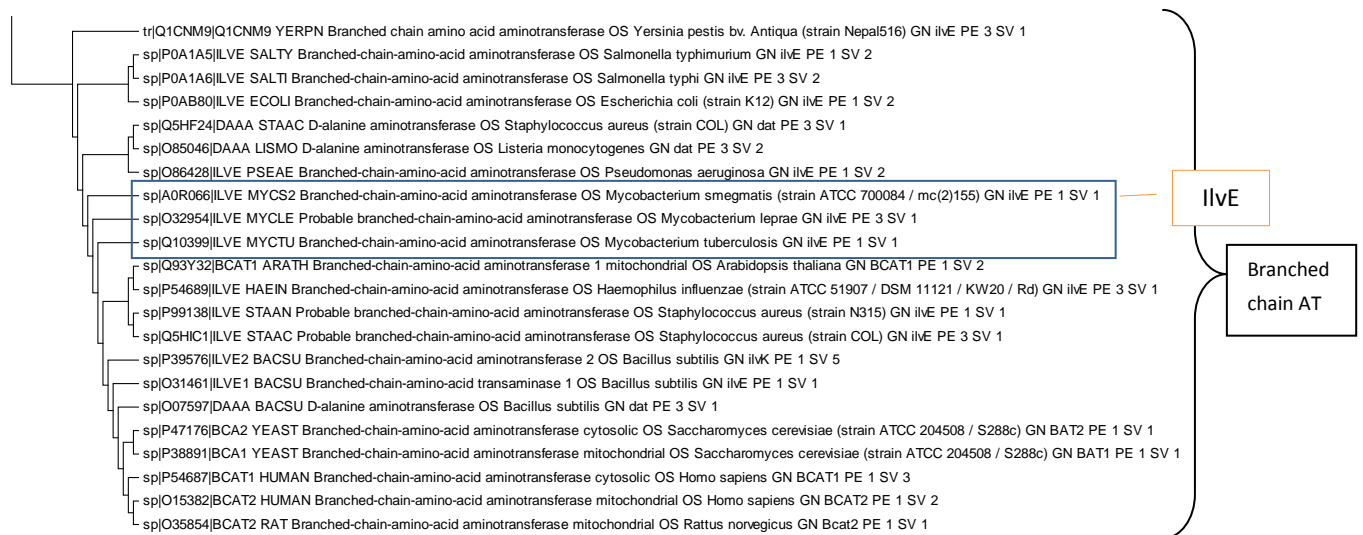


Figure 20. Phylogenetic tree showing amino acid homology of various aminotransferases: Both AspB and AspC clustered with other aspartate aminotransferase sequences. The phylogenetic tree was constructed with full-length amino acid sequences using MEGA 5.0. , based on Figure found in [127]. As a control the sequences of the branched chain aminotransferase (IlvE) of *M.tuberculosis* and *M.smegmatis* were included and both clustered with other branched chain aminotransferase sequences showing that amino acid sequences of functionally similar proteins cluster together in this tree.

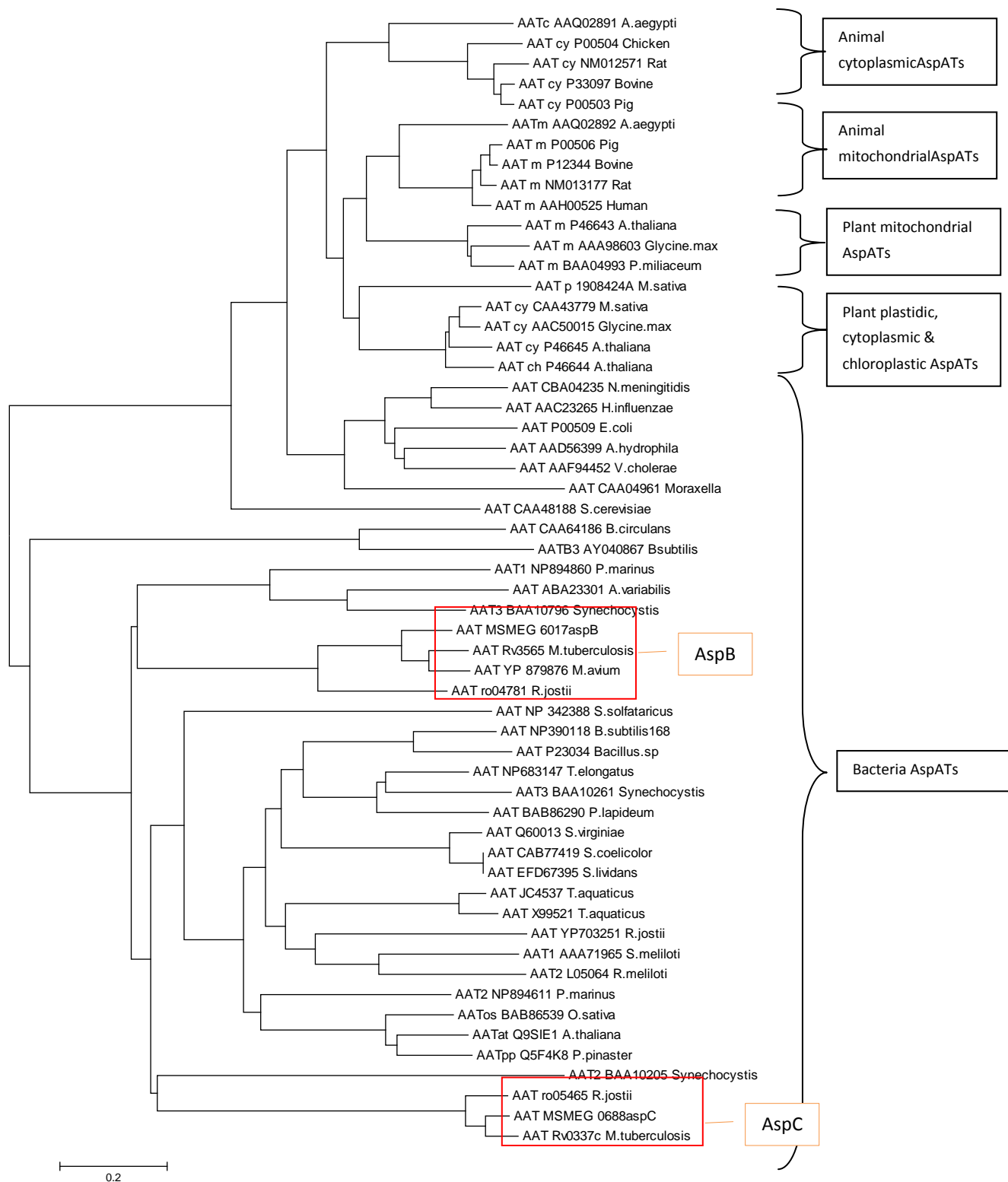


Figure 21. Neighbor-joining phylogenetic tree of aspartate aminotransferases from different organisms: AspB and AspC from *M.tuberculosis* and *M.smegmatis* were found to have strong sequence homology with other bacterial aspartate aminotransferases. The phylogenetic tree was based on figure in [128] and constructed with full-length amino acid sequences using MEGA 5.0.

Table 6. Functions of anchor residues in family I aminotransferases. Based on [127]

hierarchical level of invariance	residue	functional role	Residue in			
			AspB <sub>Mtb</sub>	AspC <sub>Mtb</sub>	AspB <sub>Msm</sub>	AspC <sub>Msm</sub>
Alpha division of PLP-dependent proteins	K-258	forms Schiff base with PLP	K-234	K-265	K-237	K-260
	D-222	forms salt bridge by H-bonding with the pyridine N-1 of PLP	D-202	D-232	D-205	D-227
Aminotransferase superfamily	G-197	accommodates the turn at the interdomain interface	G-177	G-207	G-180	G-202
	R-386	forms salt bridge by H-bonding with $\alpha$ -COO <sup>-</sup> of substrate	R-364	R-403	R-364	R-404
Family I aminotransferases	Y-70	H-bond to phosphate OP2 of PLP and stabilizes transition state	Y-64	Y-92	Y-67	Y-87
	G-110	unknown role	G-102	NF	G-105	NF
	N-194	H bonds to hydroxyl O-3' of PLP regulating electron distribution	N-174	N-204	N-177	N-199
	P-195	has <i>cis</i> conformation within span of interdomain interface	P-175	P-205	P-178	P-200
	Y-225	H bonds to hydroxyl O-3' of PLP regulating electron distribution	Y-205	Y-235	Y-208	Y-230
	R-266	H bonds with phosphates OP2 and OP4 of PLP	R-242	R-273	R-245	R-268
	G-268	unknown role	G-244	G-275	G-247	G-270
Subgroup I $\alpha$	R-292	recognizes the distal carboxyl groups of dicarboxylate substrates	NF	R-299	NF	R-300
Subgroup I $\beta$	Y-109	recognizes the distal carboxyl groups of dicarboxylate substrates	NF	NF	NF	NF

NF: residue not found

### 3. 19. Complementation of aspartate auxotrophy in *E. coli* with $AspB_{Mtb}$ and $AspC_{Mtb}$

The homologies of AspB and AspC suggested their functions as transaminases but did not clarify their substrates. Furthermore, since the *M. smegmatis* strain with mutations in both *aspB* and *aspC* had no amino acid auxotrophy (Figure 10), the metabolic functions of these genes were unclear. *E. coli* was used to explore the metabolic function of  $AspB_{Mtb}$  and  $AspC_{Mtb}$ . In *E. coli* (and by analogy Mycobacterium), aspartate auxotrophy is dependent on several alleles, including the *aspC* ortholog. In order to observe auxotrophy for aspartate in an *E. coli aspC* mutant, the genes *ilvE* and *tyrB*, encoding a branched-chain aminotransferase and aromatic amino acid aminotransferase respectively, also need to be mutated [129]. Aminotransferases have discrete specificities but there is also cross-specificities and activities. Aromatic amino acid aminotransferase TyrB and branched-chain amino acid aminotransferase IlvE can complement the mutation in the other gene [130]. Aspartate aminotransferase AspC can also catalyze the transamination of the keto-acids phenylpyruvate and 4-hydroxyphenylpyruvate to form phenylalanine and tyrosine respectively, albeit at a lower rate with lower affinity for the substrates [129,131]. We obtained the auxotroph DL39 with mutations in *aspC*, *ilvE*, and *tyrB* auxotrophy for leucine, isoleucine, valine, tyrosine, phenylalanine and aspartate [98] from the *E. coli* Genetic Stock Center. We hypothesized that extra-chromosomal expression of  $aspB_{Mtb}$  and  $aspC_{Mtb}$  would be able to complement the activity of the mutated *aspC* in DL39 if AspB and AspC were indeed able to catalyze the aspartate aminotransferase reaction. The genes  $aspB_{Mtb}$  and  $aspC_{Mtb}$  along with the hsp60 promoter was cloned from pMV361-*aspB* and pMV361-*aspC* respectively using restriction sites XbaI and HindIII and ligated into pUC19 (Figure 22). The mycobacterial hsp60 promoter is active in *E. coli* as it is orthologous to the GroEL protein of *E. coli* [132]. The constructs pUC19::hsp- $aspB_{Mtb}$  and pUC19::hsp- $aspC_{Mtb}$  were transformed into DL39 and plated onto LB plates with ampicillin selection. The transformants were grown onto 56/2 minimal media agar plates [99] with and without amino acids (leucine, isoleucine, valine, tyrosine, phenylalanine, and aspartate at 0.3 mM). Both DL39 pUC19:: $aspB_{Mtb}$  and DL39 pUC19:: $aspC_{Mtb}$  exhibited the same auxotrophy as DL39, requiring supplementation of all the six amino acids for growth.

The hsp60 promoter drives constitutive expression of  $aspB_{Mtb}$  and  $aspC_{Mtb}$  although higher levels of expression might be required to complement the auxotrophy. AspB and AspC may have lower catalytic efficiency and lower substrate affinity than *E. coli* AspC for the transamination of aspartate thus requiring higher expression levels to compensate for the mutation. Also, cloning the indigenous *aspC<sub>Eco</sub>* gene in the same manner to act as a positive control would help indicate whether the hsp60 promoter is driving sufficient levels of expression.

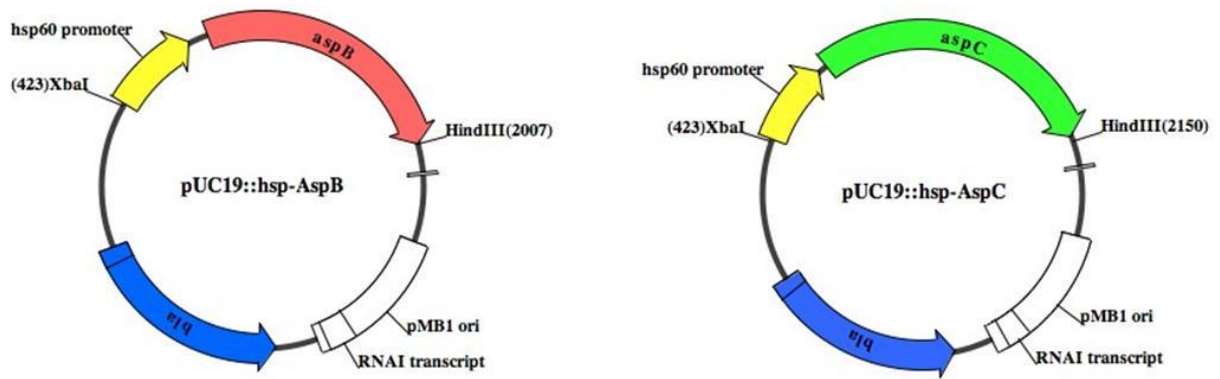


Figure 22. Vector maps of pUC19::hsp-*aspB* and pUC19::hsp-*aspC*. Constructs were transformed into the amino acid auxotroph DL39.

### **3. 20. Amino acid auxotroph DL39 does not exhibit general growth deficiencies and does not show increased antibiotic susceptibility**

The deletion of *aspC* in *M. smegmatis* caused many growth deficiencies in the strain (Figure 7). To determine whether this phenomenon can be extended to other bacteria, the growth kinetics of the amino acid auxotroph DL39, which has also has a mutation in its *aspC* gene, was studied. The growth curve of DL39 was very similar to that of its wild-type, MG1655. The two strains entered into exponential growth at similar time and the doubling rates during exponential growth were similar. The growth of DL39 decreased more quickly than MG1655 growth resulting in a lower cell density at stationary phase; the *M. smegmatis* mutant  $\Delta$ *aspC* also displayed a decreased cell density in stationary phase (Figure 23).

The *M. smegmatis*  $\Delta$ *aspC* mutant also showed increased antibiotic susceptibility. To test whether deletion of *aspC* would also cause increased antibiotic susceptibility in *E. coli*, the MICs of amino acid auxotroph DL39 against tetracycline, clarithromycin, and spectinomycin were determined using MTT assay and compared with the MICs of those antibiotics in wild-type MG1655. There was no significant difference in antibiotic susceptibility between wild-type MG1655 and amino acid auxotroph DL39 (Table 7).

Additionally, oxaloacetate was able to delay growth of *M. smegmatis* at high concentrations (40-80 mM) leading us to test whether oxaloacetate can also be toxic to *E. coli*. At 40 mM oxaloacetate, growth of *E. coli* MG1655 was inhibited by approximately 45% while at 80 mM growth was further depressed to 22% of untreated control. There was no significant difference in susceptibility towards oxaloacetate between wild-type MG1655 and amino acid auxotroph DL39 (Figure 24).

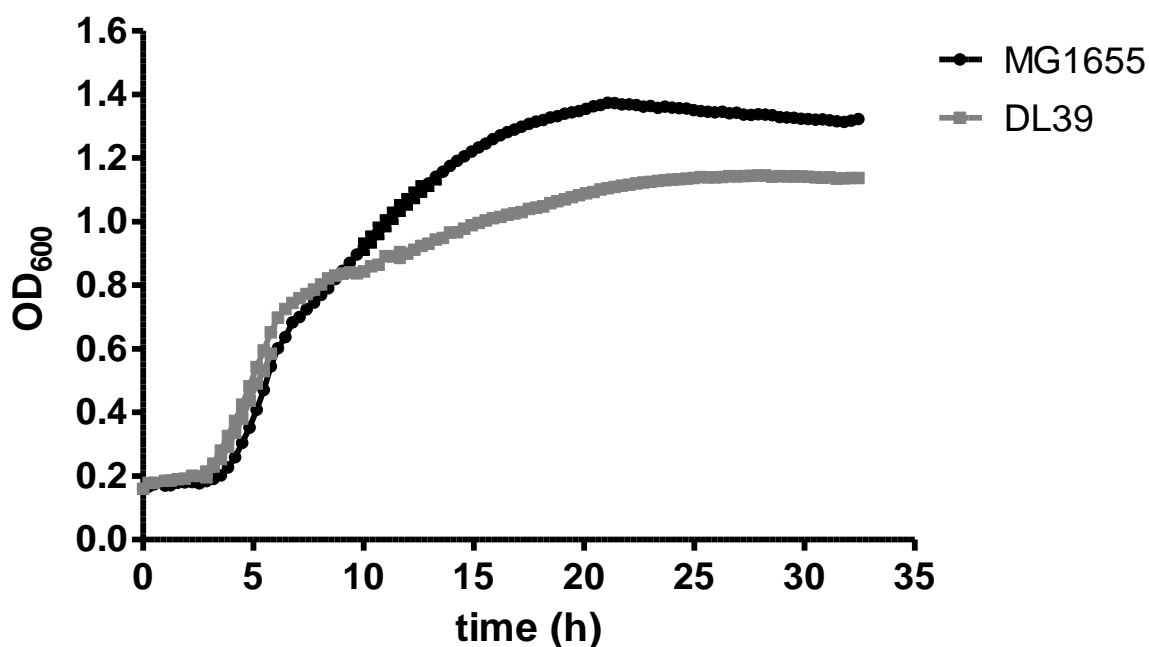


Figure 23. Amino acid auxotroph DL39 has a lower cell density at stationary phase. *E. coli* strains MG1655 and DL39 in quadruplicate wells were grown in a Bioscreen C kinetic growth reader at 37 °C with constant shaking at maximum amplitude. Growth was monitored by the Bioscreen by measuring OD<sub>600nm</sub>. The growth kinetics of *E. coli* MG1655 and amino acid auxotroph DL39 in LB show that the mutant has a similar doubling rate as compared to wild-type but enters into stationary phase earlier, resulting in a lower final cell.

Table 7. Amino acid auxotrophic strain DL39 does not show changes in antibiotic susceptibility. The MICs of wild-type (MG1655) and amino acid auxotroph DL39 for antibiotics tetracycline, clarithromycin, and spectinomycin were determined by MTT assay in LB medium. The MICs of wild-type (MG1655) and amino acid auxotroph DL39 for antibiotics tetracycline, clarithromycin, and spectinomycin were similar.

	MIC <sub>90</sub> (µg/ml)	
	MG1655	DL39
tetracycline	0.16	0.31
clarithromycin	16	16
spectinomycin	16	16

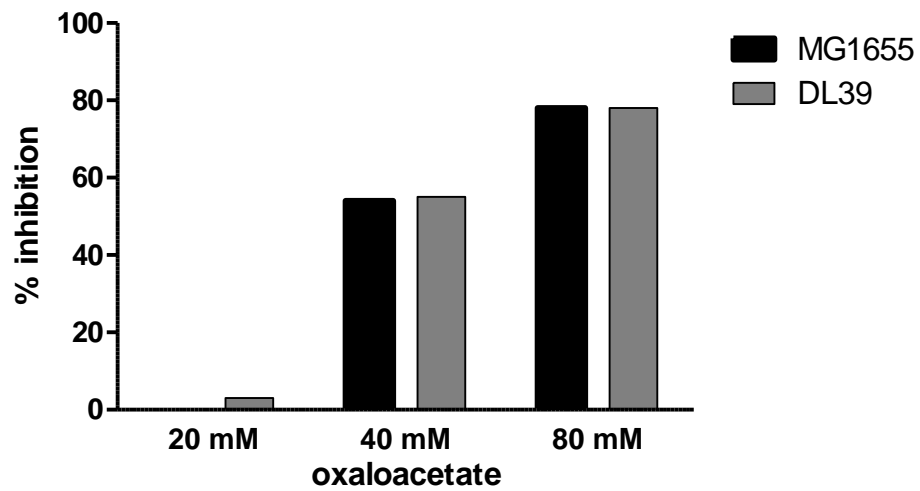


Figure 24. Oxaloacetate inhibited growth of *E. coli* at 40mM and 80mM. MG1655 and DL39 were grown in LB in the presence of oxaloacetate. Percent inhibition compared to untreated control of the strains was determined using MTT viability assay. No difference in oxaloacetate susceptibility was observed between wild-type MG1655 and amino acid auxotroph DL39.

### 3. 21. Expression and purification of AspB<sub>Mtb</sub> and AspC<sub>Mtb</sub>

To confirm AspB and AspC as aspartate aminotransferases, the activities of the purified enzymes would need to be determined experimentally. The *asp* genes were cloned into a pGEX-based vector (GELifesciences) for expression as recombinant GST-tagged proteins (Figure 25). Protein production in *E. coli* BL21 was verified after overnight induction with IPTG at room temperature. While the GST affinity purification system was chosen for properties of increasing protein solubility and purifying soluble GST fusion proteins, most of the GST-tagged AspB and AspC were insoluble under non-denaturing conditions. Inclusion of 1.5% sarkosyl in the lysis buffer increased solubility of the proteins and 2% triton increased binding to glutathione matrix [107].

Affinity purification on a glutathione sepharose column yielded purified GST-AspB and GST-AspC as observed by SDS PAGE and silver staining (Figure 26). The purified GST-tagged proteins were assayed for aspartate aminotransferase activity using the assay described in section 2.25 but no catalysis was observed suggesting that the GST moiety may be sterically hindering the activities of the Asp proteins due to its relatively large size. Thus, we proceeded to remove the GST-tag via cleavage of an engineered thrombin cleavage site between the tag and the Asp proteins.

Thrombin specifically cleaved and released AspB from the GST tag. However, attempts at removing free GST using the same glutathione matrix left a significant amount of free GST in the flow-through with the cleaved AspB protein. Additional purification steps were required to separate the free GST from AspB<sub>Mtb</sub> after protease cleavage (Figure 27).

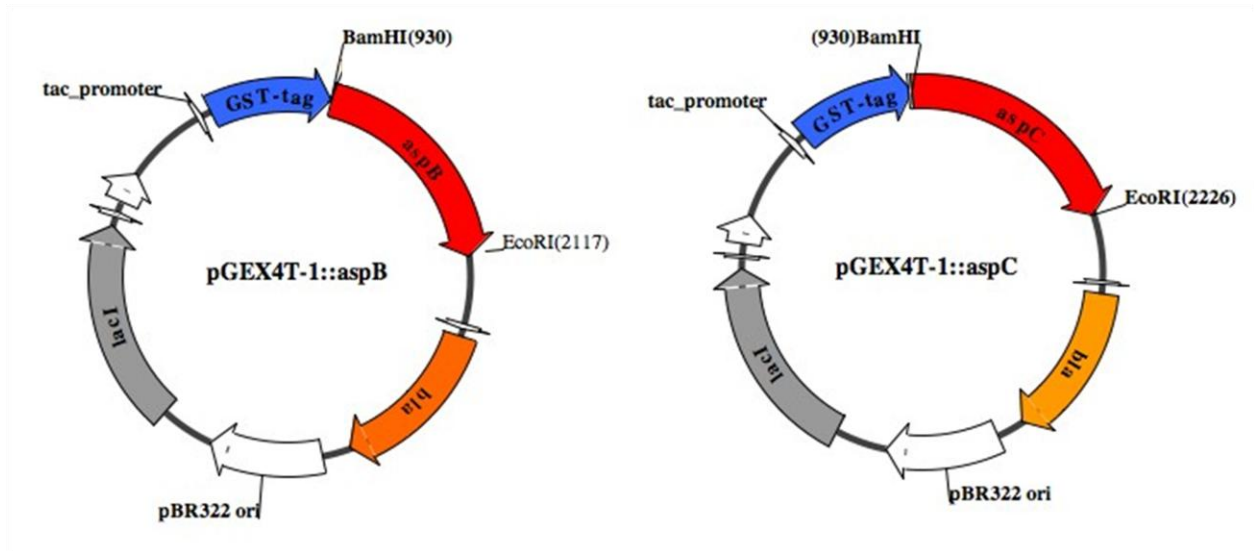


Figure 25. Expression vector maps for GST-tagged recombinant protein expression. The genes *aspB* and *aspC* from *M. tuberculosis* were cloned into pGEX4T-1 (GE) for expression of GST-tagged recombinant AspB and AspC in *E. coli* BL21.

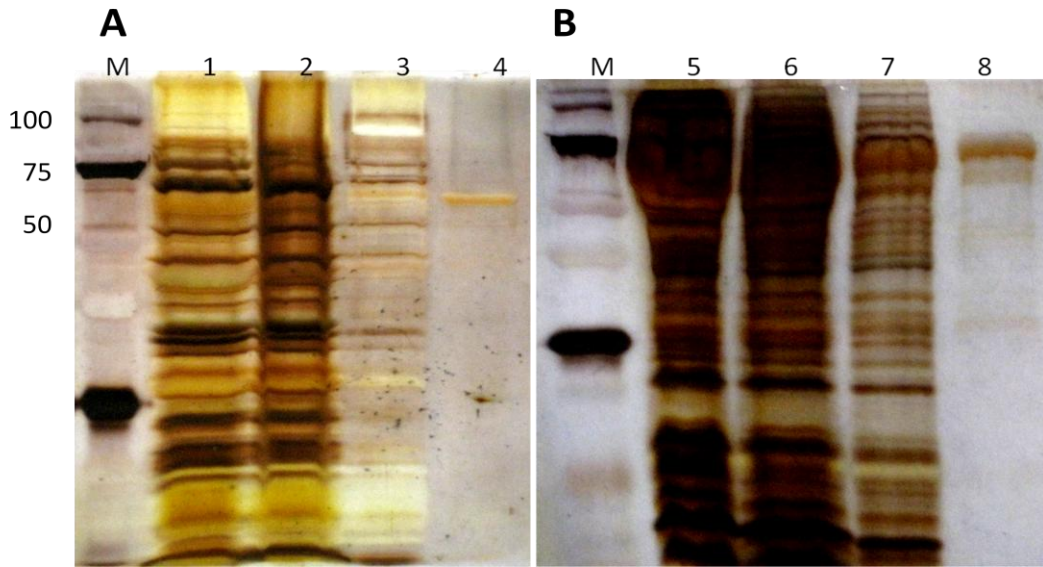


Figure 26. Purification of AspB<sub>Mtb</sub> and AspC<sub>Mtb</sub> using GST affinity chromatography. GST-tagged AspB and AspC were expressed in BL21 *E. coli* and purified on a Glutathione Sepharose 4B column. (A) Purification of GST-AspB. Lane 1 whole cell lysate. Lane 2 unbound fraction. Lane 3 wash fraction. Lane 4 GST-AspB elution. (B) Purification of GST-AspC. Lane 5 whole cell lysate. Lane 6 unbound fraction. Lane 7 wash fraction. Lane 8 GST-AspC elution. M, molecular weight marker. The eluted tagged proteins were of the expected size: AspB approximately 67 kDa. and AspC approximately 73 kDa.

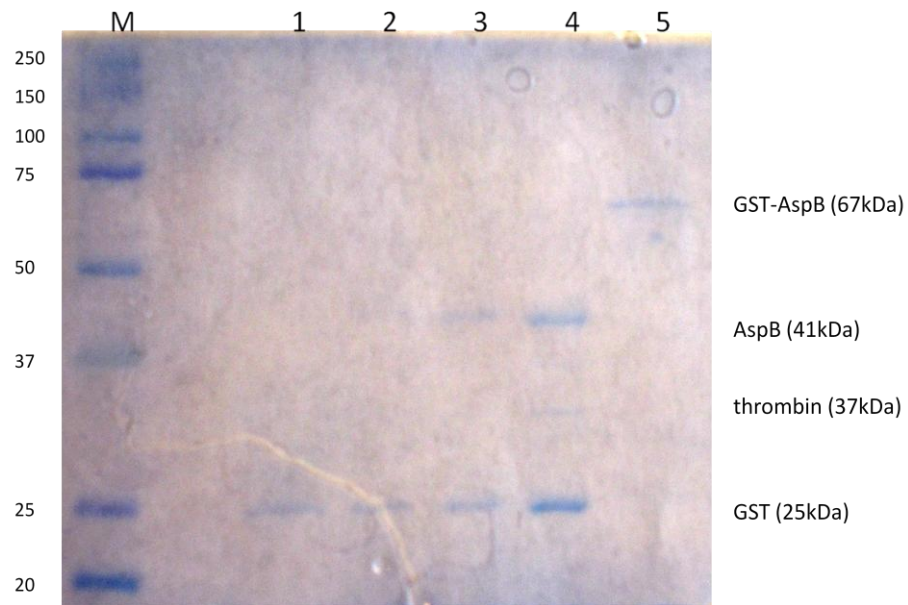


Figure 27. Removal of GST-tag from recombinant protein GST-AspB<sub>Mtb</sub>. Lane 1 to 4 GST protein still remaining in solution along with cleaved AspB after clean-up with a glutathione sepharose column. Lane 5 uncut GST-AspB. M, molecular weight marker. Thrombin successfully removed the GST-tag from AspB but free GST was difficult to remove from solution.

Removal of the GST fusion tag from GST-AspC using the engineered thrombin cleavage site was unsuccessful. Thrombin has secondary recognition sites that cleaved within AspC<sub>Mtb</sub> (Figure 28). The primary recognition site for thrombin is P4-P3-P-R/K● P1'-P2' with the bond between R/K●P1' being the scissile bond (as denoted by ●). At P4 and P3 are hydrophobic residues and residues at P1' and P2' are non-acidic [133]. The thrombin cut site between the GST and recombinant AspC<sub>Mtb</sub> is LVPR●GS. However, thrombin also cuts at secondary sites such as P2-R/K●P1' where P2 or P1' is a glycine residue (Figure 28). This less stringent secondary site can be found throughout AspC<sub>Mtb</sub> and this could allow for the many degradation products observed when GST-AspC<sub>Mtb</sub> was cleaved with thrombin (Figure 29). Many conditions, including shortened incubation time, lower protease to protein ratio, and lower reaction temperature, were altered in attempt to reduce the affinity of thrombin for the secondary recognition sites but all were found to be ineffective (Figure 29). In addition, the AspC protein appeared unstable and seemed to degrade spontaneously.

The GST tag expression system was effective at achieving expression of both AspB and AspC in soluble form. However, the relatively large size of the GST protein, 26 kDa compared to 41 kDa and 47 kDa for AspB and AspC respectively, made it necessary to remove the fusion tag as it hindered the catalytic activities of AspB and AspC. Moreover, the fusion tag removal system with thrombin was problematic as thrombin possesses too many secondary activities.

**A**

Amino acid position								reference
P4	P3	P2	P1	P1'	P2'	P3'	P4'	
L	V	P	R	G	S			[133]
hydrophobic	hydrophobic	G	R/K	G				[133]
	hydrophobic	P	R					[134]
L/G	G/T/R/M/V	P/G/V	R	S/A/G/T	W/G/F/S	R	V/L/S/R	[135]

**B**

MSPILGYWKI**K**GLVQPTRLLEYLEEKYEELHYERDEGDKWRNKKFELGLEFPNLPYYIDGDVKTQSMAIRYIADKHNMLGGCPKERAEISMLEGAVLDIRYGVSRVIAYSKDFETLKVDLFLSKLPEMLKMFEDRLCHKTYLNGDHVTHPDFMLYDALDVLYMDPMCLDAFPKLVCFKKRIEAIPIQIDKYLKSSKYIAWPLQGWQATFGGGDHPKSD**LVPRGS****VDNDGTIVDVTT****HQLPWHTASHQRQRAFAQSAKLQDVLYEIRGPVHQHAARLEAEGHRILKLNIGNPAPFGFEAPDVIMRDIIQALPYAQGYSDSQGILSARRAVVTRYELVPGF**PR**FDVDDVYLVNGVSELITMTLQALLDNGDQVLIPSPDYPLWTASTSLAGGTPVHYLCDETQGWQPDIADLESKITERTKALVVINPNNPTGAVYSCEILTQMVDL**ARK**HQLLLLADEIYDKILYDDAKHISLASIAPDMLCLTFNGLSKAYRVAGYRAGWLAITGPKEHASSFIEGIGLLANMRLCPNVPAQHAIQVALGGHQSIEDLVLPGGRLLQRDIAWTKLNEIPGVSCVKPAGALYAF**PR**LDPEVYDIDDDEQLVLDLLLSEKILVTQGTGFNWPAPDHLRLVTLPWSRDAAAIERLGNFLVSYRQZ**

Figure 28. GST-AspC<sub>Mtb</sub> contain many putative secondary thrombin cleavage sites. (A) thrombin recognition cleavage sites. Thrombin cleaves bond between P1 and P1'. While thrombin typically cuts the bond on the carboxyl end of an arginine residue, many other residues can be substituted in the recognition sequence. (B) Amino acid sequence of recombinant fusion protein GST-AspC<sub>Mtb</sub>. The AspC<sub>Mtb</sub> sequence is in bold print. The engineered thrombin cut site is highlighted in yellow while putative secondary cut sites are highlight in blue.

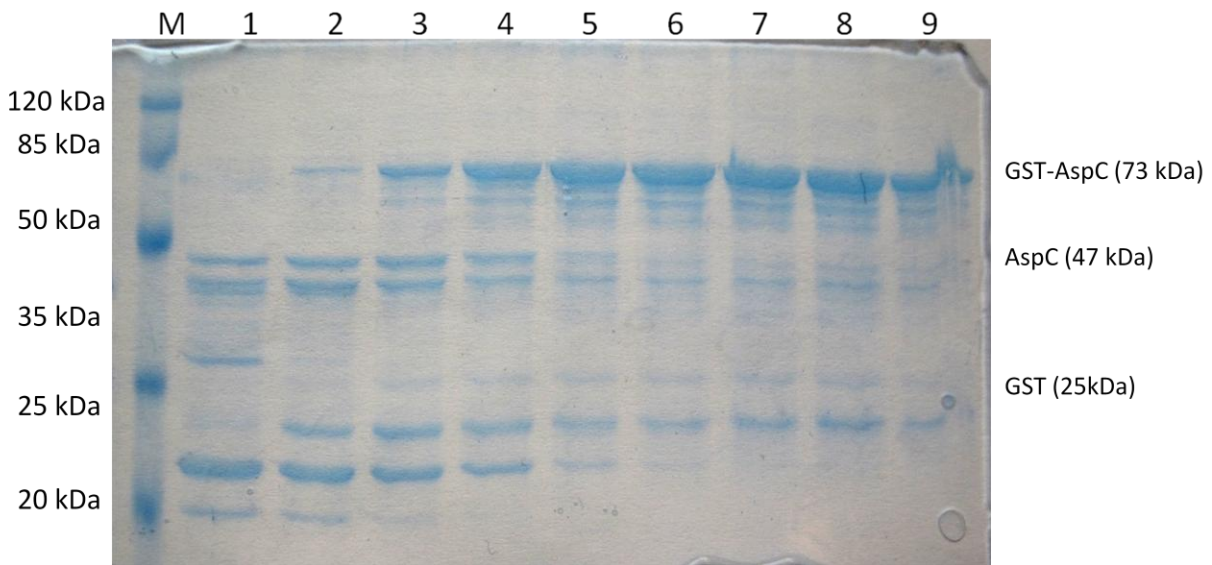


Figure 29. Thrombin cleavage of GST-AspC<sub>Mtb</sub>. 50 µg of GST-AspC<sub>Mtb</sub> was cleaved by varying amount of thrombin at 4°C for 18 hours: Lane 1 9000 ng. Lane 2 1800 ng. Lane 3 360 ng. Lane 4 72 ng Lane 5 15 ng. Lane 6 3 ng. Lane 7 0.6 ng. Lane 8 0.12 ng. Lane 9 no thrombin control. M, molecular weight marker. . Protein instability and secondary thrombin recognition sites cause non-specific degradation of GST-AspC<sub>Mtb</sub>. Low temperature and high protein to protease ratio did not diminish non-specific cleavage.

Given the difficulties with the GST constructs, His affinity purification was chosen for purification of AspB and AspC as the His tag is a relatively small fusion tag. The *aspB* and *aspC* genes were cloned into pET-based vectors for expression (Figure 30) in Rosetta2 *E. coli* which possesses the plasmid pRARE2 (Novagen) allowing for the expression of tRNAs for rare codons as mycobacteria have a G/C-rich genome while the genome of *E. coli* is A/T-rich. His-AspB was expressed in *E. coli*, found to be soluble and then purified using affinity chromatography on a nickel column followed by removal of His tag via enterokinase cleavage (Figure 31). N-terminal His tagged AspC was expressed but was found in inclusion bodies so another vector for addition of a C-terminus His tagged onto AspC was cloned as well (Figure 30B). As with purification of GST-AspC, addition of sarkosyl in the lysis buffer increased solubility of His-AspC and allowed for purification on a nickel column (Figure 32). However, due to the low yield (100 µg per litre of culture) of His-AspC purification, other expression systems were explored.

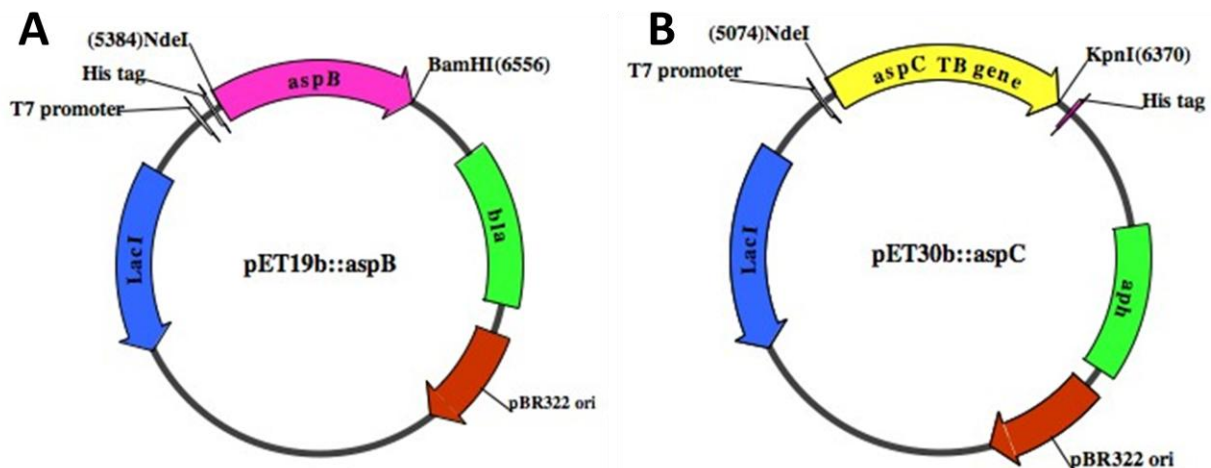


Figure 30. His-tagged AspB<sub>Mtb</sub> and AspC<sub>Mtb</sub> expression vectors. *aspB*<sub>Mtb</sub> was cloned into pET19b for expression of recombinant AspB with a N-terminus histidine tag. *aspC*<sub>Mtb</sub> was cloned into pET30b for expression of recombinant AspC with a C-terminus histidine tag.

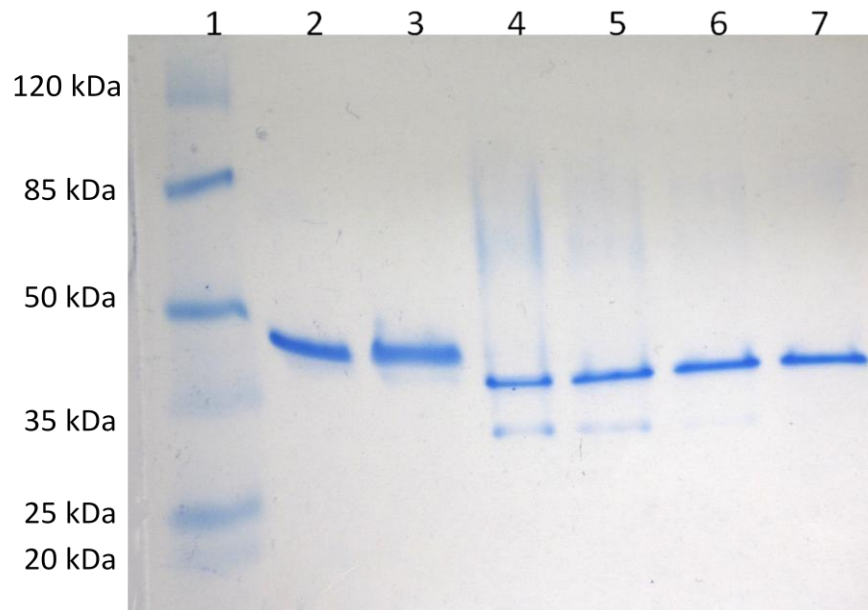


Figure 31. Purified AspB<sub>Mtb</sub> and His-tag removal. N-terminal His-tagged AspB<sub>Mtb</sub> (~ 45 kDa) was expressed in *E. coli* Rosetta 2 (DE3) and purified to apparent purity using nickel column affinity chromatography. Tag removal using the engineered enterokinase cleavage site proceeded at room temperature for 2 h. Lane 1 Marker; Lane 2 purified His-AspB; Lane 3 cleavage negative control (no enterokinase added); Lane 4 protein to enterokinase ratio at 500:1; Lane 5 1000: 1; Lane 6 2500:1; Lane 7 5000:1. Addition of too much protease resulted in a secondary cleavage product at approximately 31 kDa (Lanes 4, 5 and 6). The optimal ratio of protein to protease was determined to be 5000:1 (Lane 7)

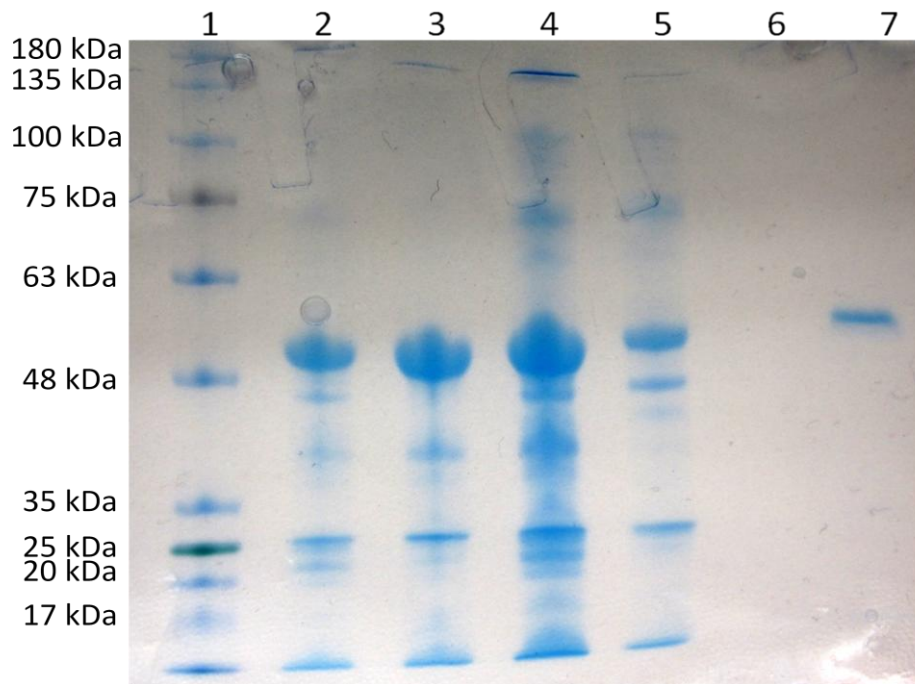


Figure 32. Purification of C-terminal His-tagged AspC<sub>Mtb</sub>. His-tagged AspC<sub>Mtb</sub> (~ 51 kDa) was expressed in *E. coli* Rosetta 2 (DE3) and purified to apparent purity using nickel column affinity chromatography. Lane 1 Marker; Lane 2 total expression in whole cells; Lane 3 insoluble fraction; Lane 4 cell free lysate; Lane 5 unbound fraction; Lane 6 blank; Lane 7 eluted His-AspC<sub>Mtb</sub>. A large portion of recombinant AspC was found in the insoluble fraction (Lane 3) reducing the yield of the purification.

In order to obtain soluble AspC for purification many different systems were tested. Expression conditions such as low IPTG concentration induction, low temperatures, or heat shock did not increase protein solubility. Variation of the His tag placement or even expression without His tag also did not improve solubility. Co-expression of AspC with chaperone proteins such as GroEL-ES that can aid in protein folding and increase the recovery of soluble proteins did not improve the solubility of AspC. Even expression in *M. smegmatis* [97], a close relative of *M. tuberculosis*, generated mostly insoluble AspC. The systems tested for expression of soluble AspC are summarized in Table 8.

Table 8. Expression of AspC<sub>Mtb</sub> in *E. coli* and *M. smegmatis*. A variety of systems were explored to generate enzymatically active *M. tuberculosis* AspC protein. One *M. smegmatis* and four *E. coli* and *aspC* expression plasmids were constructed and tested for expression under a variety of conditions. All constructs generated recombinant AspC<sub>Mtb</sub> detectable as bands using SDS PAGE, only one (designated in bold print) was used for protein purification (in bold) that was subsequently used in biochemical analyses (aspartate aminotransferase activity using methods described in section 2.21 and 2.25). The results are found in Figure 32 and Table 9.

Expression plasmid	Fusion tag	Expression strain	Expression conditions	comments
pGEX4T-1::aspC	N-terminal GST	BL21	0.25 mM IPTG, 17 h, room temperature	soluble with 1.5% sarkosyl and 2% triton
pET19b::aspC	N-terminal His	Rosetta 2 (DE3)	42°C for 30 min then 0.5 mM IPTG, 17 h, room temperature	tRNAs for rare codons supplied by pRARE2
<b>pET30b::aspC</b>	<b>C-terminal His</b>	<b>Rosetta 2 (DE3)</b>	42°C for 30 min then 0.5 mM IPTG, 4 h, 37°C	tRNAs for rare codons supplied by pRARE2
			<b>42°C for 30 min then 0.2 mM IPTG, 17 h, room temperature</b>	<b>tRNAs for rare codons supplied by pRARE2</b>
			42°C for 30 min then 0.1 mM IPTG, 17 h, 10°C	tRNAs for rare codons supplied by pRARE2
pET30b::aspC	C-terminal His	BL21 (DE3)	1 mM IPTG, 5 h, 37°C	
			1 mM IPTG, 5 h, 37°C	dnaK-dnaJ-grpE and groES-groEL co-expression (pG-KJE8, Takara Bio Inc.)
			1 mM IPTG, 5 h, 37°C	groES-groEL co-expression (pGro7, Takara Bio Inc.)
			1 mM IPTG, 5 h, 37°C	groES-groEL-tig co-expression (pG-Tf2, Takara Bio Inc.)
			1 mM IPTG, 5 h, 37°C	tig co-expression (pTf16, Takara Bio Inc.)
pET30b::aspC	no fusion tag	Rosetta 2 (DE3)	0.5 mM IPTG, 3 h, 37°C	tRNAs for rare codons supplied by pRARE2
			0.05 mM IPTG, 20 h, 15°C	tRNAs for rare codons supplied by pRARE2
pYUB1062::aspC	C-terminal His	mc <sup>2</sup> 4517	0.05 mM IPTG, 22 h, 37°C	Expression in <i>M. smegmatis</i>

### 3. 22. Aspartate aminotransferase activity of AspB<sub>Mtb</sub> and AspC<sub>Mtb</sub>

Purified recombinant his-tagged AspB<sub>Mtb</sub> and AspC<sub>Mtb</sub> expressed from *E. coli* each migrated as a single band on SDS-PAGE at their predicted theoretical masses (45 kDa and 51 kDa respectively) (Figures 31 and 32). The preparations were assayed for aspartate aminotransferase activity. The assay measures glutamate formation by transamination from aspartate to  $\alpha$ -ketoglutarate. The specific activity measured for recombinant AspB<sub>Mtb</sub> was measured at  $2.62 \times 10^{-2}$  units per milligram and recombinant AspC<sub>Mtb</sub> has a specific activity for aspartate transamination at  $5.34 \times 10^{-2}$  units per milligram (Table 9). The specific activities of purified AspB and AspC were comparable to reported specific activities of other purified aspartate aminotransferases (Table 9)

Steady-state kinetic parameters for AspB<sub>Mtb</sub> were determined for the reaction of glutamate formation by transamination from aspartate to  $\alpha$ -ketoglutarate (Table 10). The Michaelis constants,  $K_m$  for aspartate and  $\alpha$ -ketoglutarate determined for AspB<sub>Mtb</sub> is comparable to that reported for *E. coli* aspartate aminotransferase AspC<sub>Eco</sub> by Toney and Kirsch [136]. However, the catalytic constant,  $k_{cat}$ , is over 500-fold smaller than AspC<sub>Eco</sub> making the efficiency of AspB<sub>Mtb</sub>, as calculated by  $k_{cat}/K_m$ , a poor aspartate aminotransferase.

Table 9. Specific activities of purified aspartate aminotransferases.

Enzyme	Organism	Specific activity (U/mg)	Reference
aspartate aminotransferase (from heart)	<i>Sus scrofa</i> (pig)	620-690	[137]
AspC	<i>E. coli</i>	200-232	[138] [139]
aspartate aminotransferase -2	<i>Medicago sativa</i> L.(alfalfa root)	130-240	[140]
aspartate aminotransferase	<i>Bacillus</i> sp. strain YM-2	220	[141]
AspB	<i>M. tuberculosis</i>	$2.62 \times 10^{-2}$	this study
AspC	<i>M. tuberculosis</i>	$5.34 \times 10^{-2}$	this study

Table 10. Comparison of steady state kinetic parameters determined for AspB<sub>Mtb</sub> and AspC<sub>Eco</sub>. Kinetic data for AspC from *E. coli* retrieved from Toney and Kirsch [136]

Substrate	AspB ( <i>Mtb</i> )			AspC ( <i>Eco</i> )		
	$k_{cat}$ (s <sup>-1</sup> )	$K_m$ (mM)	$k_{cat}/K_m$ (M <sup>-1</sup> s <sup>-1</sup> )	$k_{cat}$ (s <sup>-1</sup> )	$K_m$ (mM)	$k_{cat}/K_m$ (M <sup>-1</sup> s <sup>-1</sup> )
aspartate	0.29 ± 0.01	1.07 ± 0.07	270 ± 10	160	1.83	87 000
α -ketoglutarate		0.36 ± 0.03	800 ± 50		0.47	340 000

## 4. Discussion

### 4. 1. *aspB* and *aspC* expression is linked to *whiB7* expression

The putative aspartate aminotransferases *aspB* and *aspC* were both identified as genes in the WhiB7-controlled regulon, suggesting that they might have roles in intermediary metabolism and intrinsic drug resistance. The transcription regulator WhiB7 is expressed in response to antibiotics as well as other stress conditions such as heat shock, iron starvation, and entry into stationary phase [24]. *whiB7* is also implicated in *M. tuberculosis* virulence because it is upregulated within resting or activated macrophages [36]. A screen of hundreds of bioactive compounds revealed that the expression of *whiB7* can be induced by compounds having diverse structures and targets and that the induction of *whiB7* expression is strongly affected by the reducing potential of the cytoplasm [35]. Here we further explore the link between metabolism and intrinsic drug resistance showing *aspB* and *aspC* have essential roles in both processes.

In *E. coli*, aspartate is synthesized by *aspC<sub>Eco</sub>* in which oxaloacetate receives an amino group from glutamate. The expression of *aspC<sub>Eco</sub>* is reported to be constitutive [142] [143], based only on the observation that aspartate does not repress expression, unlike other transaminase paralogues [144]. The *aspB* and *aspC* genes were first linked to antibiotic resistance through microarray studies of the WhiB7-controlled transcriptome of *M. tuberculosis*. Given the homologies of *M. tuberculosis* and *M. smegmatis* *aspB*, *aspC*, and *whiB7* genes (80%, 88%, and 71% amino acid identity respectively), we decided to study their regulation using qRT-PCR in the *M. smegmatis* model system. WhiB7 induced expression of *aspC* when *whiB7* was either constitutively expressed from a heat shock promoter or highly induced by tetracycline (Figure 4 and 5B). However, there was no measurable change in *aspB<sub>SMG</sub>* in response to *whiB7<sub>Mtb</sub>* expression or tetracycline induction, suggesting that *aspB* is not antibiotic induced or under WhiB7's control. The fact that *aspC<sub>Msm</sub>* expression responded to tetracycline as well as either *whiB7<sub>Mtb</sub>* (heat shock promoter expression) or *whiB7<sub>Msm</sub>* (heat shock promoter and tetracycline induced) demonstrated that *whiB7* regulation of *aspC* is similar in both organisms and that *M. smegmatis* was a reliable surrogate model. The observations that expression of *aspC* was regulated by WhiB7 and *aspC* was upregulated by tetracycline pointed towards a role for AspC in the intrinsic resistance mechanisms of mycobacteria.

*whiB7* expression is autoregulated [29,35] and its activity as a transcriptional activator depends on other regulatory signals including the reducing potential of the cytoplasm [35]. One of these elements could be AspC (or dependent genes) because the activation (often over 1000-fold) of *whiB7* in response to tetracycline was diminished (but not eliminated) in the  $\Delta$ *aspC* mutant (Figure 5A). While *aspC* expression alone upregulated *whiB7* slightly, the fact that there was no significant change in *whiB7* expression in response to tetracycline in the *hsp-aspC<sub>Mtb</sub>* strain provided evidence that *aspC* acts generally to amplify *whiB7* expression in response to a primary metabolic inducer (Figure 6A). Results showed that while

expression of *whiB7* is autoregulatory, full activation of the *whiB7* promoter depends on WhiB7 [35] as well as AspC. It is likely that in response to antibiotics AspC expression acts to change the physiological state of the bacterium, which then promotes *whiB7* expression. Thus *whiB7* and *aspC* are components of the same autoregulatory loop.

In contrast, constitutive expression of *aspB* strongly inhibited both *whiB7* and *aspC*. Even under non-inducing (no tetracycline) conditions, the expression of *whiB7* was reduced by more than 90% (Figure 6A). After tetracycline treatment, *whiB7* induction was reduced by 99.98% in the strain constitutively expressing *aspB<sub>Mtb</sub>* (Figure 6A). AspB activity appears to generate a signal for downregulation of *whiB7* that overrides the strong upregulatory signal generated by tetracycline. It would follow that if AspB expression prevented *whiB7* expression, then *aspC* would also not be upregulated. Indeed, levels of *aspC* in  $\Delta$ *whiB7* (Figure 5B) and *aspB<sub>Mtb</sub>* constitutive expression strains (Figure 6B) were very similar. *aspB* expression was unaffected by tetracycline treatment (Figure 5B), *whiB7* or *aspC* expression; other aspects of *aspB* regulation remain to be elucidated.

A model used for coordinated regulation of both *aspB* and *aspC* by *whiB7* is presented schematically in Figure 33. Expression of *aspB* causes downregulation of *whiB7* by suppressing signals generated by antibiotics that upregulate *whiB7*. The expression of *aspC* is dependent on *whiB7*. When *whiB7* is upregulated in response to tetracycline, *aspC* expression is also upregulated in a *whiB7*-dependent manner; when *aspB* expression depresses the tetracycline-induced upregulation of *whiB7*, *aspC* upregulation is also abolished. The study on interrelation of *whiB7*, *aspB*, and *aspC* gene regulation showed that the regulation of expression of *whiB7*, a mycobacterial regulator of intrinsic resistance, is connected to expression of metabolic genes *aspB* and *aspC*.

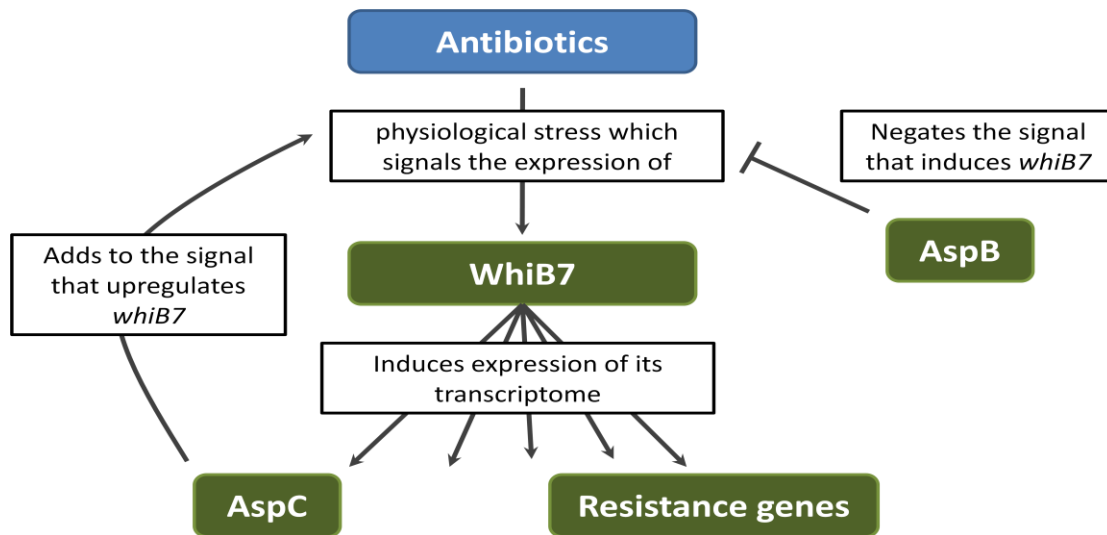


Figure 33. Schematic representation of the proposed antibiotic induced regulatory network of *whiB7*, *aspB*, and *aspC*. Antibiotic treatment results in physiological stress which upregulates expression of *whiB7*. *WhiB7* induces expression of the transcriptome which includes *aspC*. *AspC* acts to enhance the *whiB7*-inducing signals, which further amplifies *whiB7* expression. *AspB* neutralizes/suppresses the signal, so that *whiB7* and *aspC* are not upregulated when *aspB* is expressed.

## 4. 2. Intermediary metabolism of mycobacteria is linked to intrinsic antibiotic resistance

Because expression of *aspB* and *aspC* were tightly linked to regulation of *whiB7* and associated intrinsic resistance in mycobacteria, we reasoned that there might be a link between these aspartate aminotransferases and antibiotic resistance. Knock-out mutants of *aspB* and *aspC* were made using recombineering [95]. Both genes were non-essential, however *aspC* was required for optimal growth. This observation seemed consistent with results of transposon site hybridization (TraSH) screen of an insertion mutant library [93] as well as a high-density mutagenesis and deep sequencing study [52,93] to identify mutations that impair *in vitro* growth of *M. tuberculosis*. A deep sequencing transposon insertion mapping study recently revealed that certain portions of the coding sequence within the *aspB* coding sequence are required and function as non-protein-coding RNAs or cis regulatory elements [52]. The growth of the *aspC* transposon mutant was reduced compared to wild-type *M. tuberculosis* leading to the conclusion that *aspC* is essential for optimal growth. Observations that mutation of *aspC* affects growth of *M. smegmatis*, *M. bovis* BCG, and *M. tuberculosis* in culture suggest that the role of AspC is conserved across mycobacteria [93]. By analogy, it is also likely that *aspC* is required for optimal growth *in vivo*. However there is a complication with this analysis, it cannot be excluded that the preculture used for infection no longer contained *aspC* mutants and thus was not reported as required for survival during infection [145]. Our studies showed that intermediary metabolism of *M. smegmatis* was affected by the disruption of *aspC*; the  $\Delta$ *aspC* mutant was impaired in using aspartate as nitrogen or carbon source (Table 3). Furthermore, the *M. smegmatis*  $\Delta$ *aspC* mutant exhibited generalized growth defects such as slower growth rate and prolonged lag phase (Figure 7). Addition of  $\alpha$ -ketoglutarate to the medium restored the growth rate to wild-type levels but the prolonged lag phase remained, suggesting that a different element caused that defect (Figure 8A). Passaging the  $\Delta$ *aspC* mutant in  $\alpha$ -ketoglutarate-containing media to allow the strain to acclimatize did not shorten the lag, showing that the delay in growth was not due to the strain requiring time to activate alternative metabolic pathways (Figure 9).  $\alpha$ -ketoglutarate was able to suppress other physiological deficiencies and consequently the antibiotic susceptibility of  $\Delta$ *aspC* mutant. This demonstrates that AspC has roles in growth as well as antibiotic resistance (Figure 12), providing further evidence that mycobacterial intermediary metabolism is linked to intrinsic antibiotic resistance.

Interestingly, the addition of oxaloacetate to the growth media produced a greater effect than  $\alpha$ -ketoglutarate on the growth of wild-type. Oxaloacetate inhibited the growth of wild-type (Figure 16B-D). In essence,  $\alpha$ -ketoglutarate seemed to increase bacterial fitness while oxaloacetate decreased fitness. The cause of the growth rate decrease in  $\Delta$ *aspC* may be due to increased oxaloacetate in a model where AspC uses it as a substrate.  $\alpha$ -ketoglutarate and oxaloacetate appeared to modulate the growth inhibitory effects of bacteriostatic antibiotic treatments (Table 5, Figure 16).

Oxaloacetate consistently potentiated the growth inhibition activity of tetracycline, clarithromycin and spectinomycin while  $\alpha$ -ketoglutarate partially suppressed the inhibition by antibiotics. Similarly, growth of  $\Delta aspC$  was multi-drug sensitive and addition of  $\alpha$ -ketoglutarate to the medium suppressed this effect (Figure 12). It is hypothesized that increased oxaloacetate in  $\Delta aspC$  leads to growth inhibition and antibiotic sensitivity. The fact that the antibiotic sensitivity profile of the  $\Delta aspC$  mutant was similar to that of  $\Delta whiB7$  suggested that oxaloacetate metabolism may also be disrupted in the *whiB7* mutant. Considering the transcriptional activation of *aspC* by WhiB7, WhiB7 may act to regulate oxaloacetate and  $\alpha$ -ketoglutarate pools in the bacterium and AspC may be a primary determinant of intrinsic resistance. Oxaloacetate toxicity has been reported in Lactococcus fermentation causing reduced growth rates and lower biomass yields [146,147]. Although the reason for its toxicity was not explained, it was speculated that high oxaloacetate concentrations can competitively inhibit other essential metabolic enzymes, such as those in the TCA cycle. Transamination of oxaloacetate would relieve the stress [148]. Another method to detoxify oxaloacetate is to export it out of the cell via malate and citrate transporters [148,149]. These transporters have broad specificities and also transport other 2-oxocarboxylates. The transport of 2-oxocarboxylates such as oxaloacetate requires exchange with a partner (precursor/product exchange) and results in the generation of a membrane potential [149]. Addition of  $\alpha$ -ketoglutarate may relieve the transmembrane stress generated by oxaloacetate (Figure 16B-D) either by acting as an exchange molecule having similar ionic properties, or by inducing expression of additional transporters.

The opacification of 7H10 agar by the  $\Delta aspC$  mutant suggested precipitation of components in the medium, perhaps involving the export of acidic metabolites. The precipitate might be the metabolite itself or other components of the medium 7H10. Acidic metabolites such as pyruvate, malate, succinate, lactate, and fumarate have been detected in *M. tuberculosis* culture supernatant during growth [150]. Extracellular accumulation of secreted succinic acid and lactic acid was observed in anaerobic cultures of *M. tuberculosis* [74]. Under these conditions, decreased growth rates as well as accumulation of reduced cofactors such as NADH (resulting in a high NADH/NAD<sup>+</sup> ratio), are probably due to the absence of oxygen as the terminal electron acceptor [74]. The secretion of succinic acid was due to reversal of the TCA cycle, allowing the bacterium to maintain sufficient membrane proton gradient for persistence, but not active growth [74]. The  $\Delta aspC$  mutant exhibited shared features of *M. tuberculosis* physiology during hypoxic/anaerobic growth, including reduced growth rate, acid secretion, and a more reduced pool of NADH. It is plausible that deletion of *aspC* perturbed the metabolism of bacterium in such a way to cause the reversal of the TCA cycle. An atypical TCA cycle in the  $\Delta aspC$  mutant could have implications in antibiotic resistance, as the activity of bactericidal antibiotics has been suggested to be linked to the TCA cycle [67]. Metabolic distress due to the deletion of *aspC* is not yet fully understood but is likely due to oxaloacetate toxicity (Figure 16B-D). Work thus far has shown that inactivation of *aspC* has widespread

consequences on the physiology of *M. smegmatis* and additional study is required to understand the mechanism.

Similar to the  $\Delta aspC$  mutant, constitutive expression of  $aspB_{Mtb}$  also increased susceptibility of *M. smegmatis* to antibiotics (Table 4), an effect that is likely mediated through *whiB7*. This is based on our studies demonstrating that *whiB7* expression was strongly repressed by  $aspB_{Mtb}$  expression. In addition, the susceptibility profile of  $hsp-aspB_{Mtb}$  was similar that of  $\Delta whiB7$ . We conclude that enzyme activity of AspB may create a signal which downregulates *whiB7*. Transcriptional activation of *whiB7* promoted a reduced environment while oxidizing conditions decreased *whiB7* transcription [35]. Drug susceptibility of the  $\Delta aspC$  mutant was revealed by growth kinetics analyses that agreed with MTT-based MIC determination (Table 4). When the curve representing growth kinetics of the mutant was much steeper than the wild-type curve (clarithromycin, roxithromycin, rifampicin), the fold susceptibility of mutant  $\Delta aspC$  was higher (eight to sixteen fold more susceptible as compared to wild-type). A slight increase in susceptibility (two to four compared to wild-type) was reflected in comparisons of mutant and wild-type curves. While these curves had similar slopes, the curve representing the mutant was positioned above the wild-type curve (clindamycin, fusidic acid, and spectinomycin) (Figure 22). The growth curve analysis once again showed that deletion of *aspC* caused the strain to be more susceptible to a number of antibiotics. In addition, this analysis revealed that the susceptibility increase was due to the  $\Delta aspC$  mutant having an increased lag phase, akin to the effect of oxaloacetate and antibiotics on the growth of wild-type (Table 5 and Figure 16).

Paradoxically, while deletion of *aspC* augmented inhibition of *M. smegmatis* growth by antibiotics, survival kinetics indicated this mutation reduced the bacteriocidal activity of clarithromycin (Figure 15). Clarithromycin, a macrolide, is generally considered to be bacteriostatic but the overwhelmingly high concentration used in our experiments was sufficient to reduce the cell viability of both wild-type and mutant. The difference in log reduction of cell numbers can be partly attributed to the fact that the growth of the  $\Delta aspC$  mutant may have already plateaued when the antibiotic was added. Slow-growing or nongrowing cells are not very susceptible to many antimicrobial agents [151]. Indeed the  $\Delta aspC$  mutant exhibits growth defects and doubles much more slowly than wild-type *M. smegmatis*, which could contribute to the reduced killing by clarithromycin and also promote more persisters that are tolerant to antibiotics. This resistance phenomenon may also be due to a subpopulation of persisters that are genetically identical (not mutants) but are less sensitive to killing by antibiotics because they are either not actively growing or metabolising very slowly [152] [153]. The observation that the  $\Delta aspC$  mutant was simultaneously sensitive to the bacteriostatic effects of clarithromycin but resistant to the bacteriocidal killing by clarithromycin at higher concentrations highlights that *aspC* has varied effects on the bacteria's physiology. The hypothesized increased oxaloacetate in the  $\Delta aspC$  mutant may potentiate the activity of bacteriostatic antibiotics while redox stress, reflected by the increased catalase activity may protect the bacteria from killing by bacteriocidal antibiotics. More experimentation using actively

growing cultures is required to determine whether the bactericidal and bacteriostatic effects of clarithromycin reflect independent physiological effects elicited by the *aspC* inactivation.

### 4. 3. Role of AspB and AspC in mycobacteria physiology

Bioinformatic analysis of the sequences of *aspB* and *aspC* from *M. tuberculosis* and *M. smegmatis* suggested that both genes encode aspartate aminotransferases (Figures 20, 21, and Table 6). Both AspB and AspC from *M. tuberculosis* showed aspartate transaminase activity. The specific activities of AspB and AspC were much lower than specific activities reported for other aspartate aminotransferases (Table 9). Steady-state kinetic parameters for AspB<sub>Mtb</sub> were determined for the reaction of glutamate formation by transamination from aspartate to  $\alpha$ -ketoglutarate (Table 10) (experiments performed by Mr. Antonio Ruzzini). The Michaelis constants,  $K_m$  for aspartate and  $\alpha$ -ketoglutarate determined for AspB<sub>Mtb</sub> were comparable to those reported for *E. coli* aspartate aminotransferase AspC<sub>Eco</sub> by Toney and Kirsch [136]. However, the catalytic constant,  $k_{cat}$  is over 500-fold smaller than AspC<sub>Eco</sub> making AspB<sub>Mtb</sub> a poor aspartate aminotransferase, as calculated by  $k_{cat}/K_m$ . The physiological role of AspB has yet to be fully characterized; perhaps AspB requires different conditions or substrates. Purified recombinant AspC<sub>Mtb</sub> was also shown biochemically to possess aspartate aminotransferase activity.

Over-expression of *M. tuberculosis* proteins in *E. coli* often results in the proteins aggregating to form insoluble inclusion bodies. It is estimated that only 30-50% of tuberculosis proteins can be expressed in a soluble form by *E. coli* [154]. We experienced similar problems with over-expression of AspB and AspC. AspB was expressed as a soluble recombinant protein, while AspC could be over-expressed, but was mostly present in inclusion bodies making purification of native protein difficult. Expression of AspC with GST protein tag (Figure 25) significantly improved solubility and allowed subsequent purification using affinity chromatography (Figure 26), but since the size of the GST tag is comparable to AspC (25 kDa and 47 kDa, respectively) its removal was required so that the activity of AspC would not be sterically hindered by the GST tag. Unfortunately, due to the presence of secondary protease cleavage sites and general instability of the protein, it was not possible to obtain purified, tag-free, AspC from this construct (Figures 28 and 29). Mycobacterial chaperones may be required to aid in the folding and soluble expression of *M. tuberculosis* proteins. Alternatively, codon usage might need to be optimized for expression of high GC content genes in *E. coli*, a more AT rich organism. *M. smegmatis* has been used successfully to produce soluble recombinant protein of *M. tuberculosis* proteins that were previously insoluble in *E. coli* [97,154,155]. Expression in Rosetta2™ *E. coli* and *M. smegmatis* [97] was attempted but recombinant AspC was still only found in inclusion bodies (Table 8).

*aspB* maps within a cluster of cholesterol catabolic genes in the *M. tuberculosis* and *M. smegmatis* genomes that may be related to virulence of *M. tuberculosis*. *aspB* is within a putative operon controlled by a tetR-type transcriptional repressor, KstR2 [92]. *aspB* (MSMEG\_6017) was expressed 100-fold more when *kstR2* was deleted in *M. smegmatis* showing that KstR2 exerts negative regulation of *aspB* [92]. KstR2 controls the expression of genes in the cholesterol degradation pathway, a function that is important in *M. tuberculosis* virulence as cholesterol is a critical carbon source during chronic infection

[156,157]. Other genes in the operon, *fadD3* (Rv3561), *fadE32* (Rv3563), *fadE33* (Rv3564), are essential for growth on cholesterol [158]. While *aspB* was not identified as an essential gene for growth on cholesterol, it is upregulated along with other genes in the operon during infection of both the resting and IFN- $\gamma$ -activated macrophages [159], suggesting that AspB may be part of the metabolic adaptive pathway that *M. tuberculosis* requires for growth on cholesterol. Other genes in the KstR2 operon in addition to *aspB* are putative fatty acid CoA synthetase (*fadD3*) and acyl CoA dehydrogenases (*fadE31*, *fadE32*, and *fadE33*) with roles in  $\beta$ -oxidation.  $\beta$ -oxidative degradation of odd-chain-length fatty acids and cholesterol can yield molecules like propionyl CoA and acetyl CoA [160,161]. The degradation of branched chain amino acids (valine, leucine, and isoleucine) also produces propionate and requires actions of transaminases [162]. It has been speculated that AspB may act on a metabolite or intermediate of cholesterol degradation that mimics the structure of branched chain amino acids during  $\beta$ -oxidation-like degradation of a cholesterol degradation intermediate to produce propionyl CoA which can enter the methyl citrate cycle and be used for energy generation in [163].

#### 4. 4. Implicated roles for AspC in redox homeostasis and oxidative stress detoxification

Homologs AspB and AspC may both have aspartate aminotransferase activity but their roles in redox homeostasis, antioxidation, and antibiotic resistance differ. AspC acts in the WhiB7-directed pathway to modulate physiology, and may serve to counteract damage by oxidative stress. AspB, however, does not appear to do the same; deletion or constitutive expression strains of *aspB* did not show any significant changes in catalase activity or NAD<sup>+</sup>/H pools compared to wild-type. Moreover, AspB appears not to be the primary aspartate aminotransferase as deletion of the gene did not affect *M. smegmatis* growth whereas *aspC* was required for optimal aspartate catabolism and general fitness of the strain (Figure 7, Table 3). Deletion of both *aspB* and *aspC* did not cause *M. smegmatis* to become auxotrophic (Figure 10A). Amino acid transaminases have broad activities; aspartate auxotrophy in *E. coli* required deletion of three genes: *aspC* (aspartate aminotransferase), *tyrB* (aromatic amino acid aminotransferase), and *ilvE* (branched chain amino acid aminotransferase) [144]. Therefore, inactivation of additional transaminase genes may be needed to generate a *M. smegmatis* aspartate auxotroph. The  $\Delta aspB\Delta aspC$  double mutant displayed many of the same growth defects of  $\Delta aspC$  (Figures 7 and 10), further demonstrating that deletion of *aspB* does not significantly affect *in vitro* growth on glycerol.

Antibiotics triggered changes in the cytoplasmic redox potential activated *whiB7* expression. WhiB7 contributes to the maintenance of mycothiol pools (MSH and MSSM) in addition to regulating the reduction of oxidized mycothiol (MSSM) in response to antibiotics (erythromycin) [35]. Since *aspC* expression was positively regulated by WhiB7 and the deletion of *aspC* caused increased sensitivity to many antibiotics, we hypothesized that AspC may play a role in WhiB7-mediated maintenance of redox homeostasis. Quantification of NADH and NAD<sup>+</sup> pools revealed that deletion of *aspC* resulted in a large increase in the pools of NADH and NAD<sup>+</sup>, as well as the NADH/NAD<sup>+</sup> ratio (Figure 17). Inability to maintain redox homeostasis increases susceptibility to oxidative stress, as evidenced by mycothiol mutants exhibiting hypersensitivity to reactive oxygen compounds [164] [165] [166] [167] [168].

The  $\Delta aspC$  mutant exhibited increased sensitivity to oxidative stress inducers like hydrogen peroxide and menadione (Figure 18). The growth deficiencies of the  $\Delta aspC$  mutant may have contributed to this phenotype so additional experiments would need to be performed (such as a kinetic kill analysis) to confirm the sensitivity of the  $\Delta aspC$  mutant to ROS inducers. We measured catalase activity in the  $\Delta aspB$  and  $\Delta aspC$  mutants to determine whether the sensitivity to oxidative stress inducers was due to changes in the detoxifying enzymes that maintain oxidative homeostasis. The catalase assay used in this study measured the disappearance of hydrogen peroxide and could reflect the activity of either catalase (KatG) or alkyl hydroperoxidase (AhpC). Paradoxically, while the  $\Delta aspC$  mutant was apparently sensitive to peroxide, it had four-fold higher levels of catalase activity compared to wild-type indicating that the mutant requires the presence of more detoxifying enzymes to maintain oxidative homeostasis (Figure 19A). The increased catalase activity correlates with the  $\Delta aspC$  mutant displaying increased sensitivity to

isoniazid, as KatG is responsible for activation of this prodrug [169] [170] [171]. It is interesting to note that while addition of  $\alpha$ -ketoglutarate to the growth medium suppressed the drug susceptibility of the  $\Delta aspC$  mutant to tetracycline, clarithromycin, and spectinomycin, the presence of  $\alpha$ -ketoglutarate significantly increased the MIC of the strain to isoniazid making the strain 32-fold more resistant to isoniazid than wild-type (Figure 12). As previously noted, the activity of isoniazid, a prodrug, relies on a conversion catalyzed by KatG and the resistance to isoniazid in the presence of  $\alpha$ -ketoglutarate represents a link between  $\alpha$ -ketoglutarate and KatG and therefore oxidative stress detoxification.

*katG* expression is induced in *M. tuberculosis*, *M. bovis* BCG, *M. avium*, and *M. marinum* in response to hydrogen peroxide [172] [173] [174] [175] [176]. With similar regulation by *furA*, one would expect *katG* would also be upregulated in *M. smegmatis* in response to hydrogen peroxide. However, the KatG response to hydrogen peroxide in *M. smegmatis* is still unclear. There has been evidence for [172] and against [176] the transcriptional upregulation of *katG* in *M. smegmatis* in response to hydrogen peroxide. Our measurement of catalase activity in wild-type cell lysates showed no change in catalase activity after hydrogen peroxide exposure (Figure 19B). It would seem that our results support lack of *katG* upregulation in response to hydrogen peroxide in *M. smegmatis* but it is plausible that there is post-transcriptional regulation of KatG. Nonetheless, the  $\Delta aspC$  mutant, whose levels of catalase activity prior to hydrogen peroxide challenge are already elevated, responded to hydrogen peroxide with a decrease in catalase activity. The reason for this decrease in catalase activity detected after hydrogen peroxide exposure is unclear; the decrease in catalase activity may be due to activation of other detoxification enzymes such as AhpC. Alkyl hydroperoxidase is sufficient to protect *M. tuberculosis* from organic peroxides when *katG* is mutated [174]. Nonetheless, deletion of *aspC* results in a change in oxidative stress sensitivity and response of *M. smegmatis* to hydrogen peroxide oxidative stress. Paradoxically, the increased KatG activity could potentially increase oxygen radical formation; mycobacterial KatG possesses NADH oxidase activity in addition to catalase and peroxidase activities. KatG could oxidize NADH in an oxygen-dependent manner, forming either hydrogen peroxide or superoxide radicals [177]. The  $\Delta aspC$  mutant concurrently has both increased catalase and NADH levels, supplying the substrates for radical formation via NADH oxidation, further adding to oxidative stress levels.

The deletion of *aspC* may shift the metabolism of the bacterium to produce more ROS by-products during regular respiration. Aspartate is the precursor molecule in the mycobacterial NAD biosynthesis pathway. In the first step in this biosynthetic pathway aspartate is oxidized to  $\alpha$ -iminosuccinate, producing hydrogen peroxide as a by-product. Deletion of *aspC* renders the strain unable to transaminate aspartate, leading to an accumulation of aspartate that may be fed into NAD<sup>+</sup> biosynthesis reactions generating hydrogen peroxide and redox imbalance through increased NADH. Reducing NADH can drive the production of reactive oxygen from hydrogen peroxide through Fenton's reaction, resulting in DNA damage (Figure 2) [178]. Bactericidal antibiotics have also been shown to cause cell

death via the generation of hydroxyl radicals [67]. AspC has a critical role in redox homeostasis and deletion of *aspC* causes an imbalance in redox homeostasis that increases susceptibility to antibiotic-generated oxidative stress.

#### **4. 5. Concluding remarks**

Traditional understanding of antibiotic resistance focuses on the idea that antibiotics have one target and resistance is based on modification of that target or antibiotic. However, there is increasing evidence showing that physiology plays a role in determining intrinsic levels of antibiotic resistance. Intrinsic antibiotic resistance can be due to genes that are induced by antibiotics and when expressed, become functional antibiotic resistance determinants. In this study, we have presented evidence that AspB and AspC are aspartate aminotransferases that are involved in amino acid intermediary metabolism and WhiB7-controlled intrinsic resistance. Understanding of the microbial factors that affect intrinsic resistance in *M. tuberculosis* could be beneficial to the design of new regimens for the management of tuberculosis, contributing to the elimination of tuberculosis as a global health problem.

## References

1. WHO (2011) Global tuberculosis control: WHO report 2011. WHO Press.
2. Gandhi NR, Nunn P, Dheda K, Schaaf HS, Zignol M, et al. (2010) Multidrug-resistant and extensively drug-resistant tuberculosis: a threat to global control of tuberculosis. *Lancet* 375: 1830-1843.
3. Snider DE, Jr., Castro KG (1998) The global threat of drug-resistant tuberculosis. *The New England journal of medicine* 338: 1689-1690.
4. Cohn DL, Bustreo F, Raviglione MC (1997) Drug-resistant tuberculosis: review of the worldwide situation and the WHO/IUATLD Global Surveillance Project. *International Union Against Tuberculosis and Lung Disease. Clinical infectious diseases : an official publication of the Infectious Diseases Society of America* 24 Suppl 1: S121-130.
5. Chryssanthou E, Angeby K (2012) The GenoType(R) MTBDRplus assay for detection of drug resistance in *Mycobacterium tuberculosis* in Sweden. *APMIS : acta pathologica, microbiologica, et immunologica Scandinavica* 120: 405-409.
6. Nguyen L, Chinnapapagari S, Thompson CJ (2005) FbpA-Dependent biosynthesis of trehalose dimycolate is required for the intrinsic multidrug resistance, cell wall structure, and colonial morphology of *Mycobacterium smegmatis*. *Journal of bacteriology* 187: 6603-6611.
7. Silva PE, Bigi F, Santangelo MP, Romano MI, Martin C, et al. (2001) Characterization of P55, a multidrug efflux pump in *Mycobacterium bovis* and *Mycobacterium tuberculosis*. *Antimicrobial agents and chemotherapy* 45: 800-804.
8. Pasca MR, Guglierame P, Arcesi F, Bellinzoni M, De Rossi E, et al. (2004) Rv2686c-Rv2687c-Rv2688c, an ABC fluoroquinolone efflux pump in *Mycobacterium tuberculosis*. *Antimicrobial agents and chemotherapy* 48: 3175-3178.
9. Flores AR, Parsons LM, Pavelka MS, Jr. (2005) Genetic analysis of the beta-lactamases of *Mycobacterium tuberculosis* and *Mycobacterium smegmatis* and susceptibility to beta-lactam antibiotics. *Microbiology* 151: 521-532.
10. Nash DR, Wallace RJ, Jr., Steingrube VA, Udou T, Steele LC, et al. (1986) Characterization of beta-lactamases in *Mycobacterium fortuitum* including a role in beta-lactam resistance and evidence of partial inducibility. *The American review of respiratory disease* 134: 1276-1282.
11. Madsen CT, Jakobsen L, Buriankova K, Doucet-Populaire F, Pernodet JL, et al. (2005) Methyltransferase Erm(37) slips on rRNA to confer atypical resistance in *Mycobacterium tuberculosis*. *The Journal of biological chemistry* 280: 38942-38947.
12. Buriankova K, Doucet-Populaire F, Dorson O, Gondran A, Ghnassia JC, et al. (2004) Molecular basis of intrinsic macrolide resistance in the *Mycobacterium tuberculosis* complex. *Antimicrobial agents and chemotherapy* 48: 143-150.
13. Bottger EC, Springer B, Pletschette M, Sander P (1998) Fitness of antibiotic-resistant microorganisms and compensatory mutations. *Nature medicine* 4: 1343-1344.
14. Gagneux S, Long CD, Small PM, Van T, Schoolnik GK, et al. (2006) The competitive cost of antibiotic resistance in *Mycobacterium tuberculosis*. *Science* 312: 1944-1946.
15. Manabe YC, Bishai WR (2000) Latent *Mycobacterium tuberculosis*-persistence, patience, and winning by waiting. *Nature medicine* 6: 1327-1329.
16. Parrish NM, Dick JD, Bishai WR (1998) Mechanisms of latency in *Mycobacterium tuberculosis*. *Trends in microbiology* 6: 107-112.
17. Davis NK, Chater KF (1992) The *Streptomyces coelicolor* whiB gene encodes a small transcription factor-like protein dispensable for growth but essential for sporulation. *Molecular & general genetics* : MGG 232: 351-358.

18. Soliveri JA, Gomez J, Bishai WR, Chater KF (2000) Multiple paralogous genes related to the *Streptomyces coelicolor* developmental regulatory gene *whiB* are present in *Streptomyces* and other actinomycetes. *Microbiology* 146 ( Pt 2): 333-343.
19. Kim TH, Park JS, Kim HJ, Kim Y, Kim P, et al. (2005) The *whcE* gene of *Corynebacterium glutamicum* is important for survival following heat and oxidative stress. *Biochemical and biophysical research communications* 337: 757-764.
20. Alam MS, Garg SK, Agrawal P (2009) Studies on structural and functional divergence among seven *WhiB* proteins of *Mycobacterium tuberculosis* H37Rv. *The FEBS journal* 276: 76-93.
21. Garg S, Alam MS, Bajpai R, Kishan KR, Agrawal P (2009) Redox biology of *Mycobacterium tuberculosis* H37Rv: protein-protein interaction between *GlgB* and *WhiB1* involves exchange of thiol-disulfide. *BMC biochemistry* 10: 1.
22. Raghunand TR, Bishai WR (2006) *Mycobacterium smegmatis whmD* and its homologue *Mycobacterium tuberculosis whiB2* are functionally equivalent. *Microbiology* 152: 2735-2747.
23. Steyn AJ, Collins DM, Hondalus MK, Jacobs WR, Jr., Kawakami RP, et al. (2002) *Mycobacterium tuberculosis WhiB3* interacts with *RpoV* to affect host survival but is dispensable for in vivo growth. *Proceedings of the National Academy of Sciences of the United States of America* 99: 3147-3152.
24. Geiman DE, Raghunand TR, Agarwal N, Bishai WR (2006) Differential gene expression in response to exposure to antimycobacterial agents and other stress conditions among seven *Mycobacterium tuberculosis whiB*-like genes. *Antimicrobial agents and chemotherapy* 50: 2836-2841.
25. Ramakrishnan L, Federspiel NA, Falkow S (2000) Granuloma-specific expression of *Mycobacterium* virulence proteins from the glycine-rich PE-PGRS family. *Science* 288: 1436-1439.
26. Betts JC, Lukey PT, Robb LC, McAdam RA, Duncan K (2002) Evaluation of a nutrient starvation model of *Mycobacterium tuberculosis* persistence by gene and protein expression profiling. *Molecular microbiology* 43: 717-731.
27. Smith LJ, Stapleton MR, Fullstone GJ, Crack JC, Thomson AJ, et al. (2010) *Mycobacterium tuberculosis WhiB1* is an essential DNA-binding protein with a nitric oxide-sensitive iron-sulfur cluster. *The Biochemical journal* 432: 417-427.
28. Singh A, Guidry L, Narasimhulu KV, Mai D, Trombley J, et al. (2007) *Mycobacterium tuberculosis WhiB3* responds to O<sub>2</sub> and nitric oxide via its [4Fe-4S] cluster and is essential for nutrient starvation survival. *Proceedings of the National Academy of Sciences of the United States of America* 104: 11562-11567.
29. Morris RP, Nguyen L, Gatfield J, Visconti K, Nguyen K, et al. (2005) Ancestral antibiotic resistance in *Mycobacterium tuberculosis*. *Proceedings of the National Academy of Sciences of the United States of America* 102: 12200-12205.
30. Ainsa JA, Blokpoel MC, Otal I, Young DB, De Smet KA, et al. (1998) Molecular cloning and characterization of *Tap*, a putative multidrug efflux pump present in *Mycobacterium fortuitum* and *Mycobacterium tuberculosis*. *Journal of bacteriology* 180: 5836-5843.
31. Ramon-Garcia S, Martin C, Ainsa JA, De Rossi E (2006) Characterization of tetracycline resistance mediated by the efflux pump *Tap* from *Mycobacterium fortuitum*. *The Journal of antimicrobial chemotherapy* 57: 252-259.
32. Lella RK, Sharma C (2007) *Eis* (enhanced intracellular survival) protein of *Mycobacterium tuberculosis* disturbs the cross regulation of T-cells. *The Journal of biological chemistry* 282: 18671-18675.
33. Kim KH, An DR, Song J, Yoon JY, Kim HS, et al. (2012) *Mycobacterium tuberculosis Eis* protein initiates suppression of host immune responses by acetylation of *DUSP16/MKP-7*. *Proceedings of the National Academy of Sciences of the United States of America* 109: 7729-7734.
34. Zaunbrecher MA, Sikes RD, Jr., Metchock B, Shinnick TM, Posey JE (2009) Overexpression of the chromosomally encoded aminoglycoside acetyltransferase *eis* confers kanamycin resistance in

- Mycobacterium tuberculosis. Proceedings of the National Academy of Sciences of the United States of America 106: 20004-20009.
35. Burian J, Ramon-Garcia S, Sweet G, Gomez-Velasco A, Av-Gay Y, et al. (2012) The mycobacterial transcriptional regulator whiB7 gene links redox homeostasis and intrinsic antibiotic resistance. The Journal of biological chemistry 287: 299-310.
  36. Homolka S, Niemann S, Russell DG, Rohde KH (2010) Functional genetic diversity among Mycobacterium tuberculosis complex clinical isolates: delineation of conserved core and lineage-specific transcriptomes during intracellular survival. PLoS pathogens 6: e1000988.
  37. Nathan C, Shiloh MU (2000) Reactive oxygen and nitrogen intermediates in the relationship between mammalian hosts and microbial pathogens. Proceedings of the National Academy of Sciences of the United States of America 97: 8841-8848.
  38. MacMicking JD, North RJ, LaCourse R, Mudgett JS, Shah SK, et al. (1997) Identification of nitric oxide synthase as a protective locus against tuberculosis. Proceedings of the National Academy of Sciences of the United States of America 94: 5243-5248.
  39. Rybniker J, Nowag A, van Gumpel E, Nissen N, Robinson N, et al. (2010) Insights into the function of the WhiB-like protein of mycobacteriophage TM4--a transcriptional inhibitor of WhiB2. Molecular microbiology 77: 642-657.
  40. Singh A, Crossman DK, Mai D, Guidry L, Voskuil MI, et al. (2009) Mycobacterium tuberculosis WhiB3 maintains redox homeostasis by regulating virulence lipid anabolism to modulate macrophage response. PLoS pathogens 5: e1000545.
  41. Ehrh S, Schnappinger D (2009) Mycobacterial survival strategies in the phagosome: defence against host stresses. Cellular microbiology 11: 1170-1178.
  42. Bedard K, Krause KH (2007) The NOX family of ROS-generating NADPH oxidases: physiology and pathophysiology. Physiological reviews 87: 245-313.
  43. Marcinkeviciene JA, Magliozzo RS, Blanchard JS (1995) Purification and characterization of the Mycobacterium smegmatis catalase-peroxidase involved in isoniazid activation. The Journal of biological chemistry 270: 22290-22295.
  44. Heym B, Zhang Y, Poulet S, Young D, Cole ST (1993) Characterization of the katG gene encoding a catalase-peroxidase required for the isoniazid susceptibility of Mycobacterium tuberculosis. Journal of bacteriology 175: 4255-4259.
  45. Wengenack NL, Jensen MP, Rusnak F, Stern MK (1999) Mycobacterium tuberculosis KatG is a peroxynitritase. Biochemical and biophysical research communications 256: 485-487.
  46. Trivedi A, Singh N, Bhat SA, Gupta P, Kumar A (2012) Redox biology of tuberculosis pathogenesis. Advances in microbial physiology 60: 263-324.
  47. Farivar TN, Varnousfaderani PJ, Borji A (2008) Mutation in alkylhydroperoxidase D gene dramatically decreases persistence of Mycobacterium bovis bacillus calmette-guerin in infected macrophage. Indian journal of medical sciences 62: 275-282.
  48. Guimaraes BG, Souchon H, Honore N, Saint-Joanis B, Brosch R, et al. (2005) Structure and mechanism of the alkyl hydroperoxidase AhpC, a key element of the Mycobacterium tuberculosis defense system against oxidative stress. The Journal of biological chemistry 280: 25735-25742.
  49. Sherman DR, Mdluli K, Hickey MJ, Barry CE, 3rd, Stover CK (1999) AhpC, oxidative stress and drug resistance in Mycobacterium tuberculosis. BioFactors 10: 211-217.
  50. Wu CH, Tsai-Wu JJ, Huang YT, Lin CY, Liou GG, et al. (1998) Identification and subcellular localization of a novel Cu,Zn superoxide dismutase of Mycobacterium tuberculosis. FEBS letters 439: 192-196.

51. Piddington DL, Fang FC, Laessig T, Cooper AM, Orme IM, et al. (2001) Cu,Zn superoxide dismutase of *Mycobacterium tuberculosis* contributes to survival in activated macrophages that are generating an oxidative burst. *Infection and immunity* 69: 4980-4987.
52. Zhang YJ, Ioerger TR, Huttenhower C, Long JE, Sasseti CM, et al. (2012) Global Assessment of Genomic Regions Required for Growth in *Mycobacterium tuberculosis*. *PLoS pathogens* 8: e1002946.
53. Braunstein M, Espinosa BJ, Chan J, Belisle JT, Jacobs WR, Jr. (2003) SecA2 functions in the secretion of superoxide dismutase A and in the virulence of *Mycobacterium tuberculosis*. *Molecular microbiology* 48: 453-464.
54. Kurtz S, McKinnon KP, Runge MS, Ting JP, Braunstein M (2006) The SecA2 secretion factor of *Mycobacterium tuberculosis* promotes growth in macrophages and inhibits the host immune response. *Infection and immunity* 74: 6855-6864.
55. Mitchison DA, Selkon JB, Lloyd J (1963) Virulence in the Guinea-Pig, Susceptibility to Hydrogen Peroxide, and Catalase Activity of Isoniazid-Sensitive Tubercle Bacilli from South Indian and British Patients. *The Journal of pathology and bacteriology* 86: 377-386.
56. Ng VH, Cox JS, Sousa AO, MacMicking JD, McKinney JD (2004) Role of KatG catalase-peroxidase in mycobacterial pathogenesis: countering the phagocyte oxidative burst. *Molecular microbiology* 52: 1291-1302.
57. Davies J, Spiegelman GB, Yim G (2006) The world of subinhibitory antibiotic concentrations. *Current opinion in microbiology* 9: 445-453.
58. Yim G, Wang HH, Davies J (2006) The truth about antibiotics. *International journal of medical microbiology : IJMM* 296: 163-170.
59. Goh EB, Yim G, Tsui W, McClure J, Surette MG, et al. (2002) Transcriptional modulation of bacterial gene expression by subinhibitory concentrations of antibiotics. *Proceedings of the National Academy of Sciences of the United States of America* 99: 17025-17030.
60. Ng WL, Kazmierczak KM, Robertson GT, Gilmour R, Winkler ME (2003) Transcriptional regulation and signature patterns revealed by microarray analyses of *Streptococcus pneumoniae* R6 challenged with sublethal concentrations of translation inhibitors. *Journal of bacteriology* 185: 359-370.
61. Shaw KJ, Miller N, Liu X, Lerner D, Wan J, et al. (2003) Comparison of the changes in global gene expression of *Escherichia coli* induced by four bactericidal agents. *Journal of molecular microbiology and biotechnology* 5: 105-122.
62. Tsui WH, Yim G, Wang HH, McClure JE, Surette MG, et al. (2004) Dual effects of MLS antibiotics: transcriptional modulation and interactions on the ribosome. *Chemistry & biology* 11: 1307-1316.
63. Stephan J, Mailaender C, Etienne G, Daffe M, Niederweis M (2004) Multidrug resistance of a porin deletion mutant of *Mycobacterium smegmatis*. *Antimicrobial agents and chemotherapy* 48: 4163-4170.
64. Cowley S, Ko M, Pick N, Chow R, Downing KJ, et al. (2004) The *Mycobacterium tuberculosis* protein serine/threonine kinase PknG is linked to cellular glutamate/glutamine levels and is important for growth in vivo. *Molecular microbiology* 52: 1691-1702.
65. Wolff KA, Nguyen HT, Cartabuke RH, Singh A, Ogowang S, et al. (2009) Protein kinase G is required for intrinsic antibiotic resistance in mycobacteria. *Antimicrobial agents and chemotherapy* 53: 3515-3519.
66. Ren H, Liu J (2006) AsnB is involved in natural resistance of *Mycobacterium smegmatis* to multiple drugs. *Antimicrobial agents and chemotherapy* 50: 250-255.
67. Kohanski MA, Dwyer DJ, Hayete B, Lawrence CA, Collins JJ (2007) A common mechanism of cellular death induced by bactericidal antibiotics. *Cell* 130: 797-810.

68. Bizzini A, Zhao C, Auffray Y, Hartke A (2009) The *Enterococcus faecalis* superoxide dismutase is essential for its tolerance to vancomycin and penicillin. *The Journal of antimicrobial chemotherapy* 64: 1196-1202.
69. Feld L, Knudsen GM, Gram L (2012) Bactericidal antibiotics do not appear to cause oxidative stress in *Listeria monocytogenes*. *Applied and environmental microbiology* 78: 4353-4357.
70. Kohanski MA, Dwyer DJ, Collins JJ (2010) How antibiotics kill bacteria: from targets to networks. *Nature reviews Microbiology* 8: 423-435.
71. Dwyer DJ, Kohanski MA, Collins JJ (2009) Role of reactive oxygen species in antibiotic action and resistance. *Current opinion in microbiology* 12: 482-489.
72. Imlay JA (2008) Cellular defenses against superoxide and hydrogen peroxide. *Annual review of biochemistry* 77: 755-776.
73. Seaver LC, Imlay JA (2001) Alkyl hydroperoxide reductase is the primary scavenger of endogenous hydrogen peroxide in *Escherichia coli*. *Journal of bacteriology* 183: 7173-7181.
74. Watanabe S, Zimmermann M, Goodwin MB, Sauer U, Barry CE, 3rd, et al. (2011) Fumarate reductase activity maintains an energized membrane in anaerobic *Mycobacterium tuberculosis*. *PLoS pathogens* 7: e1002287.
75. Boshoff HI, Xu X, Tahlan K, Dowd CS, Pethe K, et al. (2008) Biosynthesis and recycling of nicotinamide cofactors in *mycobacterium tuberculosis*. An essential role for NAD in nonreplicating bacilli. *The Journal of biological chemistry* 283: 19329-19341.
76. Wayne LG, Lin KY (1982) Glyoxylate metabolism and adaptation of *Mycobacterium tuberculosis* to survival under anaerobic conditions. *Infection and immunity* 37: 1042-1049.
77. Kohanski MA, Dwyer DJ, Wierzbowski J, Cottarel G, Collins JJ (2008) Mistranslation of membrane proteins and two-component system activation trigger antibiotic-mediated cell death. *Cell* 135: 679-690.
78. Imlay JA, Linn S (1986) Bimodal pattern of killing of DNA-repair-defective or anoxically grown *Escherichia coli* by hydrogen peroxide. *Journal of bacteriology* 166: 519-527.
79. Park S, Imlay JA (2003) High levels of intracellular cysteine promote oxidative DNA damage by driving the fenton reaction. *Journal of bacteriology* 185: 1942-1950.
80. Yeom J, Imlay JA, Park W (2010) Iron homeostasis affects antibiotic-mediated cell death in *Pseudomonas* species. *The Journal of biological chemistry* 285: 22689-22695.
81. van der Veen S, Abee T (2011) Generation of variants in *Listeria monocytogenes* continuous-flow biofilms is dependent on radical-induced DNA damage and RecA-mediated repair. *PLoS one* 6: e28590.
82. Moreira W, Leprohon P, Ouellette M (2011) Tolerance to drug-induced cell death favours the acquisition of multidrug resistance in *Leishmania*. *Cell death & disease* 2: e201.
83. Aranda J, Bardina C, Beceiro A, Rumbo S, Cabral MP, et al. (2011) *Acinetobacter baumannii* RecA protein in repair of DNA damage, antimicrobial resistance, general stress response, and virulence. *Journal of bacteriology* 193: 3740-3747.
84. Cole ST, Brosch R, Parkhill J, Garnier T, Churcher C, et al. (1998) Deciphering the biology of *Mycobacterium tuberculosis* from the complete genome sequence. *Nature* 393: 537-544.
85. Coulibaly F, Lassalle E, Baker HM, Baker EN (2012) Structure of phosphoserine aminotransferase from *Mycobacterium tuberculosis*. *Acta crystallographica Section D, Biological crystallography* 68: 553-563.
86. Nasir N, Vyas R, Chugh C, Ahangar MS, Biswal BK (2012) Molecular cloning, overexpression, purification, crystallization and preliminary X-ray diffraction studies of histidinol phosphate aminotransferase (HisC2) from *Mycobacterium tuberculosis*. *Acta crystallographica Section F, Structural biology and crystallization communications* 68: 32-36.

87. Tremblay LW, Blanchard JS (2009) The 1.9 Å structure of the branched-chain amino-acid transaminase (IlvE) from *Mycobacterium tuberculosis*. *Acta crystallographica Section F, Structural biology and crystallization communications* 65: 1071-1077.
88. Willey JM, Sherwood L, Woolverton CJ, Prescott LM (2011) *Prescott's microbiology*. New York: McGraw-Hill.
89. Yano T, Mizuno T, Kagamiyama H (1993) A hydrogen-bonding network modulating enzyme function: asparagine-194 and tyrosine-225 of *Escherichia coli* aspartate aminotransferase. *Biochemistry* 32: 1810-1815.
90. Van der Geize R, Yam K, Heuser T, Wilbrink MH, Hara H, et al. (2007) A gene cluster encoding cholesterol catabolism in a soil actinomycete provides insight into *Mycobacterium tuberculosis* survival in macrophages. *Proceedings of the National Academy of Sciences of the United States of America* 104: 1947-1952.
91. Kendall SL, Withers M, Soffair CN, Moreland NJ, Gurcha S, et al. (2007) A highly conserved transcriptional repressor controls a large regulon involved in lipid degradation in *Mycobacterium smegmatis* and *Mycobacterium tuberculosis*. *Molecular microbiology* 65: 684-699.
92. Kendall SL, Burgess P, Balhana R, Withers M, Ten Bokum A, et al. (2010) Cholesterol utilization in mycobacteria is controlled by two TetR-type transcriptional regulators: *kstR* and *kstR2*. *Microbiology* 156: 1362-1371.
93. Sassetti CM, Boyd DH, Rubin EJ (2003) Genes required for mycobacterial growth defined by high density mutagenesis. *Molecular microbiology* 48: 77-84.
94. Stover CK, de la Cruz VF, Fuerst TR, Burlein JE, Benson LA, et al. (1991) New use of BCG for recombinant vaccines. *Nature* 351: 456-460.
95. van Kessel JC, Hatfull GF (2007) Recombineering in *Mycobacterium tuberculosis*. *Nature methods* 4: 147-152.
96. Bardarov S, Bardarov Jr S, Jr., Pavelka Jr MS, Jr., Sambandamurthy V, Larsen M, et al. (2002) Specialized transduction: an efficient method for generating marked and unmarked targeted gene disruptions in *Mycobacterium tuberculosis*, *M. bovis* BCG and *M. smegmatis*. *Microbiology* 148: 3007-3017.
97. Wang F, Jain P, Gulten G, Liu Z, Feng Y, et al. (2010) *Mycobacterium tuberculosis* dihydrofolate reductase is not a target relevant to the antitubercular activity of isoniazid. *Antimicrobial agents and chemotherapy* 54: 3776-3782.
98. LeMaster DM, Richards FM (1988) NMR sequential assignment of *Escherichia coli* thioredoxin utilizing random fractional deuteration. *Biochemistry* 27: 142-150.
99. Low B (1973) Rapid mapping of conditional and auxotrophic mutations in *Escherichia coli* K-12. *Journal of bacteriology* 113: 798-812.
100. Mangan JA, Sole KM, Mitchison DA, Butcher PD (1997) An effective method of RNA extraction from bacteria refractory to disruption, including mycobacteria. *Nucleic acids research* 25: 675-676.
101. Bernofsky C, Swan M (1973) An improved cycling assay for nicotinamide adenine dinucleotide. *Analytical biochemistry* 53: 452-458.
102. Boshoff HI, Myers TG, Copp BR, McNeil MR, Wilson MA, et al. (2004) The transcriptional responses of *Mycobacterium tuberculosis* to inhibitors of metabolism: novel insights into drug mechanisms of action. *The Journal of biological chemistry* 279: 40174-40184.
103. Leonardo MR, Dailly Y, Clark DP (1996) Role of NAD in regulating the *adhE* gene of *Escherichia coli*. *Journal of bacteriology* 178: 6013-6018.
104. Beers RF, Jr., Sizer IW (1952) A spectrophotometric method for measuring the breakdown of hydrogen peroxide by catalase. *The Journal of biological chemistry* 195: 133-140.

105. Larkin MA, Blackshields G, Brown NP, Chenna R, McGettigan PA, et al. (2007) Clustal W and Clustal X version 2.0. *Bioinformatics* 23: 2947-2948.
106. Tamura K, Peterson D, Peterson N, Stecher G, Nei M, et al. (2011) MEGA5: molecular evolutionary genetics analysis using maximum likelihood, evolutionary distance, and maximum parsimony methods. *Molecular biology and evolution* 28: 2731-2739.
107. Frangioni JV, Neel BG (1993) Solubilization and purification of enzymatically active glutathione S-transferase (pGEX) fusion proteins. *Analytical biochemistry* 210: 179-187.
108. Huang AH, Liu KD, Youle RJ (1976) Organelle-specific Isozymes of Aspartate-alpha-Ketoglutarate Transaminase in Spinach Leaves. *Plant physiology* 58: 110-113.
109. Turano FJ, Wilson BJ, Matthews BF (1990) Purification and characterization of aspartate aminotransferase isoenzymes from carrot suspension cultures. *Plant physiology* 92: 587-594.
110. Chen W, Green KD, Tsodikov OV, Garneau-Tsodikova S (2012) Aminoglycoside Multiacetylating Activity of the Enhanced Intracellular Survival Protein from *Mycobacterium smegmatis* and Its Inhibition. *Biochemistry*.
111. Green KD, Chen W, Garneau-Tsodikova S (2012) Identification and characterization of inhibitors of the aminoglycoside resistance acetyltransferase Eis from *Mycobacterium tuberculosis*. *ChemMedChem* 7: 73-77.
112. Doucet-Populaire F, Buriankova K, Weiser J, Pernodet JL (2002) Natural and acquired macrolide resistance in mycobacteria. *Current drug targets Infectious disorders* 2: 355-370.
113. De Rossi E, Arrigo P, Bellinzoni M, Silva PA, Martin C, et al. (2002) The multidrug transporters belonging to major facilitator superfamily in *Mycobacterium tuberculosis*. *Molecular medicine* 8: 714-724.
114. John RA (1995) Pyridoxal phosphate-dependent enzymes. *Biochimica et biophysica acta* 1248: 81-96.
115. Danishefsky AT, Onnufer JJ, Petsko GA, Ringe D (1991) Activity and structure of the active-site mutants R386Y and R386F of *Escherichia coli* aspartate aminotransferase. *Biochemistry* 30: 1980-1985.
116. Vodkin MH, Williams JC (1988) A heat shock operon in *Coxiella burnetii* produces a major antigen homologous to a protein in both mycobacteria and *Escherichia coli*. *Journal of bacteriology* 170: 1227-1234.
117. Young RA (1990) Stress proteins and immunology. *Annual review of immunology* 8: 401-420.
118. Saunders AH, Griffiths AE, Lee KH, Cicchillo RM, Tu L, et al. (2008) Characterization of quinolate synthases from *Escherichia coli*, *Mycobacterium tuberculosis*, and *Pyrococcus horikoshii* indicates that [4Fe-4S] clusters are common cofactors throughout this class of enzymes. *Biochemistry* 47: 10999-11012.
119. Dhandayuthapani S, Mudd M, Deretic V (1997) Interactions of OxyR with the promoter region of the oxyR and ahpC genes from *Mycobacterium leprae* and *Mycobacterium tuberculosis*. *Journal of bacteriology* 179: 2401-2409.
120. Domenech P, Honore N, Heym B, Cole ST (2001) Role of OxyS of *Mycobacterium tuberculosis* in oxidative stress: overexpression confers increased sensitivity to organic hydroperoxides. *Microbes and infection / Institut Pasteur* 3: 713-721.
121. Li Y, He ZG (2012) The mycobacterial LysR-type regulator OxyS responds to oxidative stress and negatively regulates expression of the catalase-peroxidase gene. *PloS one* 7: e30186.
122. Jensen RA, Gu W (1996) Evolutionary recruitment of biochemically specialized subdivisions of Family I within the protein superfamily of aminotransferases. *Journal of bacteriology* 178: 2161-2171.

123. Okamoto A, Kato R, Masui R, Yamagishi A, Oshima T, et al. (1996) An aspartate aminotransferase from an extremely thermophilic bacterium, *Thermus thermophilus* HB8. *Journal of biochemistry* 119: 135-144.
124. Sung MH, Tanizawa K, Tanaka H, Kuramitsu S, Kagamiyama H, et al. (1991) Thermostable aspartate aminotransferase from a thermophilic *Bacillus* species. Gene cloning, sequence determination, and preliminary x-ray characterization. *The Journal of biological chemistry* 266: 2567-2572.
125. Wu HJ, Yang Y, Wang S, Qiao JQ, Xia YF, et al. (2011) Cloning, expression and characterization of a new aspartate aminotransferase from *Bacillus subtilis* B3. *The FEBS journal* 278: 1345-1357.
126. Vacca RA, Giannattasio S, Graber R, Sandmeier E, Marra E, et al. (1997) Active-site Arg → Lys substitutions alter reaction and substrate specificity of aspartate aminotransferase. *The Journal of biological chemistry* 272: 21932-21937.
127. Jensen RA, Gu W (1996) Evolutionary recruitment of biochemically specialized subdivisions of Family I within the protein superfamily of aminotransferases. *J Bacteriol* 178: 2161-2171.
128. Wu HJ, Yang Y, Wang S, Qiao JQ, Xia YF, et al. (2011) Cloning, expression and characterization of a new aspartate aminotransferase from *Bacillus subtilis* B3. *FEBS J* 278: 1345-1357.
129. Gelfand DH, Steinberg RA (1977) *Escherichia coli* mutants deficient in the aspartate and aromatic amino acid aminotransferases. *Journal of bacteriology* 130: 429-440.
130. Berg CM, Wang MD, Vartak NB, Liu L (1988) Acquisition of new metabolic capabilities: multicopy suppression by cloned transaminase genes in *Escherichia coli* K-12. *Gene* 65: 195-202.
131. Gelfand DH, Rudo N (1977) Mapping of the aspartate and aromatic amino acid aminotransferase genes *tyrB* and *aspC*. *Journal of bacteriology* 130: 441-444.
132. Shinnick TM, Vodkin MH, Williams JC (1988) The *Mycobacterium tuberculosis* 65-kilodalton antigen is a heat shock protein which corresponds to common antigen and to the *Escherichia coli* GroEL protein. *Infection and immunity* 56: 446-451.
133. Chang JY (1985) Thrombin specificity. Requirement for apolar amino acids adjacent to the thrombin cleavage site of polypeptide substrate. *European journal of biochemistry / FEBS* 151: 217-224.
134. Lottenberg R, Hall JA, Blinder M, Binder EP, Jackson CM (1983) The action of thrombin on peptide p-nitroanilide substrates. Substrate selectivity and examination of hydrolysis under different reaction conditions. *Biochimica et biophysica acta* 742: 539-557.
135. Gallwitz M, Enoksson M, Thorpe M, Hellman L (2012) The extended cleavage specificity of human thrombin. *PloS one* 7: e31756.
136. Toney MD, Kirsch JF (1991) Tyrosine 70 fine-tunes the catalytic efficiency of aspartate aminotransferase. *Biochemistry* 30: 7456-7461.
137. Banks BE, Doonan S, Lawrence AJ, Vernon CA (1968) The molecular weight and other properties of aspartate aminotransferase from pig heart muscle. *European journal of biochemistry / FEBS* 5: 528-539.
138. Kamitori S, Hirotsu K, Higuchi T, Kondo K, Inoue K, et al. (1987) Overproduction and preliminary X-ray characterization of aspartate aminotransferase from *Escherichia coli*. *Journal of biochemistry* 101: 813-816.
139. Yagi T, Kagamiyama H, Motosugi K, Nozaki M, Soda K (1979) Crystallization and properties of aspartate aminotransferase from *Escherichia coli* B. *FEBS letters* 100: 81-84.
140. Griffith SM, Vance CP (1989) Aspartate aminotransferase in alfalfa root nodules : I. Purification and partial characterization. *Plant physiology* 90: 1622-1629.
141. Sung MH, Tanizawa K, Tanaka H, Kuramitsu S, Kagamiyama H, et al. (1990) Purification and characterization of thermostable aspartate aminotransferase from a thermophilic *Bacillus* species. *Journal of bacteriology* 172: 1345-1351.
142. Umbarger HE (1978) Amino acid biosynthesis and its regulation. *Annual review of biochemistry* 47: 532-606.

143. Neidhardt FC, Curtiss R (1996) *Escherichia coli* and *Salmonella* : cellular and molecular biology. Washington, D.C.: ASM Press.
144. Gelfand DH, Steinberg RA (1977) *Escherichia coli* mutants deficient in the aspartate and aromatic amino acid aminotransferases. *J Bacteriol* 130: 429-440.
145. Sassetti CM, Rubin EJ (2003) Genetic requirements for mycobacterial survival during infection. *Proceedings of the National Academy of Sciences of the United States of America* 100: 12989-12994.
146. Augagneur Y, Garmyn D, Guzzo J (2008) Mutation of the oxaloacetate decarboxylase gene of *Lactococcus lactis* subsp. *lactis* impairs the growth during citrate metabolism. *Journal of applied microbiology* 104: 260-268.
147. Pudlik AM, Lolkema JS (2011) Mechanism of citrate metabolism by an oxaloacetate decarboxylase-deficient mutant of *Lactococcus lactis* IL1403. *Journal of bacteriology* 193: 4049-4056.
148. Pudlik AM, Lolkema JS (2012) Rerouting Citrate Metabolism in *Lactococcus lactis*: Citrate Driven Transamination. *Applied and environmental microbiology*.
149. Bandell M, Ansanay V, Rachidi N, Dequin S, Lolkema JS (1997) Membrane potential-generating malate (MleP) and citrate (CitP) transporters of lactic acid bacteria are homologous proteins. Substrate specificity of the 2-hydroxycarboxylate transporter family. *The Journal of biological chemistry* 272: 18140-18146.
150. Goodwin MB, Boshoff HI, Barry CE, 3rd, Dowd CS (2006) Quantification of small molecule organic acids from *Mycobacterium tuberculosis* culture supernatant using ion exclusion liquid chromatography/mass spectrometry. *Rapid communications in mass spectrometry : RCM* 20: 3345-3350.
151. Brown MR, Allison DG, Gilbert P (1988) Resistance of bacterial biofilms to antibiotics: a growth-rate related effect? *The Journal of antimicrobial chemotherapy* 22: 777-780.
152. Massey RC, Buckling A, Peacock SJ (2001) Phenotypic switching of antibiotic resistance circumvents permanent costs in *Staphylococcus aureus*. *Current biology : CB* 11: 1810-1814.
153. Balaban NQ, Merrin J, Chait R, Kowalik L, Leibler S (2004) Bacterial persistence as a phenotypic switch. *Science* 305: 1622-1625.
154. Goldstone RM, Moreland NJ, Bashiri G, Baker EN, Shaun Lott J (2008) A new Gateway vector and expression protocol for fast and efficient recombinant protein expression in *Mycobacterium smegmatis*. *Protein expression and purification* 57: 81-87.
155. Bashiri G, Squire CJ, Baker EN, Moreland NJ (2007) Expression, purification and crystallization of native and selenomethionine labeled *Mycobacterium tuberculosis* FGD1 (Rv0407) using a *Mycobacterium smegmatis* expression system. *Protein expression and purification* 54: 38-44.
156. Nesbitt NM, Yang X, Fontan P, Kolesnikova I, Smith I, et al. (2010) A thiolase of *Mycobacterium tuberculosis* is required for virulence and production of androstenedione and androstadienedione from cholesterol. *Infection and immunity* 78: 275-282.
157. Pandey AK, Sassetti CM (2008) Mycobacterial persistence requires the utilization of host cholesterol. *Proceedings of the National Academy of Sciences of the United States of America* 105: 4376-4380.
158. Griffin JE, Gawronski JD, Dejesus MA, Ioerger TR, Akerley BJ, et al. (2011) High-resolution phenotypic profiling defines genes essential for mycobacterial growth and cholesterol catabolism. *PLoS pathogens* 7: e1002251.
159. Schnappinger D, Ehrt S, Voskuil MI, Liu Y, Mangan JA, et al. (2003) Transcriptional Adaptation of *Mycobacterium tuberculosis* within Macrophages: Insights into the Phagosomal Environment. *The Journal of experimental medicine* 198: 693-704.

160. Savvi S, Warner DF, Kana BD, McKinney JD, Mizrahi V, et al. (2008) Functional characterization of a vitamin B12-dependent methylmalonyl pathway in *Mycobacterium tuberculosis*: implications for propionate metabolism during growth on fatty acids. *Journal of bacteriology* 190: 3886-3895.
161. Munoz-Elias EJ, Upton AM, Cherian J, McKinney JD (2006) Role of the methylcitrate cycle in *Mycobacterium tuberculosis* metabolism, intracellular growth, and virulence. *Molecular microbiology* 60: 1109-1122.
162. Martin RR, Marshall VD, Sokatch JR, Unger L (1973) Common enzymes of branched-chain amino acid catabolism in *Pseudomonas putida*. *Journal of bacteriology* 115: 198-204.
163. Upton AM, McKinney JD (2007) Role of the methylcitrate cycle in propionate metabolism and detoxification in *Mycobacterium smegmatis*. *Microbiology* 153: 3973-3982.
164. Sareen D, Newton GL, Fahey RC, Buchmeier NA (2003) Mycothiol is essential for growth of *Mycobacterium tuberculosis* Erdman. *Journal of bacteriology* 185: 6736-6740.
165. Buchmeier NA, Newton GL, Fahey RC (2006) A mycothiol synthase mutant of *Mycobacterium tuberculosis* has an altered thiol-disulfide content and limited tolerance to stress. *Journal of bacteriology* 188: 6245-6252.
166. Rawat M, Newton GL, Ko M, Martinez GJ, Fahey RC, et al. (2002) Mycothiol-deficient *Mycobacterium smegmatis* mutants are hypersensitive to alkylating agents, free radicals, and antibiotics. *Antimicrobial agents and chemotherapy* 46: 3348-3355.
167. Miller CC, Rawat M, Johnson T, Av-Gay Y (2007) Innate protection of *Mycobacterium smegmatis* against the antimicrobial activity of nitric oxide is provided by mycothiol. *Antimicrobial agents and chemotherapy* 51: 3364-3366.
168. Ung KS, Av-Gay Y (2006) Mycothiol-dependent mycobacterial response to oxidative stress. *FEBS letters* 580: 2712-2716.
169. Zhang Y, Heym B, Allen B, Young D, Cole S (1992) The catalase-peroxidase gene and isoniazid resistance of *Mycobacterium tuberculosis*. *Nature* 358: 591-593.
170. Heym B, Alzari PM, Honore N, Cole ST (1995) Missense mutations in the catalase-peroxidase gene, *katG*, are associated with isoniazid resistance in *Mycobacterium tuberculosis*. *Molecular microbiology* 15: 235-245.
171. Scior T, Meneses Morales I, Garces Eisele SJ, Domeyer D, Laufer S (2002) Antitubercular isoniazid and drug resistance of *Mycobacterium tuberculosis*--a review. *Archiv der Pharmazie* 335: 511-525.
172. Milano A, Forti F, Sala C, Riccardi G, Ghisotti D (2001) Transcriptional regulation of *furA* and *katG* upon oxidative stress in *Mycobacterium smegmatis*. *Journal of bacteriology* 183: 6801-6806.
173. Master SS, Springer B, Sander P, Boettger EC, Deretic V, et al. (2002) Oxidative stress response genes in *Mycobacterium tuberculosis*: role of *ahpC* in resistance to peroxynitrite and stage-specific survival in macrophages. *Microbiology* 148: 3139-3144.
174. Sherman DR, Mdluli K, Hickey MJ, Arain TM, Morris SL, et al. (1996) Compensatory *ahpC* gene expression in isoniazid-resistant *Mycobacterium tuberculosis*. *Science* 272: 1641-1643.
175. Pagan-Ramos E, Song J, McFalone M, Mudd MH, Deretic V (1998) Oxidative stress response and characterization of the *oxyR-ahpC* and *furA-katG* loci in *Mycobacterium marinum*. *Journal of bacteriology* 180: 4856-4864.
176. Sherman DR, Sabo PJ, Hickey MJ, Arain TM, Mahairas GG, et al. (1995) Disparate responses to oxidative stress in saprophytic and pathogenic mycobacteria. *Proceedings of the National Academy of Sciences of the United States of America* 92: 6625-6629.
177. Singh R, Wiseman B, Deemagarn T, Donald LJ, Duckworth HW, et al. (2004) Catalase-peroxidases (*KatG*) exhibit NADH oxidase activity. *The Journal of biological chemistry* 279: 43098-43106.
178. Imlay JA, Chin SM, Linn S (1988) Toxic DNA damage by hydrogen peroxide through the Fenton reaction in vivo and in vitro. *Science* 240: 640-642.

